Regulation of *C.elegans* Vulval Morphogenesis by LIN-12 Notch Signaling

---

Dissertation

zur

Erlangung der naturwissenschaftlichen Doktorwürde
(Dr. sc. nat.)

vorgelegt der

Mathematisch-naturwissenschaftlichen Fakultät

der

Universität Zürich

von

Sarfarazhussain Farooqui

aus

Indien

Promotionskomitee

Prof. Dr. Alex Hajnal, Universität Zürich
(Vorsitz, Leitung der Dissertation)

Prof. Dr. Michael Hengartner, UZH Zürich

Prof. Dr. Peter Gallant, Universitat Würzburg

Prof. Dr. Freddy Radtke, EPFL Lausanne

Zürich, 2012

Dedicated to MY PARENTS, FAMILY and MY MENTORS

Table of Contents

Zusammenfassung

Einer der grundlegenden Gesichtspunkte während der Entwicklung eines Tieres ist die Bildung der Epithelschicht. Epithelzellen sind polarisierte Zellen, deren basolateraler Teil vom apikalen Teil durch Adhäsionsverbindungen (*engl.:adherens junctions*) getrennt ist. Diese Adhäsionsverbindungen enthalten E-Cadherin und andere Proteine, die das Aneinanderhaften von Zellen herbeiführen; Zudem ist die basale Zelloberfläche typischerweise mit einer Basallamina verbunden. Diese Epithelzellen können mittels Morphogenese zu Röhren und darüber hinaus zu ganzen Röhrennetzen umgeformt werden. Einige Studien zeigen bereits, dass im Mittelpunkt der Morphogenese die Anhaftung und die Anordnung von Zellen stehen; jedoch ist über die Kontrolle der Signalwege bei der morphogenese wenig bekannt.

Die Entwicklung der Vulva von *C.elegans* stelt ein bedeutendes Modellsystem für die Festlegung und für die strukturelle Ausbildung der Schicksale der Epithelzellen dar. Auf der Suche nach Genen, die im Epithelgewebe der Vulva direkt durch den ubiquitären Notch-Signalweg reguliert werden, stießen wir auf das *C.elegans* Gen Rho-Kinase (ROCK) *let-502*, das ein indirektes zielgen von Notch darstellt. Rho-Kinasen (ROCKs) sind die Hauptüberträger der Signale von aktivierten Rho-GTPasen und wurden oft aufgrund ihrer Fähigkeit die Kontraktilität von Actomyosin zu beeinflussen, mit den über Rho-GTPasen vermittelten Effekten auf Form und Bewegung von Zellen in Verbindung gebracht. Eine Funktion von ROCKs ist das Herbeiführen von Formänderung und Bewegung von Zellen, was auf eine wichtige Rolle der von Rho-ROCKs übermittelten Signaltransduktion während der Gewebsmorphogenese schließen lässt. Die Identifizierung einer Rho-Kinase als ein durch den Notch-Signalweg indirekt reguliertes Gen ermöglichte es, die strukturelle Ausbildung der Vulva von *C.elegans* als ein Instrument für die Erforschung von Signaltransduktion beider Umgestaltung von der Epithelschicht zu verwenden.

Auf Grund seines Expressionsmuster kann das Gen *let-502* als ein indirektes Notch-Target bezeichnet werden. Durch weitere Untersuchungen des Expressionsmusters von *let-502* in verschiedenen Mutanten konnten wir zeigen, dass der Transkriptionsfaktor LIN-1 ETS nach Notch geschaltet ist und direkt an den Promotor von *let-502* bindet, um dessen Transkription zu starten. Somit stellt LIN-1 einen zentralen Faktor bei der Entwicklung der Vulva dar.

Die Anker zelle (AC), 1° and 2° Zellen sind die drei Bestandteile des Epithels, das die Vulva ausbildet. Ein Signal der AC führt zur Induktion des 1° Zellschicksals während die 1° Zelle direkt auch für die Ausführung des 2° Zellschicksals der Nachbarzellen verantwortlich ist. Somit können wir darüber spekulieren, dass die AC die Rolle des Anführers spielt und die 2° Zellen, die von der 1° abhängig sind, hinterherfolgen. Wir untersuchten die einzelnen Beiträge dieser Zelltypen zur Bildung der Vulva. Indem wir Weg spezielle Zellen im Wurm ablatierten, konnten wir zeigen, dass die 2° Zellen über die Rho-Kinase *let-502* eine Stoßkraft ausüben, während die AC eine Zugkraft besitzt. Beide Kräfte sind wichtig, um eine funktionsfähige Vulva zu bilden. Wir gingen noch einen Schritt weiter und wiesen die Stoß- und Zugkraft nach, indem wir zum ersten Mal die Morphogenese der Vulva filmten. Aus molekularer Sicht ist die Ordnung von Anführer und nachfolgenden Zellen wie folgt: AC-1°-2°. 2° Zellen sind also von 1° Zellen abhängig. Im Gegensatz dazu zeigten wir, dass aus mechanischer Sicht im Bezug auf die Stoßkraft die 1° Zellen von den 2° Zellen abhängen. Zusammen mit Mark Watson Pellegrino fanden wir auch, dass in 1° Zellen der RAS-Signalweg und der Transkriptionsfaktor LIN-39 HOX das neu entdeckte Gen *vab-23* aktivieren und somit - gleichermaßen wie der Notch-Signalweg in 2° Zellen – Fusion, Bewegung und ordnungsgemäße Anhaftung von Zellen während der Morphogenese der Vulva regulieren. *vab-23* ist ein DNA-bindendes Protein, das direkt das Gen *smp-1* reguliert, was wir mittels ChIP Experimente zeigen konnten. Das *C.elegans* Protein VAB-23 zeigt eine hohe Sequenzhomologie zu dem humanen HCA127 (hepatocellular carcinoma antigen), dessen Funktion bisher noch unbekannt ist.

Wir konnten schlussendlich zeigen, dass die beiden Transkriptionsfaktoren – LIN-1 in 2° Zellen und VAB-23 in 1° Zellen – im Mittelpunkt der Morphogenese der Vulva stehen. Die einfache Beschaffenheit des Modellorganismus *C.elegans* hat es uns erlaubt die Funktionen von LIN-1 und VAB-23 zu untersuchen, und wir schlagen vor, dass beide Gene konservierte Funktionen während der Morphogenese von Organen in höheren Organismen übernehmen können. Diese Moleküle gaben uns auch eine Gelegenheit dazu, die Formveränderung von einzelnen Zellen bei der Morphogenese der Vulva zu erkunden. Die Resultate dieser Studie legen bedeutende molekulare und zelluläre Wechselwirkungen offen, die zur endgültigen Struktur von Organen beitragen.

Summary

One of the fundamental aspects of development in animals is the formation of epithelia. Epithelial cells are polarized, with basolateral domains separated from apical domains by adherens junctions. The adherens junctions contain E-cadherin and other proteins that mediate cell adhesion. The basal surface of epithelial cell is associated with a basal lamina. These epithelial cells can be remodeled into tubes and further into branches of these tubes via morphogenesis. Several studies show that organization and cohesion are central to epithelial morphogenesis but the signals controling this remodeling are poorly understood.

C.elegans vulval development serves as an important system for studying cell fate determination and morphogenesis of epithelial cells. In a quest to find out the direct target genes of the universal Notch signaling pathway in the vulval epithelium, we found the *C.elegans* Rho-kinase (ROCK) *let-502* as an indirect Notch target gene. The Rho-kinases (ROCKs) are major effectors targets of the activated Rho GTPase. ROCKs have been implicated in many of the Rho-mediated effects on cell shape and movement via their ability to affect acto-myosin contractility. One of the functions of ROCKs are to bring about changes in shape and motility of cells, which suggests a potentially important role for Rho-ROCK signaling in tissue morphogenesis during development. Identification of Rho-kinase as an indirect target of the Notch signaling pathway paved the way for using *C.elegans* vulval morphogenesis as a tool for studying the signals controling of epithelial remodeling. By, analyzing the *let-502* expression pattern in several mutant backgrounds, we demonstrate that LIN-1 ETS is the transcription factor that acts downstream of the Notch signaling pathway and directly binds to the *let-502* promoter to activate its transcription. Finally, we show that LIN-1 is a central player of vulval morphogenesis.

The anchor cell (AC), the 1° and 2° cells are the three components of the vulval epithelium. Signaling from the AC leads to induction of the 1° cell fate while 1° cells are directly responsible for 2° cell fate specification, we thus propose that the AC should be the leader and the 2° cells are the lagging cells, which are dependent on the 1° cells. We analyzed the individual contribution of these cell types in building up the vulva. Using classical cell ablation techniques, we could show that 2° descendants provide a pushing force via the Rho-kinase *let-502*, while the AC provides the pulling force. We went a step further and verified the pushing and the pulling forces by visualizing and quantifying toroid morphogenesis in vivo. The order of leader to follower is AC→1°→2°, making 2° cells dependent on 1° cells. On the other hand, from the force contribution perspective, the 1° cells

are dependent on 2° cells for the pushing force. Finally, together with Mark Watson Pellegrino, we showed that in 1° cells, the RAS signaling pathway and the LIN-39 HOX transcription factor activate the novel gene *vab-23* to regulate cell fusions, movement and proper adhesion of cells during vulval morphogenesis. *vab-23* is a DNA binding protein and using ChIP, we demonstrated that *smp-1* is one of its direct target genes. It has several indirect targets too. *C.elegans* VAB-23 shows strong homology to a human hepatocellular carcinoma antigen (HCA127) of unknown function.

Thus, we could show that the two transcription factors, LIN-1 in 2° cells and VAB-23 in 1° cells, have taken the centre stage during morphogenesis. The simple nature of *C.elegans* as a model system has allowed us to investigate the functions of LIN-1 and VAB-23. We propose that LIN-1 ETS and VAB-23 zinc finger play conserved functions in organ morphogenesis of higher animals. The two transcription factors also gave us an opportunity to analyze the cell shape changes during morphogenesis of the vulva and reveal the important molecular and cellular interactions that contribute to the final shape of organs.

Abbreviations

1°	primary
2°	secondary
AC	anchor cell
AML	acute myeloid leukemia
Apf	adjacent primary fate
ChIP	chromatin immunoprecipitation
Chr.	chromosome
coIP	co-immunoprecipitation
CSL	CBF1/Su(H)/LAG-1
CtBP1	C-terminal binding protein 1
Dpy	dumpy: shortened body
DSL	DELTA/SERRATE/LAG-2
DU	dorsal uterine
ECM	extracellular matrix
EGF	epidermal growth factor
EGF	epidermal growth factor
Egl	egg-laying defective
EMS	ethyl methyl sulfonate
EMT	epithelial to mesenchymal transition
EBS	ETS binding sites
GEF	guanine nucleotide exchange factor
GFP	green fluorescent protein
LBS	*lag-1* binding sites
Lin	lineage defective
LST	lateral signal target
MAPK	mitogen-activated protein kinase
Muv	multivulva
NICD	Notch intracellular domain
PI3K	phosphoinosite-3-kinase
Pvl	protruding vulva
RAS	rat sarcoma
RNAi	RNA interference
Rol	roller: rolling movement
RTK	receptor tyrosine kinase signaling pathway
SMC	smooth muscle cells
SPh	somatic primordium of the hermaphrodite
Su(H)	suppressor of hairless
SynMuv	synthetic multivulva
Unc	uncoordinated
URS	upstream regulatory sequence
utse	uterine seam cell
VPC	vulval precursor cell
VU	ventral uterine

1 Introduction

1.1 General Introduction

Development of an organism can be described briefly as a series of changes in the state of the cell, tissue, organ, or an organism, which results in a sustainable life form. These changes give rise to the structure and the function of living organisms. The development starts as the embryo divides, followed by determination of cell fates by these cells, resulting in a clump of differentiated cells. This group of cells further undergoes morphogenesis, a process that changes their shape and migrate to form new cellular interactions to adopt a new spatial plan, in doing so, they together form a functional tissue or organ. Further coordination and connectivity between these tissues results in the formation of a life form. Thus, morphogenesis is one of the many, but an important process of development. Mostly, these processes are very tightly controlled and any change in them causes several developmental disorders so it is very important to have an in depth knowledge about the process of morphogenesis.

To date, several important aspects of cell fate determination and morphogenesis of the differentiated cells have been described (Wolpert, 2011). It is well known that the cell fate adoption or execution depends on several signaling pathways interacting with each other. This interaction among cells could be autocrine or paracrine in nature. Predominantly, these signals are paracrine in nature where a signaling molecule mostly in the form of a ligand from a cell, activates the receptor on the membrane of a different cell to transduce a signaling cascade in the ligand-receiving cell. This signaling has the potential to bring about several intracellular changes that will decide the determination of fate and eventually, the shape and size of the tissue to be formed. Thus, a hawk eye's view of these pathways is important for moving towards more complete knowledge about development of a life form.

An important aspect of the development is the conservation of the events during evolution that lead to the growth of a fully developed organism. For example, the phases of embryonic development from the fish to mammals are pretty similar (Wolpert, 2011). In addition, the molecular pathways governing certain developmental processes are conserved too. For example the mechanism and signaling molecules involved in programmed cell death or apoptosis are highly conserved from free-living nematode *C.elegans* (Figure 1.1) to humans (Adams, 2003; Danial and Korsmeyer, 2004; Horvitz, 2003). However, it is very difficult to analyze these processes in higher eukaryotes due to their large genome size and

large number of cells, which lead to more complexity and lot of redundancy in their genome. It was easily studied in *C.elegans* owing to smaller genome size, less number of cells and less redundancy. Also, the worm is viable without these dying cells thus, making it a handy system to analyze apoptosis (Hengartner and Horvitz, 1994). Similarly among vertebrates, the frog, *X.laevis*, the mouse (*mus musculus*), the chicken (*Gallus gallus*), and the zebrafish (*Danio rerio*) are the main models now studied (Wolpert, 2011). Among invertebrates, the fruitfly *D. melanogaster* similar to *C.elegans*, is well known for studying developmental genetics (Wolpert, 2011).

These model organisms have served as an excellent tool for identifying the molecular pathways important for organ development. Many advances have been made in understanding these signaling pathways which are required for cell fate determination and further morphogenesis of cells by studying important events taking place at different time points or stages of the model organs. Notch signaling is one of these pathways, which is well characterized.

1.2 Notch signaling pathway

1.2.1. Notch ligands and receptors

Mammals have four genes encoding Notch receptors (N1–N4). Each is synthesized as a single transmembrane polypeptide but subsequently cleaved and transported to the cell surface as a heterodimer (Figure. 1.2). The extracellular domains contain several (Lai, 2004) tandem epidermal growth factor (EGF)-like repeats that bind ligand. Notch ligands are classified into two structurally related groups: Delta-like ligands (Dll-1, -3, and -4) and Serrate-like ligands (Jagged-1 and -2) (Lai, 2004). Both types of ligands are transmembrane proteins with a number of tandem EGF-like repeats in their extracellular domain and a unique Delta, Serrate, and Lag-2 (DSL)-binding domain in the amino terminus necessary for receptor interaction (Lai, 2004). The Notch signaling pathway is initiated when receptor-bearing cells interact with Notch ligands expressed by adjacent cells. This interaction triggers two proteolytic cleavages that release the Notch intracellular domain (NICD) from its plasma membrane tether, allowing it to translocate to the nucleus, where it binds to a transcriptional regulator known as CBF1/Su(H)/LAG-1 (CSL). In the absence of NICD, CSL inhibits expression of target genes by binding to RTGGGAA elements and recruiting transcriptional corepressors (Figure. 1.2). However, when NICD enters the nucleus, it binds to CSL, displaces the corepressors, and recruits transcriptional coactivators that induce expression of

members of the Hairy-Enhancer of Split (HES) and Hes-related proteins (HERP) gene families. HES/HERP proteins are basic helix-loop-helix (bHLH) DNA-binding proteins that inhibit the expression and/or function of lineage-specifying bHLH genes, such as MASH-1 (neurogenesis), MyoD (myogenesis), and E2A (B lymphopoiesis) (Iso et al., 2003). Although the CSL/HES pathway mediates many effects of Notch signaling, some CSL independent mechanisms also exist (Martinez Arias et al., 2002) .

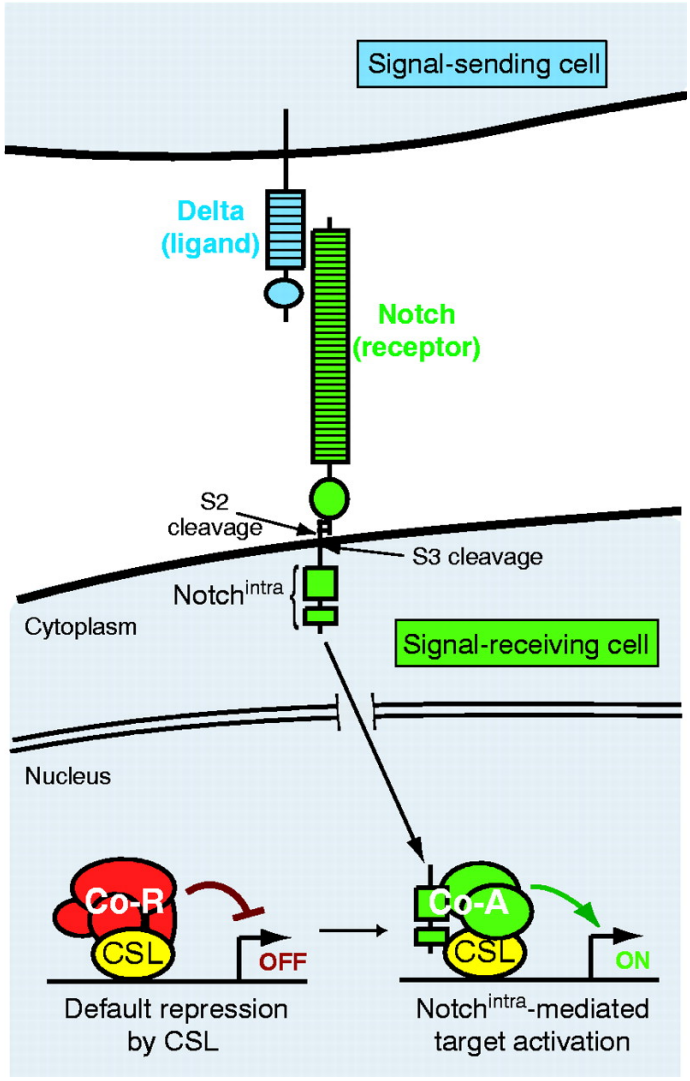

Figure 1.2. Notch signaling pathway. . Notch receptor on signal receiving cell interacts with Notch ligands such as Delta or Serrate/Jagged from signal sending cell . Upon ligand binding, Notch is cleaved by ADAM metalloprotease and Presinilin/γ-secretase to free the Notch intracellular domain. Notch intra (N-IC) initiates its downstream effects by migrating to the nucleus and binding RTGGGAA elements . (adapted from (Lai, 2004))

1.2.2. Notch regulates self-renewal and cell-lineage decisions in many tissue

Notch receptors and ligands are widely expressed during organogenesis in mammalian embryos, and studies of spontaneous or induced mutants demonstrate that Notch signaling regulates cell-lineage decisions in tissues derived from all three primary germ layers: endoderm (e.g. pancreas), mesoderm (skeleton, mammary gland, vasculature, and hematopoietic cells), and ectoderm (neuronal lineages). Some developing tissues express several different receptors and ligands, whereas others express a single receptor–ligand pair. Although some Notch receptors appear to have genetically redundant functions in some developmental contexts (e.g. N1 and N4 in vasculogenesis) (Krebs et al., 2000), others have unique and essential functions as revealed by the severe disruption of embryogenesis that results from loss-of-function mutations (Lai, 2004). Notch functions in the development of many tissues and cell lineages like hematopoiesis (Pear and Radtke, 2003), neurogenesis (de la Pompa et al., 1997), somitogenesis (Pourquie and Kusumi, 2001) and vasculogenesis (Krebs et al., 2000). Vasculogenesis is a form of tube morphogenesis, which involves a complex process of remodeling and refining. The role of Notch signaling in tube morphogenesis has been poorly understood.

1.3 Mechanisms underlying the formation of biological tubes

1.3.1. Biological tubes

Tubes are a fundamental unit of organ design. Most of our major organs including the lung, kidney, and vasculature are composed primarily of tubes. They serve as the body's plumbing for transporting critical gases, liquids, and cells from one site to another. These biological pipes are almost invariably composed of living cells, usually attached to one another to form an epithelium (sheet of cells) that is wrapped into a tube with the apical epithelial surface lining the lumen, in contact with the transport medium, and the basal surface facing outward (Figure 1.3a). Some tubes modify the transport fluid, whereas others act as passive conduits. Despite significant progress over the last decade in understanding how tubular organs are patterned during development, we are only now beginning to understand how cells assemble into tubes and how tube size and shape are regulated. A detailed mechanistic understanding of these processes is important for medicine as well as biology, because many human diseases such as polycystic kidney disease and atherosclerotic heart disease are more or less plumbing defects (Lai, 2004). A molecular understanding of tubulogenesis could lead to new ways of diagnosing and treating these conditions.

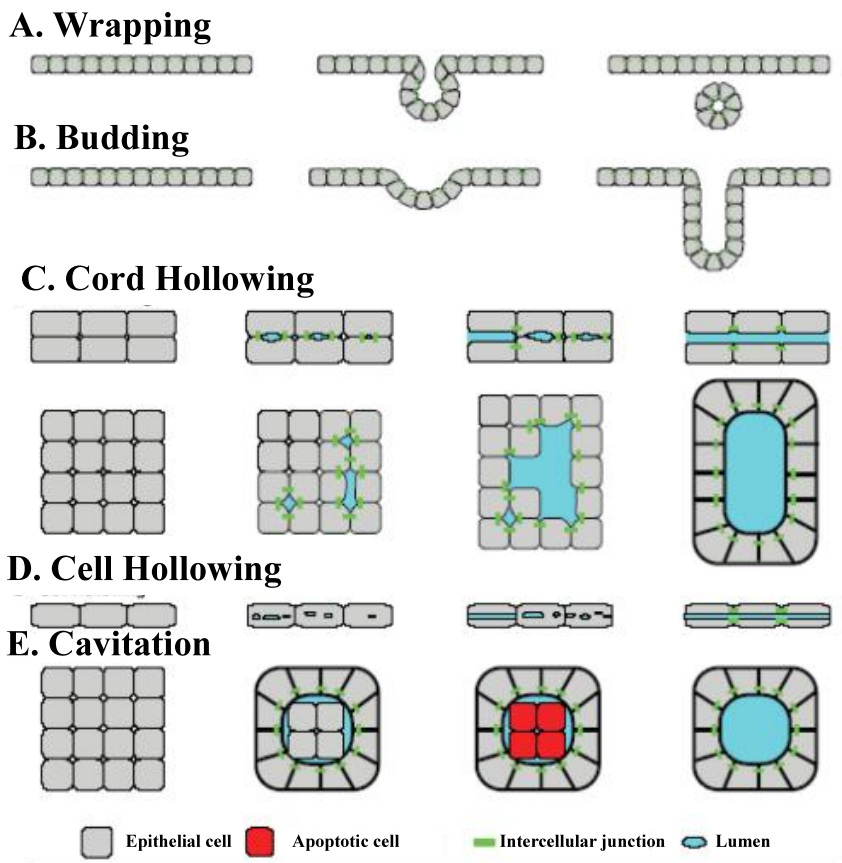

Figure 1.3a. Morphological Processes of Tube Formation A. Wrapping: a portion of an epithelial sheet invaginates and curls until the edges of the invaginating region meet and seal, forming a tube that runs parallel to the plane of the sheet. **B.** Budding: a group of cells in an existing epithelial tube (or sheet) migrates out and forms a new tube as the bud extends. The new tube is a direct extension of the original tube. **C.** Cord hollowing: a lumen is created de novo between cells in a thin cylindrical cord. **D.** Cell hollowing: a lumen forms within the cytoplasm of a single cell, spanning the length of the cell. **E.** Cavitation: the central cells of a solid cylindrical mass of cells are eliminated to convert it into a tube. Adapted from (Andrew and Ewald, 2010)

A bird's eye view of tube through physiology point of view reveals the tremendous structural diversity of biological tubes. They have different sizes, shapes, and connecting patterns, which, are tailored to their specific transport fluid and function. Tube sizes range over six orders of magnitude, from 0.1 micron or less in diameter for the smallest insect tracheal tubes to greater than 20 cm for the gut of an adult elephant. Their cellular architectures also differ. One striking difference is the number of cells in each cross section of the tube, which generally scales with tube diameter. Large diameter tubes are composed of hundreds or thousands of cells per cross section, whereas small diameter tubes can be composed of just a single cell. Tubes also differ in the presence or absence of cell junctions. Junctions serve as cell attachment sites that seal the epithelial layer to paracellular leakage, and they separate the border between apical and basolateral membrane domains. Multicellular and most

unicellular tubes contain such junctions (Figure 1.3a), whereas some unicellular tubes lack junctional structures (Lubarsky and Krasnow, 2003). Most tubes secrete specialized matrices at their apical or basal surface, or contain additional cell layers, but the simplest tubes are epithelial monolayers without any surrounding support structures (Lubarsky and Krasnow, 2003).

Inspite of all the research in tube morphogenesis and owing to the tube diversity, the important questions still remain the same for example how do such diverse tubes form, how do they grow to achieve their mature sizes and shapes. Do they use completely different cellular and molecular mechanisms, or are there common underlying mechanisms of tubulogenesis? Tubular organs develop in a wide variety of ways, and many cellular processes have been said to be involved. But recent investigations of tube formation and growth in a number of systems, from cell culture to human tubulogenesis diseases, point to critical roles for apical membrane biogenesis, vesicle fusion, and secretion. Although the full process is not well understood for any system, by drawing together results from different systems, a general model for tube morphogenesis can be sketched out. This model accommodates a variety of organ and tube specific variations that tailor tube structure to function and shows how different tube sizes and shapes are created in nature and how defects in the process cause human disease.

1.3.2. Morphological Processes of Tube Formation

Descriptions of embryonic development showed that tubular organs develop in many different ways. At a higher level, it appears that nearly every tubular organ forms in its own distinct manner, some deploying multiple tube forming mechanisms. Some of this morphogenetic diversity, however, derives from differences in events leading up to or following tube formation, such as the way the cells reach their proper positions, or the means by which extra cells are eliminated or additional cell layers are recruited around the developing tubes. If one considers only the events that occur just as the cells form tubes, then most tubulogenesis processes can be grouped into five general categories (Figure 1.3a). Wrapping occurs when an epithelial sheet curls until its edges meet and seal, forming a tubular structure. Typically, this involves only a portion of the epithelium, with the tube-forming cells first invaginating to form a crevice in the epithelium, then sealing off and separating from the rest of the epithelium, as during neural tube formation in many vertebrates (Colas and Schoenwolf, 2001). This generates a tube that runs parallel to the

plane of the epithelium from which it is derived. In budding, cells extend out from the

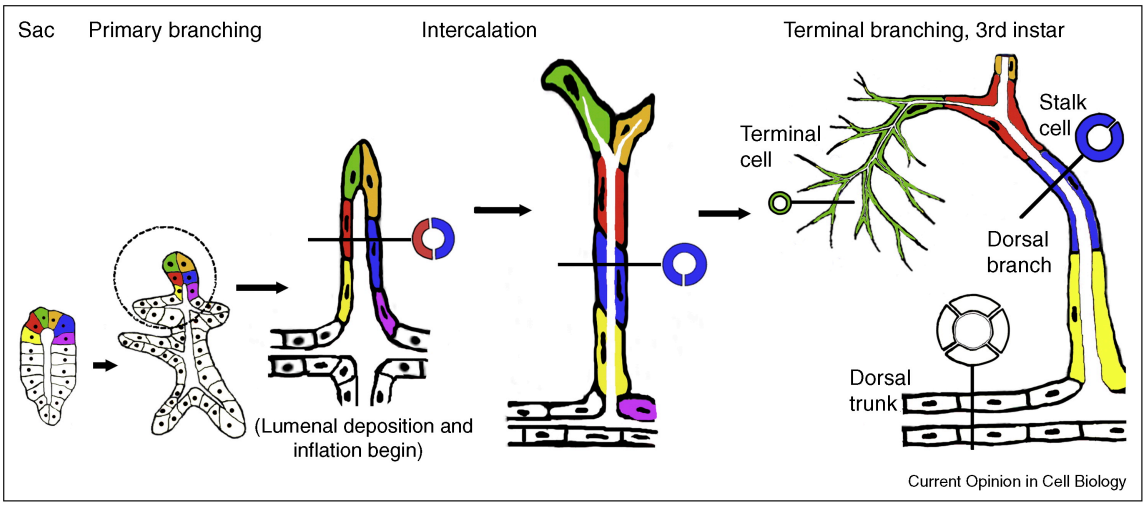

Figure 1.3b. Branching morphogenesis. Three distinct tube types generated by tracheal branching morphogenesis. From left to right: during early stages of embryogenesis, tracheal cells invaginate and form tracheal sacs composed of roughly 80 cells arranged in a polarized epithelial monolayer ('sac' schematic). Six cells are colored coded (yellow, red, green, orange, blue and magenta) to allow them to be followed over time. In response to a Branchless FGF chemoattractant cue, tip cells initiate the primary branching program (Figure 1.3c), and six primary branches bud from the tracheal sac ('primary branching' schematic). Cells within the hashed circle (dorsal trunk anterior branch, to left, dorsal branch at top) are schematized at later developmental time points shown to the right. The cells of the dorsal branch are initially arranged side by side such that a cross-section view (black line) reveals the profile of two cells (red and blue) surrounding the tube lumen ('intercalation' schematic). The cells remodel their cell–cell contacts, changing neighbors (note: blue cell no longer shares a cell–cell junction with the orange or magenta cells) and intercalating to form a longer thinner tube. In a cross-sectional view, the mature dorsal branch tube is a single cell (blue) in circumference. The dorsal branch tip cells (green and orange) become specified as terminal and fusion cells, the former undergoes extensive branching during larval life, while the latter anastamoses with a fusion cell from the contra-lateral side to produce a continuous tube spanning the dorsal midline. By the end of embryogenesis, tubes of three distinct cellular architectures are present in the tracheal system. These distinct tube types are easily recognized in the third instar larvae, where terminal cells have ramified extensively producing dozens of branched terminal tubes ('terminal branching, 3rd instar' schematic). The tubes from a single terminal cell (green) spread over areas of 100 mm or more, and are a micron or less in diameter. In cross-section the tubes are revealed to be 'seamless.' In contrast, the dorsal branch stalk cells (red, blue, yellow) wrap around a lumenal space and seal into a tube by forming autocellular adherins and septate junctions represented by the single seam visible in cross- section (blue). Dorsal trunk tubes are several cells (white) in circumference and the cells that compose them organize into a tube by making intercellular adherins and septate junctions in cross-section, a junctional seam is visible between all cells. Adapted from (Schottenfeld et al., 2010).

epithelium in a direction perpendicular to the epithelial plane, forming a tube as the bud grows. This mechanism is followed during branching morphogenesis of many organs, including the formation of major branches of the Drosophila tracheal (respiratory) system (Figure 1.3b; (Schottenfeld et al., 2010)). New branches bud from the walls of an existing branch, and the lumen of the new branch is a direct extension of the lumen of the parental branch.

During cavitation, cells are organized into a thick cylindrical mass and they create a central cavity by eliminating cells in the center of the mass, as it occurs during salivary gland morphogenesis (Melnick and Jaskoll, 2000) in vertebrate embryos. In cord hollowing, cells

assembled in a thin cylindrical cord create a lumen between cells, without cell loss (Figure 1.3a C). Examples include the Caenorhabditis elegans gut (Leung et al., 1999). Cell hollowing is distinct from the other processes in that it involves one cell rather than a group of cells (Figure 1.3a D). For instance, some capillary endothelial cells form a membrane-bound lumen within the cytoplasm that spans the length of the cell and opens to the exterior at both ends (Bar and Wolff, 1972).

1.3.3. Leaders and followers in tube outgrowth

Cell marking studies in the mammalian kidney and Drosophila trachea revealed that the elongating tubes in these systems comprise of two distinct populations: Tip cells (also known as leader cells or terminal cells) and trunk cells (also known as follower or stalk cells) (Cabernard and Affolter, 2005; Shakya et al., 2005). Tip cells in Drosophila require receptor tyrosine kinase (RTK) signaling for outgrowth, whereas the follower cells do not. Moreover, it is the cells that receive the highest levels of RTK signaling that become the tip cells and they do so by moving into the leader position, passing by cells in which RTK signaling levels are relatively lower (Figure 1.3c; (Ghabrial and Krasnow, 2006)).

Studies in Drosophila tracheal cells, demonstrated a requirement for FGF signaling in the leader but not follower cells and for relative levels of FGF signaling being important in sorting the leaders (tip cells) from followers (stalk cells) (Figure 1.3c) (Cabernard and Affolter, 2005; Ghabrial and Krasnow, 2006). Studies from Caussinus *et. al* reveal that it is the leader cells in the embryonic trachea that generate the traction forces required for the cell rearrangements of embryonic tracheal tube outgrowth (Caussinus et al., 2008). So far only Xavier *et al* reported that the physical forces from the followers or stalk cells make a bigger contribution during collective cell migration (Xavier Trepat, 2009). Thus, most of the current research focuses on leader cells as the main player in morphogenesis, while the contribution of the follower cells need to be explored. To investigate this, various organs in different model systems are being used and here we present *C. elegans* vulval development as a new model for tube morphogenesis.

1.4 *Caenorhabditis elegans* as a model system in developmental biology

C.elegans is a free living nematode approximately 1mm in size, with a short life-cycle of 3-5 days which depends on temperature and its breeding environment (Figure 1.1). Sexually, it is dimorphic in nature predominantly as hermaphrodites and occassionally

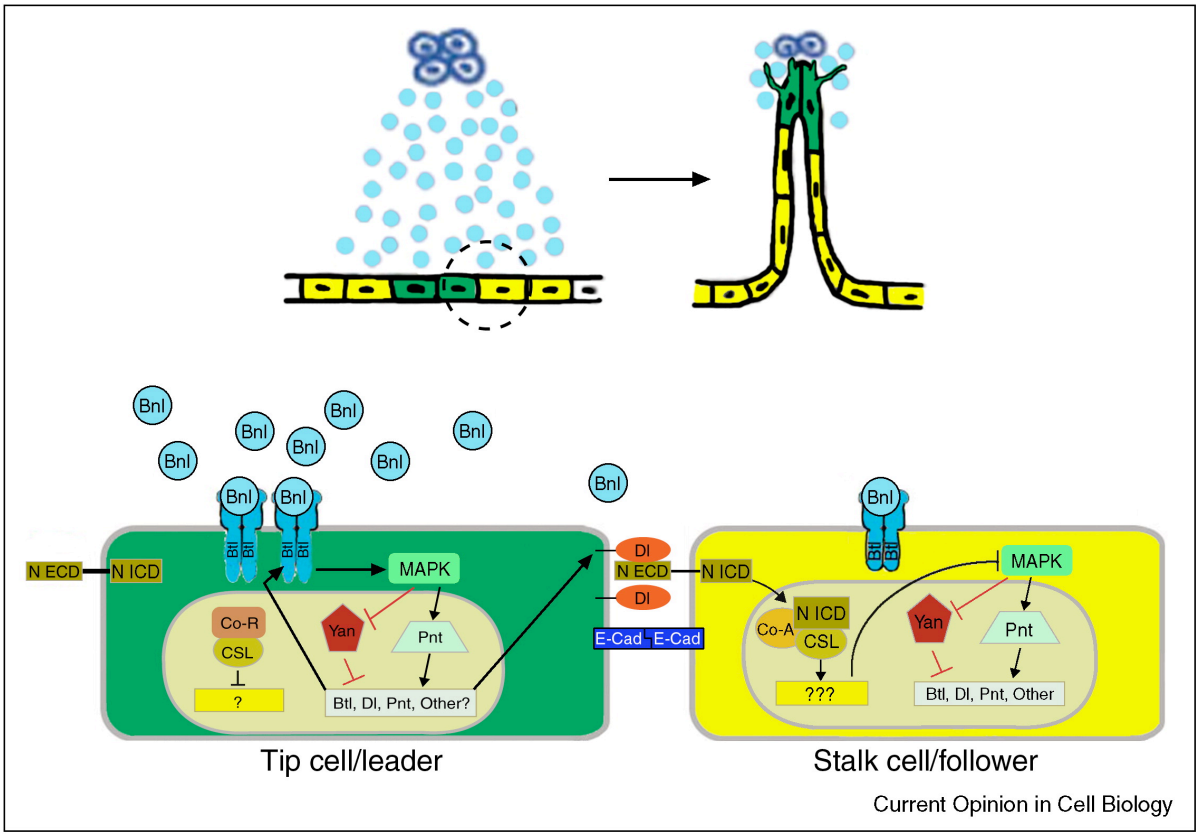

Figure 1.3c. Signaling in leader and follower cells. Tip cell selection. In the top panel, dorsal branch cells in the tracheal epithelium receive a signal (light blue) from FGF- secreting cells (dark blue). Two cells are selected as tip cells (green) while the other cells will become followers (yellow). Interactions between a leader and follower cell (circled) are shown in the enlarged bottom panel. These two tracheal epithelial cells are held together by adherens junctions, by homophilic interactions between Drosophila E-cadherin (E-Cad) on their surface. Initial slight differences in FGF signaling are amplified by positive and negative feedback loops. Breathless FGFR signaling (FGF: Branchless/Bnl, FGFR: Breathless/Btl) through the canonical MAPK pathway here represented only results in phosphorylation of the ETS box transcription factors Pointed (Pnt) and Yan (encoded by anterior open). Phosphorylation of Pointed activates transcription of breathless, Delta (Dl), and pointed itself. Transcription of breathless and pointed is expected to increase FGFR pathway activity, while Delta (Dl) activates Notch (extracellular (NECD) and intracellular (NICD) domains indicated). Proteolytic processing of the ligated Notch receptor releases the N ICD, which associates with the transcription factor CSL (CBF1/suppressor of hairless/Lag1, light gold oval), and co-activator (Co-A, in Drosophila, mastermind). Activation of Notch antagonizes MAPK, downregulating the FGFR pathway and Delta expression in the follower cell. Adapted from (Schottenfeld et al., 2010)

as males. The adult hermaphrodite comprises of several tissues including the gonad that produces oocytes, which undergo maturation and fertiliation by sperm within spermatheca. After the formation of the embryo, they undergo several rounds of cell divison within the uterine cavity to be finally laid out of the worm through vulva. This egg further undergoes morphogenesis leading to hatching of the eggshell, which results, into the L1 stage larvae. This larvae further goes through four stages of larval developments to finally form an adult animal which can lay its own eggs and the cycle continues.

Sydney Brenner isolated *C.elegans* from a soil sample in his backyard and since then, it has served as an excellent model organism (S, 1974). It is easy to maintain in laboratory

condition at 15-25 °C, is genetically tractable, can be frozen and thawed after long time, is transparent throughout and hence easy to observe all the cells in its body. Because of the transparent body, the complete cell lineage of the animals was established (HR, 1977). Remarkably, Inspite of being such a small organism, *C.elegans* has important organ systems like muscles, nervous systems which are comparable to even higher organisms such as mammals. Further, sequencing of *C.elegans* genome served as an important model for sequencing the human genome (Consortium, 1998). The genomes of closely related species such as *Caenorhabditis ramenei, Caenorhabditis briggsae, Caenorhabditis japonica* and *Caenorhabditis brenneri* are sequenced which allows us to answer several questions by doing comparative genomics using in-silico approaches (Stein LD, 2003). In order to understand the function of a gene in *C.elegans* genome, two different approaches are adopted. First, gene function can be "knocked out" using chemical mutagens or "knocked-down" using RNA interference (RNAi). Secondly, PCR products or plasmids containing fusion product of a gene loci and or protein fusion tags like green fluorescent protein (GFP) can be directly

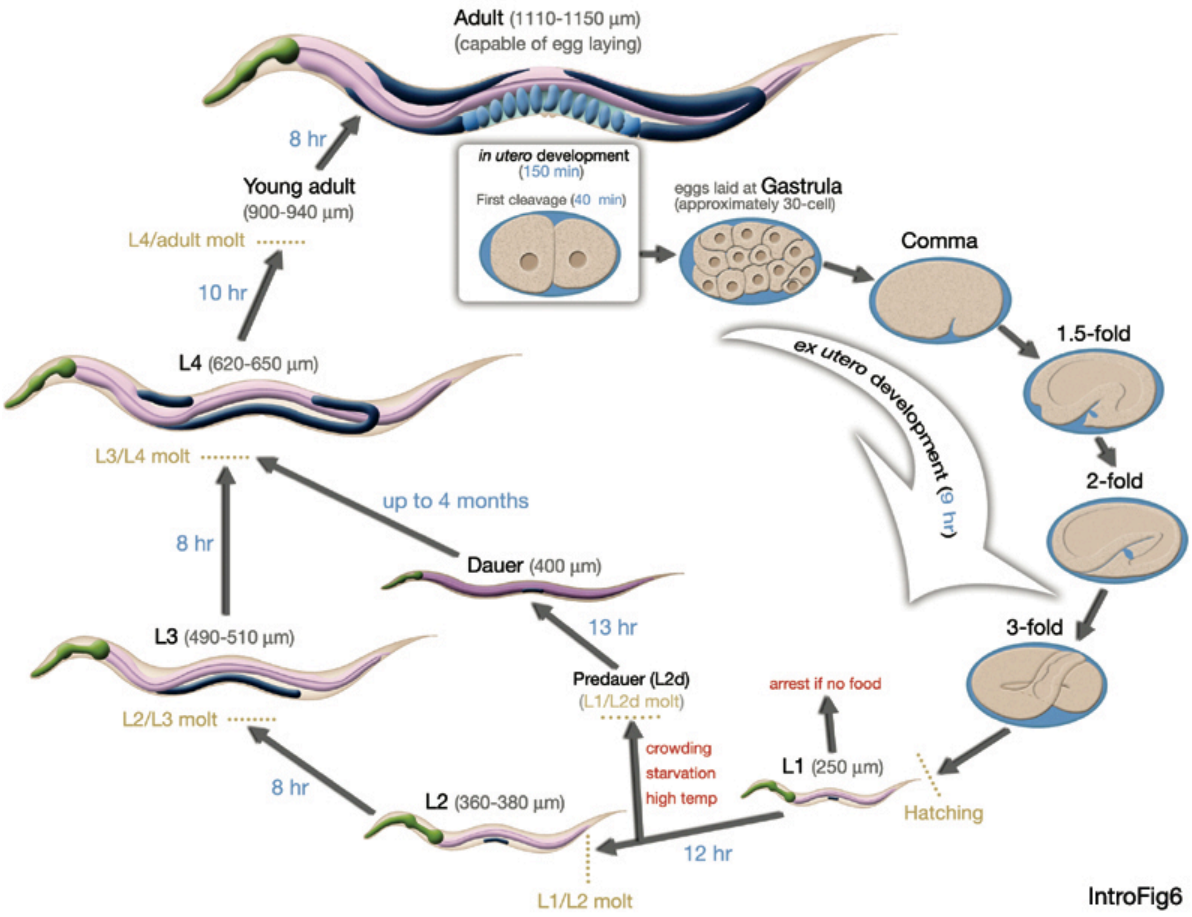

Figure 1.1. Life cycle of *C.elegans*. After fertilization of the egg, the zygote develops in the uterus till 30 cell stage. The egg is laid at this stage and it continues its development to hatch out as L1 larvae stage. Under

optimum conditions, the worm continues to develop through the L2-L4 stage till adulthood. If the conditions are not optimal for its development, the worm develops into dauer stage, in which they stay till conditions become optimum again (www.wormatlas.org).

microinjected in the animal to give rise to progeny containing extrachromosomal arrays in it (Mello CC, 1991; O, 2002). These extrachromosal arrays can be integrated into the worm genome using gamma-irradiation to form homogenously expression lines (Mello CC, 1991). Also, the cells can be directly manipulated by laser ablation to study their role in the given environment (Bargmann and Avery, 1995). Owing to the transparent nature, development of protein fusion tags and possibility of ablating cells, *C.elegans* has become an exciting model for studying organ morphongenesis. Embryonic morphogenesis is a well-studied process in *C.elegans* development. I will take a short look over important aspects of embryonic morphogenesis and vulval morphogenesis.

1.5 Embryonic morphogenesis in *C.elegans*: important lessons

1.5.1. Late embryogenesis: an overview

The first step in *C.elegans* morphogenesis is rearrangement of the three germ layers during gastrulation. First, the two ectoderm-precursor cells move from ventral surface to the interior of the embryo termed as endodermal ingression. These cells are followed by mesoderm and germline precursor cells one after another until one third of the embryonic cells are internalized. There is a gap left behind by these mass ingression of cells called as "gastrulation cleft". The neuronal precursor cells fill in this cleft. After gastrulation the hypodermal (epidermal) cells of the embryo are arranged in dorsal, lateral and ventral lines on each side of the dorsal surface of the embryo. The dorsal line of cells undergoes intercalation, wherein two lines merge to form a single and long row of cells on the dorsal surface of the embryo (Figure 1.4c). Post intercalation, ventral closure of the embryo takes place. During ventral closure, the anterior pair of ventral hypodermal cells migrate from each side of the embryo to meet on the ventral surface followed by the elongation of hypodermal cells towards ventral midline, which finally leads to closure of the ventral pocket (Figure 1.4d). After ventral closure, the embryo elongates by acto-myosin mediated contraction of circumferential actin-bundles in the hypodermis, squeezing the worm in dorso-ventral axis and leading to four-fold elongation in anterio-posterior axis (Figure 1.4e). In all of the above-mentioned morphogenesis events, actin cytoskeleton plays an important role. It becomes very

important to study the way actin generates mechanical forces and also how this force generating machinery is regulated. The two major force generating events driving morphogenesis are “protrusive events” and “contractile events”.

1.5.2. Protrusive events: polymerization of actin drives embryonic morphogenesis

Actin polymerization results into formation of microfilaments, which culminates into the movement of cells in forward direction. Biochemical studies showed that the formation of actin filaments require Arp2/3 complex. Polymerization and nucleation of these filaments lead to the formation of lamellae and filopodia, which have the capability to ratchet the plasma membrane forward. These filaments are bundled or cross-linked into 3D structures, which provide the very basis of morphogenesis.

Several factors ensure the proper migration of epidermal cells towards the ventral midline. One such factor is the Arp2/3 complex (Sawa et al., 2003). The Arp2/3 complex is composed of seven subunits: Arp3, Arp2, p41Arc, p34Arc, p21Arc, p20Arc, and p16Arc (Winter et al., 1999). Study in several systems have revealed a role for the Arp2/3 complex in actin polymerization (Pantaloni et al., 2001), and the activation of the complex is accomplished through binding of members of the WASP family (Machesky et al., 1999). Individual knock-down of each Arp2/3 subunit in *C.elegans* yields similar defects in ventral migration of epidermal cells (Sawa et al., 2003). In addition, *C.elegans* WASP members are also necessary for proper epidermal ventral enclosure (Sawa et al., 2003). The cadherin/catenin system has been involved in several processes including *C.elegans* ventral enclosure in *C.elegans* (Raich et al., 1999). Cadherin is responsible for cell-cell adhesion and functions in a calcium-dependent manner (Haussinger et al., 2002). The extracellular domain of the protein is responsible for calcium binding whereas the intracellular region indirectly associates with actin through a connected protein complex composed of three types of catenins: α, β, and γ (Pettitt, 2005). *C.elegans* cadherin gene *hmr- 1*, or catenin genes *hmp-1* and *hmp-2* deficient animals exhibit defects in ventral enclosure (Raich et al., 1999). In these mutant embryos, epidermal extensions reach the ventral midline but fail to attach to one another, leading to the rupture of internal contents. *apr-1* is a third catenin gene which also affects epidermal enclosure, in addition to its role in Wnt signalling in the regulation of gene expression (Hoier et al., 2000).

Upstream regulators such as the Rho family GTPases Rac and Cdc42 act to regulate their downstream components such as Arp2/3, WASp (Wiskott-Aldrich syn- drome protein), WIP (WASP-interacting protein) and WAVE (WASP family verprolin- homologous protein) to

coordinate new actin polymerization and the formation of these protrusive structures (Jaffe and Hall, 2005). Regulation of intracellular calcium levels is important for the formation of the protrusive actin structures, because depletion of inositol 1,4,5-tripho-sphate receptor reduces formation of filopodia and lamella in the migrating ventral hypodermal cells and prevents ventral enclosure (Thomas-Virnig et al., 2004).

During *C.elegans* embryonic morphogenesis, protrusive events are important for the initial epibolic migrations of the anterior ventral hypodermis around
the ventral surface of the embryo also known as ventral closure (Figure 1.4d); the closure of the gastrulation cleft by neuroblasts (Figure 1.4b); and the intercalation of the dorsal hypodermal cells (Figure 1.4c). *C.elegans* Rac *ced-10*, WSP-1, WVE-1, GEX-2 and GEX-3 deficient animals show defect in ventral closure (Soto et al., 2002). WVE-1,WSP-1,UNC-34 (*C.elegans* homologue of Ena) deficient animals show impaired migration of neuroblasts during gastrulation cleft closure (Bear et al., 2002). The *C.elegans* ephrin receptor receptor *vab-1* and its ligands *vab-2, efn-2, efn-3* and *efn-4* positively regulate ventral closure and gastrulation cleft closure (Chin-Sang et al., 1999; Chin-Sang et al., 2002). Two other *C.elegans* receptors, the LAR-like receptor tyrosine phosphatase *ptp-3* and the Robo receptor *sax-3*, together with *vab-1* regulate epidermal morphogenesis (Harrington et al., 2002), (Ghenea et al., 2005). Also, the semaphorin gene *mab-20*, which encodes a secreted ligand, binds to its transmembrane receptor (encoded by the *plx-2* gene) to direct neuroblast movement (Nakao et al., 2007). The ephrin gene *efn-4* acts redundantly with *ptp-3* (Harrington et al., 2002) and *mab-20*/*plx-2* (Nakao et al., 2007) during morphogenesis.

1.5.3. Contractile events: actomyosin contraction drives embryonic morphogenesis

Contractile or pulling force is generated by existing actin meshwork and the motor protein myosin (Reedy, 2000). Factors affecting the formation of actin filament and myosin II motors play an important role during acto-myosin driven contraction with later having more significant role. Myosin II contains a pair of heavy chains (NMY-2) and two pairs of light chains. The first pair of light chains (known as regulatory light chains, or MLC- 4 in the *C.elegans* early embryo) can be phosphorylated at serine 18 leading to increase in the actin binding affinity and motor activity of myosin (Somlyo and Somlyo, 2003). In *C.elegans,* endodermal ingression and embryonic elongation are governed by actomyosin-mediated contraction. At the 28-cell stage the two endoderm-precursors located on the ventral surface of the embryo start to ingress into the embryonic interior, becoming completely enclosed by their neighbors. The ingressing cells show an apical accumulation of the myosin II heavy-

chain protein NMY-2 (non-muscle myosin II) just before and during the cell movements (Figure 1.4a) (Nance and Priess, 2002). Phosphorylated myosin is shown to be present in the apical domain of the ingressing endoderm-precursors, confirming that myosin is activated during gastrulation by Wnt signaling pathway (Rohrschneider and Nance, 2009). After the completion of ventral closure the final contractile event of *C.elegans* morphogenesis takes place.

The contraction of circumferential actin bundles within the hypodermis squeezes the bean-shaped embryo leading to a four-fold increase in its length with simultaneous decrease in the circumference (Figure 1.4e) (Priess and Hirsh, 1986). Circumferential Actin Bundles (CFBs) are formed in the lateral seam cells and anchored by adherens junctions (Labouesse, 1997). *C.elegans* spectrin proteins such as SMA-1 and SPC-1, connect the CFBs to the adherens junctions (McKeown et al., 1998; Norman and Moerman, 2002). The cadherin/catenin complex of HMP-1, HMP-2 and HMR-1 co-localize to adherens junctions and are necessary for the anchoring of CFBs to the junctions (Costa et al., 1998). The loss of this complex results in defective embryonic elongation (Costa et al., 1998). The proper localization and function of the adherens junction requires the inputs of at least three crucial regulators: LET-413, DLG-1 and AJM-1. The GTPase adaptor-like protein LET-413 regulates epidermal cell polarity, whereas in let-413 mutants adherens junctions are localized to the basolateral instead of the apical side of the membrane (Legouis et al., 2000). LET-413 also regulates the proper apical localization of two other adherens junction proteins: DLG-1 and AJM-1 (McMahon et al., 2001). *C.elegans* DLG-1, a MAGUK membrane-associated guanylate kinase-family scaffolding protein, as well as the novel adherens junction-associated protein AJM-1, are necessary for proper cell-cell contact during the contraction mediated elongation (Bossinger et al., 2001; Firestein and Rongo, 2001; Koppen et al., 2001). During elongation, LET-502 Rho-kinase and MEL-11 myosin phosphatase act antagonistically to regulate phosphorylation of MLC-4 to regulate the contractile state of the actin bundles. Zygotic null of MEL-11 results into striking hyper-elongation of the embryo (Piekny et al., 2000; Wissmann et al., 1999; Wissmann et al., 1997). The serine–threonine kinase, LET- 502 is required to activate MLC-4 and *LET-502* zygotic null embryos fail to elongate (Piekny et al., 2000; Wissmann et al., 1999; Wissmann et al., 1997). Its predicted that LET- 502 might directly phosphorylate MLC-4 and thereby activate contraction. Alternatively, LET-502 can phosphorylate MEL-11, which in turn can activate MLC-4 and thus elongation indirectly by sequestering the MEL-11

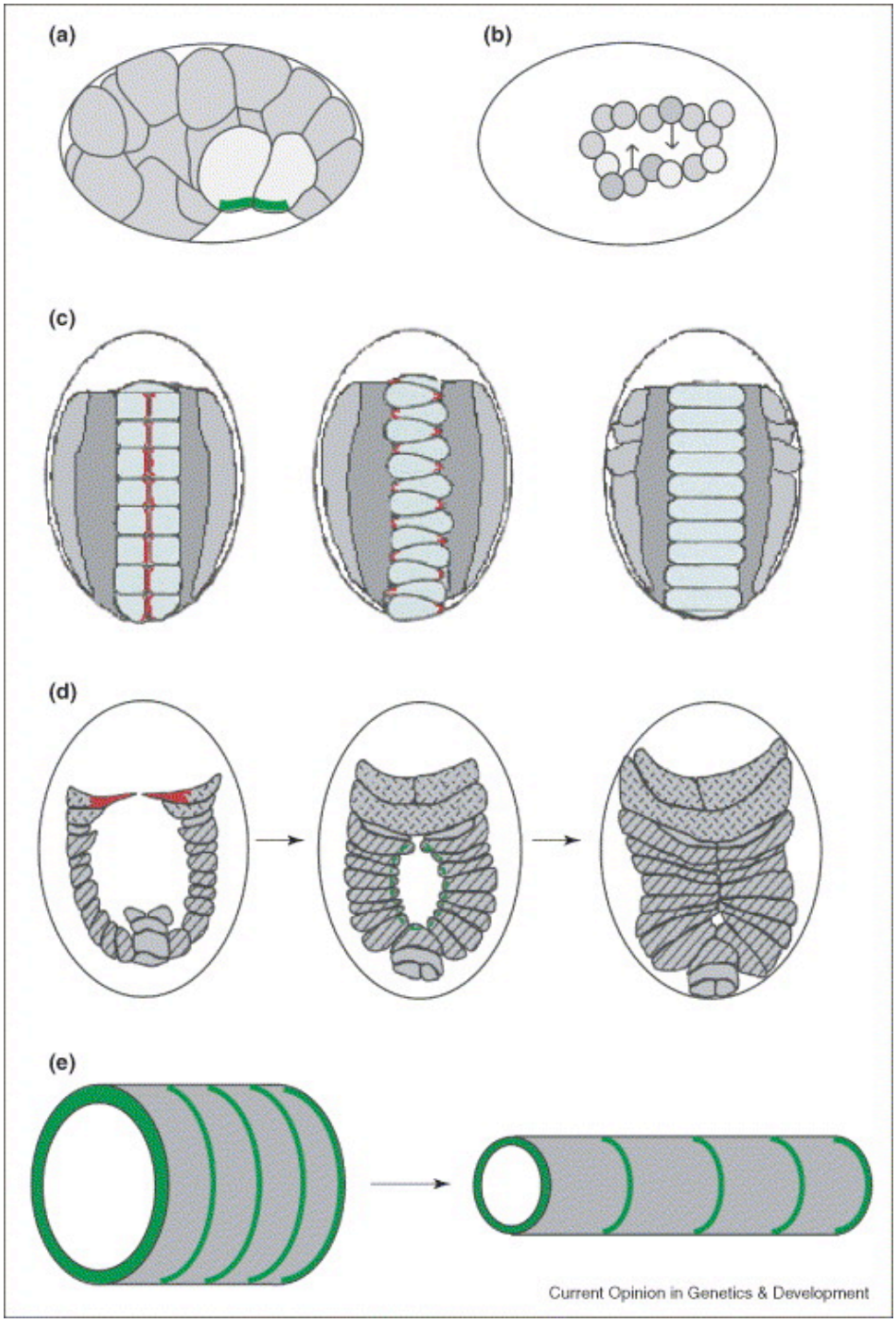

Figure 1.4 Overview of *C.elegans* embryonic morhogenesis. (A-C) dorsal view of the embryo. Dorsal intercalation involves wedging of epidermal cells together forming a single row. (D-F) These embryo illustrations depict the ventral side of the embryo. During ventral enclosure, contralateral rows of epidermal cells migrate from the dorsal side of the embryo towards the ventral side and then attach. (G-H) During the elongation phase, epidermal cells contract and form the tube-like formation of the worm. (Adapted from (Marston and Goldstein 2002)).

phosphatase away from the contraction site (Piekny et al., 2003). Embryos lacking both MEL-11 and *LET-502* elongate normally and develop further, beautfiully suggests that these

proteins antagonize each other (Piekny et al., 2003; Piekny et al., 2000; Wissmann et al., 1999; Wissmann et al., 1997). The fact that these double embryos still complete elongation shows that there must be an additional, unidentified myosin light-chain kinase. Recently, RGA-2 was proposed to be a RhoGAP for Rho-1, which plays important role during embryonic elongation (Diogon et al., 2007). Other genes showing weak phenotypes include the PP2c phosphatase fem-2, the Rho GTPases ced-10 (Rac-like) and mig-2 (Rho/Rac-like), the PI3 kinase age-1, and the insulin receptor daf-2 (Piekny et al., 2000; Wissmann et al., 1999). The downstream affectors of Rho signaling pathway during morphogenesis, are well characterized but the upstream transcriptional regulators are yet to be explored.
Embryonic development has served as an important but, owing to high saturation in research at this stage of worm development, a new model organ needs to be established for studying morphogenesis. Here we used vulval development as a model for studying various aspects of morphogenesis.

1.6 *C.elegans* vulval development: a model for organogenesis

Vulval development of the *C.elegans* hermaphrodite can be divided into three steps. First, the epithelial VPCs (Vulval Precursor Cells) are generated. Secondly, a specialized gonadal cell called the Anchor Cell (AC) triggers vulval patterning and development. Thirdly, the morphogenesis or execution of the cell fates which includes eversion after divisions to form the mature vulva (Figure 1.5) (Sternberg, 2005).

1.6.1. Vulval induction and patterning

Vulval cells are derived from the P cell lineage (HR, 1977).A group of 12 P cells migrate from the lateral sides of the worm to the ventral side during the L1 stage. After cell migration, the P cells divide along the anterior-posterior axis. As a result, 12 anterior P cells (Pn.a) are formed which differentiate into neuronal cells, while 12 posterior P cells (Pn.p) form epidermal cells (HR, 1977). During the L2 stage, the 12 epidermal Pn.p cells get aligned along the ventral midline. From these cells, P3.p to P8.p form equipotent Vulval precursor cells (VPCs) and the remaining cells, P1.p, P2.p and P9-12.p, fuse with the surrounding hypodermal syncitium hyp7. The six VPCs become equipotent to adopt a vulval fate by expressing the Hox factor LIN-39, which blocks their fusion to hyp7 (Clark et al., 1993). Vulval development is triggered by a secreted signal originating from the somatic gonadal AC in the form of LIN-3 EGF (Figure 1.5A) (Hill and Sternberg, 1992).

1.6.2. The EGFR/RAS/MAPK pathway promotes the 1° vulval cell fate

The AC is located on the dorsal side of P6.p and produces the epidermal growth factor (EGF) orthologue LIN-3 (Hill RJ, 1992), which binds and activates the epidermal growth factor receptor (EGFR) orthologue LET-23. While LET-23 is expressed in all VPCs, P6.p (the VPC closest to the AC) receives the highest level of LIN-3 ligand (figure 1.5A). Primarily P6.p sequesters LIN-3, but it is also thought to be distributed gradually in the extracellular space, resulting into activation of LET-23 in the remaining VPCs to a lesser extent (Katz et al., 1995; Sternberg and Horvitz, 1986). Binding of LIN-3 to LET-23 activates the evolutionary conserved Ras/MAPK pathway by similar mechanisms as found in mammalian systems (figure 1.5A). Firstly, ligand binding leads to the dimerization and autophosphorylation of the receptor. This generates docking sites for the adaptor proteins like SEM-5 Grb2 (Clark et al., 1992). Subsequent recruitment of SOS-1 (Chang C, 2000), the RasGEF, leads to the activation of LET-60 RAS (Beitel GJ, 1990) at peripherical membranes. As a result, the phosphorylation cascade of LIN-45/Raf (Han M, 1993), MEK- 2/MEK (Kornfeld K, 1995; Wu Y, 1995) and MPK-1/ERK (Lackner MR, 1994) is triggered. Activated MPK-1 translocates to the nucleus to phosphorylate different targets, including transcription factors, which control the expression of genes underlying the primary (1°) vulval fate (Sundaram et al., 2006). Two well characterized targets of MPK-1 are LIN-1, a transcription factor of the Ets family (Beitel GJ, 1995) and LIN-31, a member of the forkhead family of transcription factors (Miller LM, 1993). *lin-31* and *lin-1* act downstream of *mpk-1*, and both proteins can be directly phosphorylated by MAP kinase. LIN-31 binds to LIN-1, and the LIN-1/LIN-31 complex inhibits vulval induction. Phosphorylation of LIN-31 and LIN-1 by MPK-1 disrupts the LIN-1/ LIN-31 complex, relieving vulval inhibition (Tan et al., 1998). Phosphorylated LIN-31 may also act as a transcriptional activator, promoting vulval cell fates. LIN-31 is a vulval specific effector of MPK-1, while LIN-1 acts as a general effector (Tan et al., 1998). The partnership of tissue-specific and general effectors may confer specificity onto commonly used signaling pathways, creating distinct tissue-specific outcomes. The transcriptional targets of the LET-23 pathway include the gene *egl-17*, which encodes the *C.elegans* orthologue of the fibroblast growth factor FGF (Burdine RD, 1998) and *lag-2*, which represents a Delta-like Notch ligand (Chen N, 2004).

1.6.3. The LIN-12 Notch pathway promotes the 2° vulval cell fate

The gene *lag-2,* is one of the downstream targets of LET-23 pathway (Chen N, 2004) that encodes a transmembrane ligand specific for LIN-12/Notch (figure 2a and

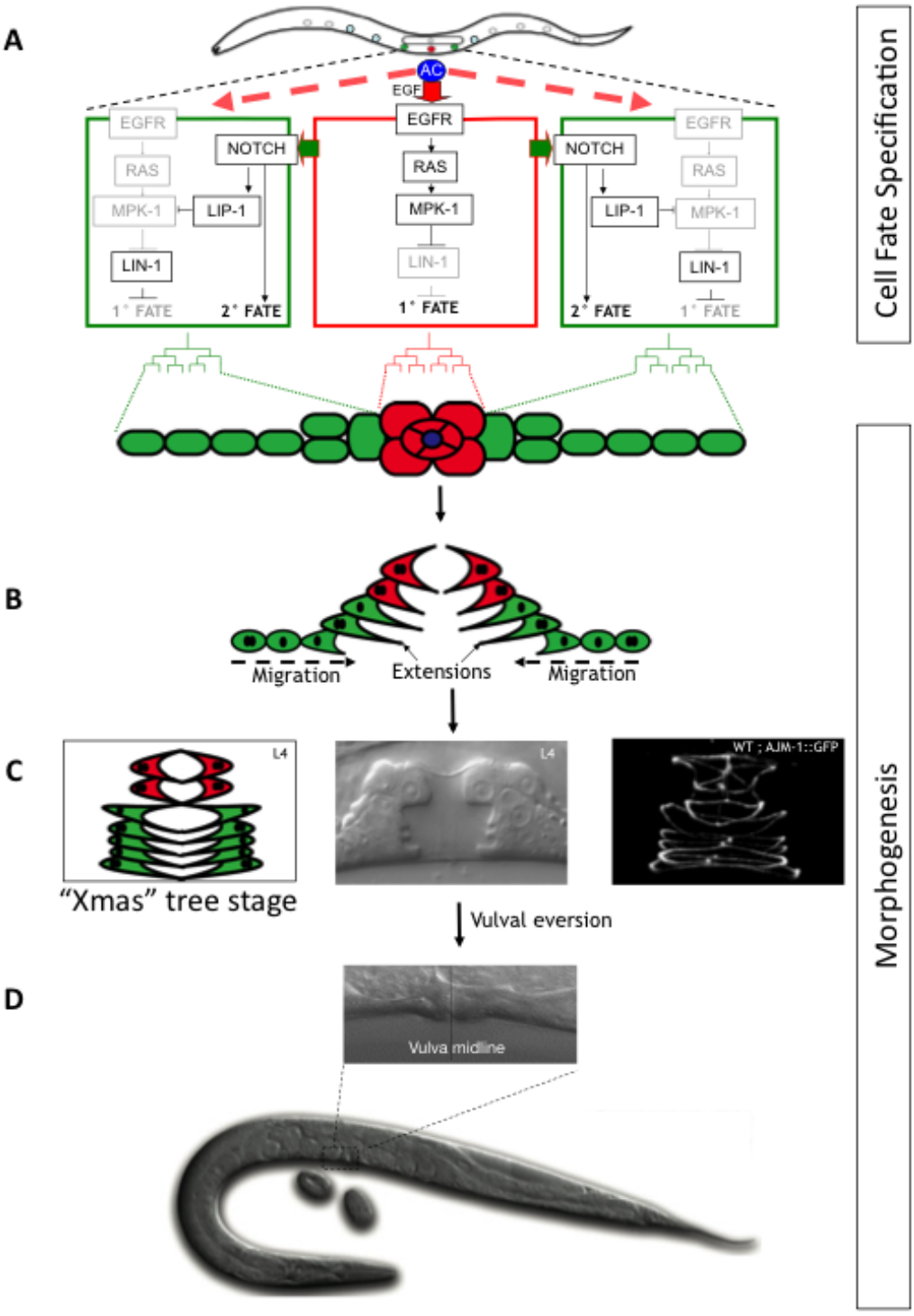

Figure 1.5. Vulval development in a nutshell. (A) Induction takes place following the establishment of the vulva equivalence group. During this stage, a signal derived from the anchor cell (A-C), located in the somatic gonad, instructs the cells to adopt a vulval cell fate. Once induced, P5.p-P7.p divide three times. (B) Following the final divisions, vulval cells begin to invaginate. (B-C) In the L4 worm, cell migration, attachment and fusion result in the formation of toroid rings, giving rise to the characteristic "Christmas tree" stage of vulva development. (D) The invaginated vulva then everts during early adulthood giving rise to the functional vulva.

(Shaye DD, 2005)). After, P6.p is induced, the LAG-2 ligand activates LIN-12 on the neighbouring VPCs P5.p and P7.p (Shaye DD, 2005). Activated LIN-12 is proteolytically processed at the plasma membrane and the intracellular domain subsequently translocates into the nucleus. In the nucleus it controls the expression of a variety of target genes together with the protein LAG-1 CSL (Shaye DD, 2005). The LIN-12 target genes are believed to encode either factors responsible to adopt the secondary (2°) vulval fate or inhibitors of the LET-23 pathway (figure 1.5 and (Berset T, 2001; Yoo AS, 2004)). As mentioned above, the LET-23 pathway is responsible for the establishment of the primary vulval fate. The LIN-12 pathway is crucial to inhibit the LET-23 pathway and therefore the primary vulval fate in P5.p and P7.p.

1.6.4. Negative regulator of MPK-1 signaling

As mentioned above, the LIN-12 pathway is activated in P5.p and P7.p to inhibit the primary vulval fate in these cells. One of the key players in this lateral inhibition is LIP-1 (Lateral induced phosphatase) (Berset T, 2001). *lip-1* is a direct target of the LIN-12 pathway (figure 1.5A , (Berset T, 2001)). It has been shown that LIP-1 interacts directly with and dephosphorylates MPK-1, which renders it inactive (Berset T, 2001). LIP-1 is mainly active in secondary VPCs, where it inhibits the LET-23 pathway at the level of MPK-1 and simultaneously the 1° vulval fate (Berset T, 2001). Transcription of other negative regulators of the LET-23 pathway have been found to be regulated by LIN-12, such as *ark-1*, *dpy-23*, *lst-1*, *lst-2*, *lst-3* and *lst-4* (Yoo AS, 2004). Also Yoo *et al* showed that a microRNA gene, *mir-61*, is a direct transcriptional target of LIN-12 and expression of *mir-61* promotes the 2° fate. They identified *vav-1*, the ortholog of the Vav oncogene, as a target of *mir-61*, and showed that down-regulation of VAV-1 promotes *lin-12* activity in specifying the 2° fate. Thus, *lin-12, mir-61*, and *vav-1* form a feedback loop which helps maximize *lin-12* activity in the presumptive 2° VPCs (Yoo and Greenwald, 2005).
These studies show that a sophisticated crosstalk between the LET-23 and the LIN-12 pathway controls the patterning of the vulval cells.

1.6.5. 1° cell fate specification is postively regulated by the small GTPase RHO-1

Canevascini et al. (2005) showed that Rho signalling positively regulates vulval development. Gain-of-function of *ect-2*, a gene encoding a RhoGEF (Guanine nucleotide exchange factor), exhibits a Multivulva phenotype in combination with a loss-of-function

allele of *gap-1*. The ubiquitous expression of a dominant negative form of RHO-1 was sufficient to neutralize the effects provoked by the *ect-2(gf)* allele. Furthermore, it was found that ECT-2 most likely represents the GEF for RHO-1 and that this pathway feeds either upstream or at the level of the RasGEF SOS-1 (Canevascini et al., 2005).

1.6.6. Morphogenesis of the vulva

Both 1° and 2° vulval lineages undergo three rounds of cell divisions Pn.p (1celled), Pnp.x (2 celled), Pnp.xx (4celled), Pnp.xxx (8celled) stage) (Figure 1.5A). P6.p gives rise to 8 descendants and P5.p and P7.p each give rise to 7 descendants. In the early L4 stage, The AC from the gonad invades vulval epithelium (Sherwood DR, 2005) and the 1° vulval cells detach from the cuticule and move dorsally, which induces the invagination of the vulval tissue. The 2° vulval cells follow their neighbouring primary cells. Vulval cells undergo migration, elongation and fusion resulting in the mid L4 stage shape called as the "Christmas Tree" stage (Figure 1.5 B,C). It is a symmetrical structure, where the primary cells make the upper building block of the "tree" and the secondary cells form the lateral branches of the "tree". Subsequent homotypic fusion of the vulval cells lead to a stack of vulval rings (toroids) (Figure 1.5C) (Sharma-Kishore R, 1999). After the formation of "Christmas Tree" vulva undergoes eversion to form a tubular structure connecting the uterine tissue to the exterior of the worm resulting into fully developed egg-laying apparatus (Figure 1.5C). The force contribution of 1°, 2° or AC for making a complete 'Christmas tree' stage are largely unknown.

Vulval development is very sensitive to changes in gene function and these changes are clearly visible in the Christmas tree stage vulva. Much is known about the molecular events determining early vulva cell fates but very less is known about how these fates are executed and how these cells are rearranged into a functional organ. After initial patterning of cells, vulval morphogenesis begins, the linearly arranged 22 cells undergo the migration, elongation and fusion of vulval cells to form the ring-like toroids (Figure 1.5 C) (Sharma-Kishore R, 1999; Shemer et al., 2000). Among the genes plexin and semaphorin are directly involved in *C.elegans* vulval morphogenesis (Dalpe et al., 2005). The ligand semaphorin and its receptor plexin act as guidance cues during neurogenesis (Nakamura et al., 2000). In *C.elegans* plexin, *plx-1*, and semaphorin, *smp-1*, are responsible for the migration of the vulval cells toward the midline of the worm (Dalpe et al., 2004). The *sqv* genes, which regulate the synthesis of glycosaminoglycans, are also important for the adhesion of vulva

cells to the basal lamina (Bulik et al., 2000; Herman et al., 1999; Hwang and Horvitz, 2002). Also, the novel protein EGL-26 regulates the proper morphology of VulF, a P6.p descendant (Hanna-Rose and Han, 2002). Additionally, *C.elegans par-1*, a gene involved in establishing cell polarity which is necessary for asymmetric cell divisions, is involved in vulval toroid formation (Hurd and Kemphues, 2003). A complex gene regulatory network was found to coordinate vulva morphogenesis (Fernandes and Sternberg, 2007). This network includes genes already described in having roles during morphogenesis like *cog-1* (Palmer et al., 2002), *lin-11* (Newman et al., 1999) and *egl-38* (Chang et al., 1999). Two components of the synMuv pathway (*lin-40* and *lin*-35) have established roles in vulva morphogenesis in addition to regulating vulva cell fate decisions (Bender et al., 2007; Chen and Han, 2001).

Cell signalling is not only necessary during early vulva development but in later stages of morphogenesis too. The Rac-encoding gene *ced-10*, the Rac-related gene *mig-2* and the *Trio*-like GEF *unc-73* are required for proper orientation of vulva cells during division and migration (Kishore RS, 2002). It is thought that *ced-10* acts downstream of the semaphorin/plexin genes *smp-1* and *plx-1*, with *mig-2* and *unc-73* acting in parallel (Dalpe et al., 2004). While there is an established role for the Rho family of GTPases, *ced-10* Rac and *cdc-42*, *rho-1* have received considerably less attention. Also, little is known about the role of Notch and Ras signaling targets, which are specifically involved in executing proper vulva morphogenesis. An in-silico screen for finding out Notch target genes has been done to uncover potential targets, but invivo follow up of the interesting candidates has been done only for the genes involved in cell fate specifications (Yoo AS, 2004). Thus the role of Notch and Ras signaling pathway during morphogenesis is an unexplored territory.

References:

Adams, J. M. (2003). Ways of dying: multiple pathways to apoptosis. *Genes Dev* **17**, 2481-95.

Andrew, D. J. and Ewald, A. J. (2010). Morphogenesis of epithelial tubes: Insights into tube formation, elongation, and elaboration. *Dev Biol* **341**, 34-55.

Bar, T. and Wolff, J. R. (1972). The formation of capillary basement membranes during internal vascularization of the rat's cerebral cortex. *Z Zellforsch Mikrosk Anat* **133**, 231-48.

Bargmann, C. I. and Avery, L. (1995). Laser killing of cells in Caenorhabditis elegans. *Methods Cell Biol* **48**, 225-50.

Bear, J. E., Svitkina, T. M., Krause, M., Schafer, D. A., Loureiro, J. J., Strasser, G. A., Maly, I. V., Chaga, O. Y., Cooper, J. A., Borisy, G. G. et al. (2002). Antagonism between Ena/VASP proteins and actin filament capping regulates fibroblast motility. *Cell* **109**, 509-21.

Beitel GJ, C. S., Horvitz HR. (1990). Caenorhabditis elegans ras gene let-60 acts as a switch in the pathway of vulval induction. *Nature* **348**, 503-9.

Beitel GJ, T. S., Greenwald I, Horvitz HR. (1995). The Caenorhabditis elegans gene lin-1 encodes an ETS-domain protein and defines a branch of the vulval induction pathway. *Genes and Development* **9**, 3149-62.

Bender, A. M., Kirienko, N. V., Olson, S. K., Esko, J. D. and Fay, D. S. (2007). lin-35/Rb and the CoREST ortholog spr-1 coordinately regulate vulval morphogenesis and gonad development in C. elegans. *Dev Biol* **302**, 448-62.

Berset T, H. E., Battu G, Canevascini S, Hajnal A. (2001). Notch inhibition of RAS signaling through MAP kinase phosphatase LIP-1 during C. elegans vulval development. *Science* **291**, 1055-8.

Bossinger, O., Klebes, A., Segbert, C., Theres, C. and Knust, E. (2001). Zonula adherens formation in Caenorhabditis elegans requires dlg-1, the homologue of the Drosophila gene discs large. *Dev Biol* **230**, 29-42.

Bulik, D. A., Wei, G., Toyoda, H., Kinoshita-Toyoda, A., Waldrip, W. R., Esko, J. D., Robbins, P. W. and Selleck, S. B. (2000). sqv-3, -7, and -8, a set of genes affecting morphogenesis in Caenorhabditis elegans, encode enzymes required for glycosaminoglycan biosynthesis. *Proc Natl Acad Sci U S A* **97**, 10838-43.

Burdine RD, B. C., Stern MJ. (1998). EGL-17(FGF) expression coordinates the attraction of the migrating sex myoblasts with vulval induction in C. elegans. *Development* **125**, 1083-93.

Cabernard, C. and Affolter, M. (2005). Distinct roles for two receptor tyrosine kinases in epithelial branching morphogenesis in Drosophila. *Dev Cell* **9**, 831-42.

Canevascini, S., Marti, M., Frohli, E. and Hajnal, A. (2005). The Caenorhabditis elegans homologue of the proto-oncogene ect-2 positively regulates RAS signalling during vulval development. *EMBO Rep* **6**, 1169-75.

Caussinus, E., Colombelli, J. and Affolter, M. (2008). Tip-cell migration controls stalk-cell intercalation during Drosophila tracheal tube elongation. *Curr Biol* **18**, 1727-34.

Chang C, H. N., Sternberg PW. (2000). Caenorhabditis elegans SOS-1 is necessary for multiple RAS-mediated developmental signals. *The EMBO Journal* **19**, 3283-94.

Chang, C., Newman, A. P. and Sternberg, P. W. (1999). Reciprocal EGF signaling back to the uterus from the induced C. elegans vulva coordinates morphogenesis of epithelia. *Curr Biol* **9**, 237-46.

Chen N, G. I. (2004). The lateral signal for LIN-12/Notch in C. elegans vulval development comprises redundant secreted and transmembrane DSL proteins. *Developmental Cell* **6**, 183-92.
Chen, Z. and Han, M. (2001). Role of C. elegans lin-40 MTA in vulval fate specification and morphogenesis. *Development* **128**, 4911-21.
Chin-Sang, I. D., George, S. E., Ding, M., Moseley, S. L., Lynch, A. S. and Chisholm, A. D. (1999). The ephrin VAB-2/EFN-1 functions in neuronal signaling to regulate epidermal morphogenesis in C. elegans. *Cell* **99**, 781-90.
Chin-Sang, I. D., Moseley, S. L., Ding, M., Harrington, R. J., George, S. E. and Chisholm, A. D. (2002). The divergent C. elegans ephrin EFN-4 functions inembryonic morphogenesis in a pathway independent of the VAB-1 Eph receptor. *Development* **129**, 5499-510.
Clark, S. G., Chisholm, A. D. and Horvitz, H. R. (1993). Control of cell fates in the central body region of C. elegans by the homeobox gene lin-39. *Cell* **74**, 43-55.
Clark, S. G., Stern, M. J. and Horvitz, H. R. (1992). Genes involved in two Caenorhabditis elegans cell-signaling pathways. *Cold Spring Harb Symp Quant Biol* **57**, 363-73.
Colas, J. F. and Schoenwolf, G. C. (2001). Towards a cellular and molecular understanding of neurulation. *Dev Dyn* **221**, 117-45.
Consortium, T. C. e. G. S. (1998). Genome sequence of the nematode C. elegans: A platform for investigating biology. *Science* **282**, 2012-18.
Costa, M., Raich, W., Agbunag, C., Leung, B., Hardin, J. and Priess, J. R. (1998). A putative catenin-cadherin system mediates morphogenesis of the Caenorhabditis elegans embryo. *J Cell Biol* **141**, 297-308.
Dalpe, G., Brown, L. and Culotti, J. G. (2005). Vulva morphogenesis involves attraction of plexin 1-expressing primordial vulva cells to semaphorin 1a sequentially expressed at the vulva midline. *Development* **132**, 1387-400.
Dalpe, G., Zhang, L. W., Zheng, H. and Culotti, J. G. (2004). Conversion of cell movement responses to Semaphorin-1 and Plexin-1 from attraction to repulsion by lowered levels of specific RAC GTPases in C. elegans. *Development* **131**, 2073-88.
Danial, N. N. and Korsmeyer, S. J. (2004). Cell death: critical control points. *Cell* **116**, 205-19.
de la Pompa, J. L., Wakeham, A., Correia, K. M., Samper, E., Brown, S., Aguilera, R. J., Nakano, T., Honjo, T., Mak, T. W., Rossant, J. et al. (1997). Conservation of the Notch signalling pathway in mammalian neurogenesis. *Development* **124**, 1139-48.
Diogon, M., Wissler, F., Quintin, S., Nagamatsu, Y., Sookhareea, S., Landmann, F., Hutter, H., Vitale, N. and Labouesse, M. (2007). The RhoGAP RGA-2 and LET-502/ROCK achieve a balance of actomyosin-dependent forces in C. elegans epidermis to control morphogenesis. *Development* **134**, 2469-79.
Fernandes, J. S. and Sternberg, P. W. (2007). The tailless ortholog nhr-67 regulates patterning of gene expression and morphogenesis in the C. elegans vulva. *PLoS Genet* **3**, e69.
Firestein, B. L. and Rongo, C. (2001). DLG-1 is a MAGUK similar to SAP97 and is required for adherens junction formation. *Mol Biol Cell* **12**, 3465-75.
Ghabrial, A. S. and Krasnow, M. A. (2006). Social interactions among epithelial cells during tracheal branching morphogenesis. *Nature* **441**, 746-9.
Ghenea, S., Boudreau, J. R., Lague, N. P. and Chin-Sang, I. D. (2005). The VAB-1 Eph receptor tyrosine kinase and SAX-3/Robo neuronal receptors function together during C. elegans embryonic morphogenesis. *Development* **132**, 3679-90.
Han M, G. A., Han Y, Sternberg PW. (1993). C. elegans lin-45 raf gene participates in let-60 ras-stimulated vulval differentiation. *Nature* **363**, 133-40.

Hanna-Rose, W. and Han, M. (2002). The Caenorhabditis elegans EGL-26 protein mediates vulval cell morphogenesis. *Dev Biol* **241**, 247-58.
Harrington, R. J., Gutch, M. J., Hengartner, M. O., Tonks, N. K. and Chisholm, A. D. (2002). The C. elegans LAR-like receptor tyrosine phosphatase PTP-3 and the VAB-1 Eph receptor tyrosine kinase have partly redundant functions in morphogenesis. *Development* **129**, 2141-53.
Haussinger, D., Ahrens, T., Sass, H. J., Pertz, O., Engel, J. and Grzesiek, S. (2002). Calcium-dependent homoassociation of E-cadherin by NMR spectroscopy: changes in mobility, conformation and mapping of contact regions. *J Mol Biol* **324**, 823-39.
Hengartner, M. O. and Horvitz, H. R. (1994). Programmed cell death in Caenorhabditis elegans. *Curr Opin Genet Dev* **4**, 581-6.
Herman, T., Hartwieg, E. and Horvitz, H. R. (1999). sqv mutants of Caenorhabditis elegans are defective in vulval epithelial invagination. *Proc Natl Acad Sci U S A* **96**, 968-73.
Hill RJ, S. P. (1992). The gene lin-3 encodes an inductive signal for vulval development in C. elegans. *Nature* **358**, 470-6.
Hill, R. J. and Sternberg, P. W. (1992). The gene lin-3 encodes an inductive signal for vulval development in C. elegans. *Nature* **358**, 470-6.
Hoier, E. F., Mohler, W. A., Kim, S. K. and Hajnal, A. (2000). The Caenorhabditis elegans APC-related gene apr-1 is required for epithelial cell migration and Hox gene expression. *Genes Dev* **14**, 874-86.
Horvitz, H. R. (2003). Worms, life, and death (Nobel lecture). *Chembiochem* **4**, 697-711.
HR, S. J. a. H. (1977). Post-embryonic cell lineages of the nematode, Caenorhabditis elegans. *Developmental Biology* **56**, 110-56.
Hurd, D. D. and Kemphues, K. J. (2003). PAR-1 is required for morphogenesis of the Caenorhabditis elegans vulva. *Dev Biol* **253**, 54-65.
Hwang, H. Y. and Horvitz, H. R. (2002). The SQV-1 UDP-glucuronic acid decarboxylase and the SQV-7 nucleotide-sugar transporter may act in the Golgi apparatus to affect Caenorhabditis elegans vulval morphogenesis and embryonic development. *Proc Natl Acad Sci U S A* **99**, 14218-23.
Iso, T., Kedes, L. and Hamamori, Y. (2003). HES and HERP families: multiple effectors of the Notch signaling pathway. *J Cell Physiol* **194**, 237-55.
Jaffe, A. B. and Hall, A. (2005). Rho GTPases: biochemistry and biology. *Annu Rev Cell Dev Biol* **21**, 247-69.
Katz, W. S., Hill, R. J., Clandinin, T. R. and Sternberg, P. W. (1995). Different levels of the C. elegans growth factor LIN-3 promote distinct vulval precursor fates. *Cell* **82**, 297-307.
Kishore RS, S. M. (2002). ced-10 Rac and mig-2 function redundantly and act with unc-73 trio to control the orientation of vulval cell divisions and migrations in Caenorhabditis elegans. *Developmental Biology* **241**, 339-348.
Koppen, M., Simske, J. S., Sims, P. A., Firestein, B. L., Hall, D. H., Radice, A. D., Rongo, C. and Hardin, J. D. (2001). Cooperative regulation of AJM-1 controls junctional integrity in Caenorhabditis elegans epithelia. *Nat Cell Biol* **3**, 983-91.
Kornfeld K, G. K., Horvitz HR. (1995). The Caenorhabditis elegans gene mek-2 is required for vulval induction and encodes a protein similar to the protein kinase MEK. *Genes and Development* **9**, 756-68.
Krebs, L. T., Xue, Y., Norton, C. R., Shutter, J. R., Maguire, M., Sundberg, J. P., Gallahan, D., Closson, V., Kitajewski, J., Callahan, R. et al. (2000). Notch signaling is essential for vascular morphogenesis in mice. *Genes Dev* **14**, 1343-52.
Labouesse, M. (1997). Deficiency screen based on the monoclonal antibody MH27 to identify genetic loci required for morphogenesis of the Caenorhabditis elegans embryo. *Dev Dyn* **210**, 19-32.

Lackner MR, K. K., Miller LM, Horvitz HR, Kim SK. (1994). A MAP kinase homolog, mpk-1, is involved in ras-mediated induction of vulval cell fates in Caenorhabditis elegans. *Genes and Development* **8**, 160-73.
Lai, E. C. (2004). Notch signaling: control of cell communication and cell fate. *Development* **131**, 965-73.
Legouis, R., Gansmuller, A., Sookhareea, S., Bosher, J. M., Baillie, D. L. and Labouesse, M. (2000). LET-413 is a basolateral protein required for the assembly of adherens junctions in Caenorhabditis elegans. *Nat Cell Biol* **2**, 415-22.
Leung, B., Hermann, G. J. and Priess, J. R. (1999). Organogenesis of the Caenorhabditis elegans intestine. *Dev Biol* **216**, 114-34.
Lubarsky, B. and Krasnow, M. A. (2003). Tube morphogenesis: making and shaping biological tubes. *Cell* **112**, 19-28.
Machesky, L. M., Mullins, R. D., Higgs, H. N., Kaiser, D. A., Blanchoin, L., May, R. C., Hall, M. E. and Pollard, T. D. (1999). Scar, a WASp-related protein, activates nucleation of actin filaments by the Arp2/3 complex. *Proc Natl Acad Sci U S A* **96**, 3739-44.
Martinez Arias, A., Zecchini, V. and Brennan, K. (2002). CSL-independent Notch signalling: a checkpoint in cell fate decisions during development? *Curr Opin Genet Dev* **12**, 524-33.
McKeown, C., Praitis, V. and Austin, J. (1998). sma-1 encodes a betaH-spectrin homolog required for Caenorhabditis elegans morphogenesis. *Development* **125**, 2087-98.
McMahon, L., Legouis, R., Vonesch, J. L. and Labouesse, M. (2001). Assembly of C. elegans apical junctions involves positioning and compaction by LET-413 and protein aggregation by the MAGUK protein DLG-1. *J Cell Sci* **114**, 2265-77.
Mello CC, K. J., Stinchcomb D and Ambros V. (1991). Efficient gene transfer in C.elegans: extrachromosomal maintenance and integration of transforming sequences. *EMBO* **10**, 3959-70.
Melnick, M. and Jaskoll, T. (2000). Mouse submandibular gland morphogenesis: a paradigm for embryonic signal processing. *Crit Rev Oral Biol Med* **11**, 199-215.
Miller LM, G. M., Morisseau BA, Kim SK. (1993). lin-31, a Caenorhabditis elegans HNF-3/fork head transcription factor homolog, specifies three alternative cell fates in vulval development. *Genes and Development* **7**, 933-47.
Nakamura, F., Kalb, R. G. and Strittmatter, S. M. (2000). Molecular basis of semaphorin-mediated axon guidance. *J Neurobiol* **44**, 219-29.
Nakao, F., Hudson, M. L., Suzuki, M., Peckler, Z., Kurokawa, R., Liu, Z., Gengyo-Ando, K., Nukazuka, A., Fujii, T., Suto, F. et al. (2007). The PLEXIN PLX-2 and the ephrin EFN-4 have distinct roles in MAB-20/Semaphorin 2A signaling in Caenorhabditis elegans morphogenesis. *Genetics* **176**, 1591-607.
Nance, J. and Priess, J. R. (2002). Cell polarity and gastrulation in C. elegans. *Development* **129**, 387-97.
Newman, A. P., Acton, G. Z., Hartwieg, E., Horvitz, H. R. and Sternberg, P. W. (1999). The lin-11 LIM domain transcription factor is necessary for morphogenesis of C. elegans uterine cells. *Development* **126**, 5319-26.
Norman, K. R. and Moerman, D. G. (2002). Alpha spectrin is essential for morphogenesis and body wall muscle formation in Caenorhabditis elegans. *J Cell Biol* **157**, 665-77.
O, H. (2002). PCR fusion-based approach to create reporter gene constructs for expression analysis in transgenic C. elegans. *Biotechniques* **32**, 728-30.
Palmer, R. E., Inoue, T., Sherwood, D. R., Jiang, L. I. and Sternberg, P. W. (2002). Caenorhabditis elegans cog-1 locus encodes GTX/Nkx6.1 homeodomain proteins and regulates multiple aspects of reproductive system development. *Dev Biol* **252**, 202-13.

Pantaloni, D., Le Clainche, C. and Carlier, M. F. (2001). Mechanism of actin-based motility. *Science* **292**, 1502-6.
Pear, W. S. and Radtke, F. (2003). Notch signaling in lymphopoiesis. *Semin Immunol* **15**, 69-79.
Pettitt, J. (2005). The cadherin superfamily. *WormBook*, 1-9.
Piekny, A. J., Johnson, J. L., Cham, G. D. and Mains, P. E. (2003). The Caenorhabditis elegans nonmuscle myosin genes nmy-1 and nmy-2 function as redundant components of the let-502/Rho-binding kinase and mel-11/myosin phosphatase pathway during embryonic morphogenesis. *Development* **130**, 5695-704.
Piekny, A. J., Wissmann, A. and Mains, P. E. (2000). Embryonic morphogenesis in Caenorhabditis elegans integrates the activity of LET-502 Rho-binding kinase, MEL-11 myosin phosphatase, DAF-2 insulin receptor and FEM-2 PP2c phosphatase. *Genetics* **156**, 1671-89.
Pourquie, O. and Kusumi, K. (2001). When body segmentation goes wrong. *Clin Genet* **60**, 409-16.
Priess, J. R. and Hirsh, D. I. (1986). Caenorhabditis elegans morphogenesis: the role of the cytoskeleton in elongation of the embryo. *Dev Biol* **117**, 156-73.
Raich, W. B., Agbunag, C. and Hardin, J. (1999). Rapid epithelial-sheet sealing in the Caenorhabditis elegans embryo requires cadherin-dependent filopodial priming. *Curr Biol* **9**, 1139-46.
Reedy, M. C. (2000). Visualizing myosin's power stroke in muscle contraction. *J Cell Sci* **113 (Pt 20)**, 3551-62.
Rohrschneider, M. R. and Nance, J. (2009). Polarity and cell fate specification in the control of Caenorhabditis elegans gastrulation. *Dev Dyn* **238**, 789-96.
S, B. (1974). The genetics of Caenorhabditis elegans. *Genetics* **77**, 71-94.
Sawa, M., Suetsugu, S., Sugimoto, A., Miki, H., Yamamoto, M. and Takenawa, T. (2003). Essential role of the C. elegans Arp2/3 complex in cell migration during ventral enclosure. *J Cell Sci* **116**, 1505-18.
Schottenfeld, J., Song, Y. and Ghabrial, A. S. (2010). Tube continued: morphogenesis of the Drosophila tracheal system. *Curr Opin Cell Biol* **22**, 633-9.
Shakya, R., Watanabe, T. and Costantini, F. (2005). The role of GDNF/Ret signaling in ureteric bud cell fate and branching morphogenesis. *Dev Cell* **8**, 65-74.
Sharma-Kishore R, W. J., Southgate E, Podbilewicz B. (1999). Formation of the vulva in Caenorhabditis elegans: a paradigm for organogenesis. *Development* **126**, 691-9.
Shaye DD, G. I. (2005). LIN-12/Notch trafficking and regulation of DSL ligand activity during vulval induction in Caenorhabditis elegans. *Development* **132**, 5081-92.
Shemer, G., Kishore, R. and Podbilewicz, B. (2000). Ring formation drives invagination of the vulva in Caenorhabditis elegans: Ras, cell fusion, and cell migration determine structural fates. *Dev Biol* **221**, 233-48.
Sherwood DR, B. J., Kramer JM, Sternberg PW. (2005). FOS-1 promotes basement-membrane removal during anchor-cell invasion in C. elegans. *Cell* **121**, 951-62.
Somlyo, A. P. and Somlyo, A. V. (2003). Ca2+ sensitivity of smooth muscle and nonmuscle myosin II: modulated by G proteins, kinases, and myosin phosphatase. *Physiol Rev* **83**, 1325-58.
Soto, M. C., Qadota, H., Kasuya, K., Inoue, M., Tsuboi, D., Mello, C. C. and Kaibuchi, K. (2002). The GEX-2 and GEX-3 proteins are required for tissue morphogenesis and cell migrations in C. elegans. *Genes Dev* **16**, 620-32.
Stein LD, B. Z., Blasiar D, Blumenthal T, Brent MR, Chen N, Chinwalla A, Clarke L, Clee C, Coghlan A, Coulson A, D'Eustachio P, Fitch DHA, Fulton LA, Fulton RE, Griffiths-Jones S, Harris TW, Hillier LW, Kamath R, Kuwabara PE, Mardis ER,

Marra MA, Miner TL, Minx P, Mullikin JC, Plumb RW, Rogers J, Schein JE, Sohrmann M, Spieth J, Stajich JE, Wei C, Willey D, Wilson RK, Durbin R, Waterston RH. (2003). The Genome Sequence of Caenorhabditis briggsae: A Platform for Comparative Genomics. *PLoS Biology* **1**, 166-92.
Sternberg, P. W. (2005). Vulval development. *WormBook*, 1-28.
Sternberg, P. W. and Horvitz, H. R. (1986). Pattern formation during vulval development in C. elegans. *Cell* **44**, 761-72.
Sundaram, P., Echalier, B., Han, W., Hull, D. and Timmons, L. (2006). ATP-binding cassette transporters are required for efficient RNA interference in Caenorhabditis elegans. *Mol Biol Cell* **17**, 3678-88.
Tan, P. B., Lackner, M. R. and Kim, S. K. (1998). MAP kinase signaling specificity mediated by the LIN-1 Ets/LIN-31 WH transcription factor complex during C. elegans vulval induction. *Cell* **93**, 569-80.
Thomas-Virnig, C. L., Sims, P. A., Simske, J. S. and Hardin, J. (2004). The inositol 1,4,5-trisphosphate receptor regulates epidermal cell migration in Caenorhabditis elegans. *Curr Biol* **14**, 1882-7.
Winter, D., Lechler, T. and Li, R. (1999). Activation of the yeast Arp2/3 complex by Bee1p, a WASP-family protein. *Curr Biol* **9**, 501-4.
Wissmann, A., Ingles, J. and Mains, P. E. (1999). The Caenorhabditis elegans mel-11 myosin phosphatase regulatory subunit affects tissue contraction in the somatic gonad and the embryonic epidermis and genetically interacts with the Rac signaling pathway. *Dev Biol* **209**, 111-27.
Wissmann, A., Ingles, J., McGhee, J. D. and Mains, P. E. (1997). Caenorhabditis elegans LET-502 is related to Rho-binding kinases and human myotonic dystrophy kinase and interacts genetically with a homolog of the regulatory subunit of smooth muscle myosin phosphatase to affect cell shape. *Genes Dev* **11**, 409-22.
Wolpert, L. (2011). Principles of development. Oxford ; New York: Oxford University Press.
Wu Y, H. M., Guan KL. (1995). MEK-2, a Caenorhabditis elegans MAP kinase kinase, functions in Ras-mediated vulval induction and other developmental events. *Genes and Development* **9**, 742-55.
Xavier Trepat, M. R. W., Thomas E. Angelini, Emil Millet, David A. Weitz, James P. Butler and Jeffrey J. Fredberg. (2009). Physical forces during collective cell migration. *Nature Physics* **5**, 426-430.
Yoo AS, B. C., Greenwald I. (2004). Crosstalk between the EGFR and LIN-12/Notch pathways in C. elegans vulval development. *Science* **303**, 663-6.
Yoo, A. S. and Greenwald, I. (2005). LIN-12/Notch activation leads to microRNA-mediated down-regulation of Vav in C. elegans. *Science* **310**, 1330-3.

2 Objective of the present study

The introduction has shown the importance of *C.elegans* as a model organism for the study of fate determination and morphogenesis. This model has been used extensively to study the role of Notch signaling pathway, mostly in the context of cell fate decisions. However, the role of Notch signaling in morphogenesis has been overlooked. Additionally, the identification of Notch target genes that are specifically involved in the execution of cell fates is lacking.

The original objective of this thesis was to identify novel direct Notch target genes involved in cell fate determination. But as it is beautifully said "whatever is simple in science, it is either wrong or you are lucky" and we were not lucky as we found the Rho-kinase homologue *let-502* as an indirect Notch target gene. The putative Notch target gene *let-502* was selected based on three criteria: (1) *let-502* promoter contained CSL binding sites (2) It was expressed selectively in the 2° lineage of vulval cells (3) RNAi of *let-502* resulted in particular phenotypes linked to vulva development (i.e. worms displaying a "protruding vulva" that were egg-laying defective (**www.wormbase.org**). As a result, the characterization of *let-502* was pursued, since preliminary experiments indicated that it was positively regulated by the Notch signaling pathway and is involved in vulval morphogenesis. Also, the examination of the role of *LET-502* in the vulva gave us an opportunity to have a closer look at the forces required for shaping the vulval tube during its development.

The specific aims of this thesis were:

1. To find out novel Notch target genes and analyze them using *in vivo* gene expression analysis (Chapter 3);
2. Molecularly characterize the transcriptional regulation of the *C.elegans* Rho-kinase *let-502* (Chapters 4)
3. Examine the role of Rho-kinase *let-502* in vulval morphogenesis (Chapters 4);
4. Characterize VAB-23 as gene required for morphogenesis (collaboration with Mark Watson Pellegrino) (Chapter 5);
5. Concluding remarks and outlook (Chapter 6).

3 Part I: Systematic identification and functional analysis of Notch target genes in *C.elegans*

3.1 Abstract

During hermaphrodite vulval development, lateral signaling from the primary vulval precursor cell (VPC) P6.p activates the LIN-12 Notch pathway in the neighbouring secondary VPCs P5.p and P7.p. The LIN-12 Notch signal inhibits primary fate specification and promotes the secondary vulval fate by activating transcription factors of the CSL family, which turn on the expression of specific target genes.

Notch target genes usually contain clusters of CSL binding sites (RTGGGAA) in their promoter/enhancer regions. Notch target genes are up regulated in secondary cells and down regulated in the primary cells of the vulva (e.g. *lip-1*). We screened the *C. elegans* genome for genes containing three or more CSL binding sites within 2 kbp upstream of their start codon. We narrowed down the list of genes depending on whether the putative CSL sites are conserved in the *C. briggsae* orthologs and further on the basis of their predicted functions. Transcriptional reporters containing promoter-GFP fusions were analyzed for the 23 best candidates by fusion PCR and microinjection into wild type worms to create transgenic lines. Reporters were analyzed for a 2° fate specific expression pattern in the vulvae. Also, the genes in which the CSL binding sites were not conserved were knocked down using RNAi in Notch gain-of-function animals to analyze their effect on vulval induction. The screen led to identification of five genes, which showed an expression pattern in the vulva typical for Notch targets. These genes are *let-502, nsh-1, f20h11.1, f28a12.4* and *lin-41*.

3.2 Introduction

The development of the vulva, which is a part of the egg laying apparatus, serves as a paradigm to study the development of an organ from six equipotent vulval precursor cells due to the interplay of different pathways like RAS, Notch and Wnt. Twelve P- cells migrate during the L1 stage from the lateral midline of the animal to the ventral midline and the posterior descendants of P3 to P8 (P3.p to P8.p) form the vulval precursor cells (VPC), which form an equivalence group. Further vulval development takes place from these VPCs (Figure 1.5). Before vulval development, Notch mediated lateral inhibition results in the differentiation of the anchor cell (AC, an organizer cell) in the somatic gonad, which initiates vulval development. AC then expresses LIN-3 to activate the EGFR and the Ras pathway in

the nearby VPCs to stimulate their differentiation. P6.p, the VPC closest to the anchor cell, receives most of the signal and adopts a primary cell fate (Hill RJ, 1992). In P6.p, Ras promotes expression of DSL Ligands to activate the Notch pathway in the neighbouring VPCs. P5.p and P7.p (Chen N, 2004) adopt the secondary 2° cell fate in a Notch dependent manner (Greenwald et al., 1983).

Initial differences in VPC position lead to differences in the relative levels and timing of the signaling that appear to be critical for cell fate patterning (Sternberg and Horvitz, 1989). The remaining distal VPCs, in which both Notch and Ras activity are low, adopt the tertiary cell fate. A combination of Ras and Notch signaling leads to the invariant 3°- 3°- 2°- 1°- 2°- 3° pattern of VPC cell fates. P5.p, P6.p and P7.p then form 22 cells to generate the egg laying apparatus called vulva. The role of the Notch signaling pathway in various cellular processes is well studied, but little is known about its downstream targets not only in *C.elegans* but also in higher organisms. We are interested in finding out the role of the genes that are activated by the Notch pathway, which bring about several decisions in the development of vulva. To find new targets, an in-silico and in-vivo screen was performed to identify genes with characteristic of Notch targets.

3.3 Results

3.3.1. *In silico* Screen for Notch target genes

To Identify the Notch target genes involved in vulval development, we performed a GFP (Green Fluorescent Protein) reporter based screen comprised of two steps. First, using a bioinformatics approach, we screened the whole *C.elegans* genome for genes containing at least three CSL binding sites (RTGGGAA) within 2 kb upstream of the inititation codon on both strands (using a perl script programme by Peter Gallant) (Figure 1). To further narrow down this list, we sorted out the genes on the basis of biological function or vulval phenotype (Pvl phenotype, Endocytosis/Sorting/Secretion, Signaling, Protein degradation/Proteases, Phosphatases, Kinases, Transcription factors) (Figure 1). In this sorted list, *ref-1* and *hlh-26*, which were previously described as a Notch targets, served as a positive control for the screen. Finally, we divided these genes into two groups. The first group (Table 1a) has conserved CSL sites in the closely related C. *briggsae* orthologs and in the second group (Table 1b) the CSL sites in C. *briggsae* orthologs are not conserved.

3.3.2. *In vivo* Screen for Notch target genes

For in vivo screening, we generated promoter GFP fusion construct (O, 2002) of the first group of genes and analyzed their expression pattern in wild type animals (Table 1a). After the analysis, four of these genes which showed 2° specific expression pattern were F20H11.1, *nsh-1* F28A12.4, *let-502* and *lin-41* and were considered putative Notch target genes (Figure 4). *F20H11.1* is expressed in the descendants of 2° cells at Christmas tree stage in L4 animals (VulA, VulB1, VulB2, VulC and VulD cells) and expression is absent in the P6.p descendents (VulE, VulF cells) (Figure 4A). *F28A12.4* is expressed from the Pnp.x stage in secondary cells and their descendants in the vulva (Figure 4B). *lin-41* is expressed from Pn.pxx -christmas tree stage. The expression is upregulated in 2° and downregulated in 1° cells mostly at Pn.pxx stage (Figure 4C). *let-502* is expressed in all vulval precursor cells before induction. It's expression is downregulated in 1° cells from Pn.px stage onwards and becomes more prominent in 2° cells from late Pn.pxxx stage onwards with onset of vulval morphogenesis (Figure 4E). Genetic regulation and functional analysis of *let-502* is investigated in Chapter 4.

Notch signaling induces 2° cell fate during vulval development. P3.p-P8.p form vulval equilance group of cells that have the potential to adopt vulval cell fates in future. Hyper activation of Notch signaling induces P3.p-P8.p cells to adopt 2° vulval cell fate (vulval index of 6) (Greenwald et al., 1983). As a result, all of these cells give rise to individual invaginations that form pseudovulva (non-functional vulva). RNAi of Notch receptor *lin-12,* in Notch gain-of-function animals decreases the vulval induction index of 6 to 4 (Figure 3). Downregulating a Notch target gene involved in Notch mediated induction of 2° cell fate should result into the decrease of vulval index of Notch gain of function mutants. Using RNAi, candidate genes were knocked down in a *lin-12* gain-of-function background for the remaining 29 genes (Table 1b) lacking conserved CSL binding sites to test if any of them suppresse the multivulva phenotype caused by *lin-12* gain-of-function. RNAi against one new gene showed mild suppression of the *lin-12 Notch* gain-of-function phenotype i.e. *nsh-1* (Figure 3). Transcriptional reporter of *nsh-1* showed higher expression in 2° than in 1° vulval cells, which is typical for Notch target genes (Figure 4D).

3.4 Discussion

Taken together, our bioinformatics screen followed by systematic expression and RNAi analysis has identified five putative Notch target genes. One gene, *let-502* was

analyzed in detail as described in the next chapter 4. The following is a summary of the proerties of the putative notch targets identified in this study.

The **F20H11.1** gene contains 6 CSL sites in its promoter region and encodes a protein with Protein kinase C, phorbol ester/diacyglycerol binding, zinc finger, RING-type and pancreatic ribonuclease domains. It is listed in wormbase as an uncharacterized protein with an unknown function during development. The presence of a protein kinase C domain indicates that it might be involved in cell signaling. The human homolog of F20H11.1, DEF-8 (72% similarity), is known to be differentially expressed in the haemopoietic system (Hotfilder et al., 1999). The molecular and phenotypic function of DEF-8 is not characterized so far. Recently, (Ivanov et al., 2009) showed that protein kinase C activation disrupts epithelial apical junctions via Rho-kinase ROCK-II dependent stimulation of actomyosin contractility in pancreatic epithelium. These observations point in the direction of the role of F20H11.1 in regulating apical junction integrity of the vulva. Further experiments for connecting the Rho-kinase *let-502* and myosin contraction with F20H11.1 might give us more insight into vulval morphogenesis. *tm3648* is a 320 bp deletion allele of F20H11.1 removing the initiation codon which makes it a protein null allelle. This strain will serve as a perfect tool to investigate the role of F20H11.1 in the vulval development.

F28A12.4 contains 5 CSL sites in its promoter. The protein contains an aspartyl protease domain. It is mentioned as an uncharacterized gene with the Gastricin precursor as human homolog. Presently, no RNAi clone and no allele except one mos transposon insertion in the promoter region is available for F28A12.4.

lin-41 encodes a protein with Zinc finger domain. *lin-41* is involved in the heterochronic pathway and null mutations of *lin-41* cause precocious expression of adult fates at larval stages while increased activity causes the opposite phenotype (Slack et al., 2000). *lin-41* has variable RNAi phenotypes including protruding vulva (Pvl). LIN-41 encodes a member of RBCC family of regulatory protein, some of which have been implicated in RNA binding or control RNA function (Slack et al., 2000). Mutants are available for *lin-41* but they do not show any vulval phenotype suggesting that *lin-41* function might be redundant or is not important for vulval development. Notch might be regulating the timing of 2° cell patterning via LIN-41.

nsh-1 contains 5 CSL sites in its promoter region. The NSH-1 protein contains a Dead like helicase domain. *nsh-1* is required for embryonic development, reproduction and genitalia development (Simms and Baillie, 2010). RNAi against *nsh-1* causes a variable Pvl

phenotype and alters the *egl-17::cfp* expression pattern at Pn.p stage of vulval development (Simms and Baillie, 2010) . *Drosophila* homolog Sno also has a well defined role in promoting the expression of the Notch ligand, Dl, downstream of EGFR during cone cell specification where it interacts with transcriptional regulatory proteins to interrupt repression of Dl by Su(H) and the co-repressor SMRTER (Nagaraj and Banerjee, 2007).

let-502 contains 4 CSL sites in its 5' promoter enhancer region. The *LET-502* protein has a Serine/Threonince protein kinase domain. It is known to be downstream effector of the Rho small GTPase and was shown to control embryonic and larval development by phosphorylation of myosin light chain. *let-502* RNAi induces several penetrant phenotypes including protruding and bursting vulva. The human homolog pROCK also acts in the Rho signaling pathways (Amano et al., 2000) but has not yet been connected with Notch signaling. *C.elegans let-502* is expressed in secondary vulval cells from the one cell (Pn.p) stage on and downregulated in the primary cells and their descendants (see chapter 4). Thus, a Rho signal transduced via *LET-502* may be required for secondary cell morphogenesis. The role of *let-502* was further analyzed in detail during *C.elegans* vulval morphogenesis in the following chapter 4.

3.5 Materials and methods

3.5.1. Strains used

C.elegans strains were maintained at 20°C on standard nematode growth media as described previously (Brenner, 1974). The wild-type strain of C.elegans used was Bristol N2. Strains used were as follows: *lin-12(n137)/unc-32(e189) lin-12(n137n720)*, *zhEx434-455[promoter::nls::gfp::lacz::unc-54 3'utr, Plin-48::gfp]*. Promoter was taken as the intergenic region which was 5' upstream of the candidate open reading frame.

3.5.2. Design of transcriptional reporter constructs

To investigate the expression pattern of candidate genes, transcriptional *gfp* reporters were produced. The reporters were made by the fusion PCR method (primers mentioned in Table 3.2d) (O, 2002). There, the promoter region including the 5' upstream regulatory sequence up to the next predicted gene and the first few nucleotides from the gene of interest were amplified by PCR. In a second PCR reaction, the *nls::gfp::lacZ* coding region from pPD96.04 was amplified. In the fusion PCR step (O, 2002) , the full-length reporter was produced by running a PCR on both products with nested primers. Since the promoter region

was amplified with a 3'-primer that includes an overlap to the *gfp*-containing PCR fragment the two PCR products were fused during PCR (Figure 3.2c).

3.5.3. Generation of transgenic lines expressing the transcriptional *gfp*-reporter

The reporter constructs were injected at a concentration of 10-100ng/ul into both syncytial gonad arms as described (Mello CC, 1991). The injected amount was estimated by DNA agarose gel electrophoresis of the PCR products. Generally, transcriptional reporters were injected with *plin-48::gfp* as the coinjection marker (50-75ng/ul) in N2 animals. As a consequence, transgenic lines that showed robust *gfp*-expression were established for all transcriptional reporters. The injection mixture contained besides the transcriptional reporter and the coinjection marker a certain amount of the plasmid pBS-KS- to reach at least a total DNA concentration of 200ng/ul.

3.5.4. Microscopical analysis of expression pattern

For each transcriptional reporter, two to three independent transgenic lines that inherited the extrachromosomal array to their progeny were established. For each line, about 20 animals at the L3 or L4 stage were observed with a microscope at high resolution to find transgenic lines that showed strong *gfp*-expression. The line showing expression of the gene in the vulva was taken as the representative line for expression.

3.5.5. RNAi of candidate genes

RNA interference

RNA interference (RNAi) was performed using the feeding method as described (Kamath et al., 2001). The worms were bleached on empty plates. The synchronized L1 worms were transferred to nematode growth media plates containing 3 mM IPTG and 50ng/ml ampicillin, seeded with the desired RNAi bacteria and allowed to grow for 3-5 days at 20-25°C. The first generation progeny F1 was analyzed. L4 Christmas tree stage animals were mounted on a Olympus microscope with normaski optics on 4% agarose pads in 20 mM Tetramisole solution. Vulval induction was scored by counting the number of vulval invaginations and their corresponding induction on the ventral side of the animal.

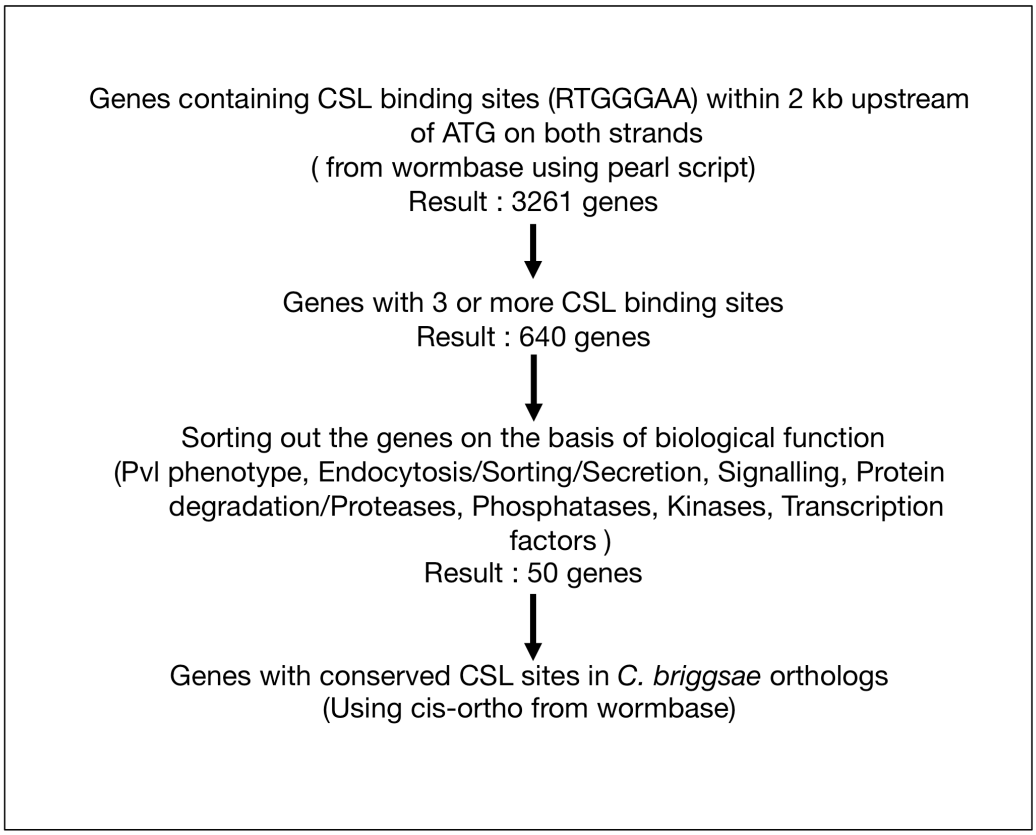

Figure 1. Bioinformatics screen for Notch target genes as described in results.

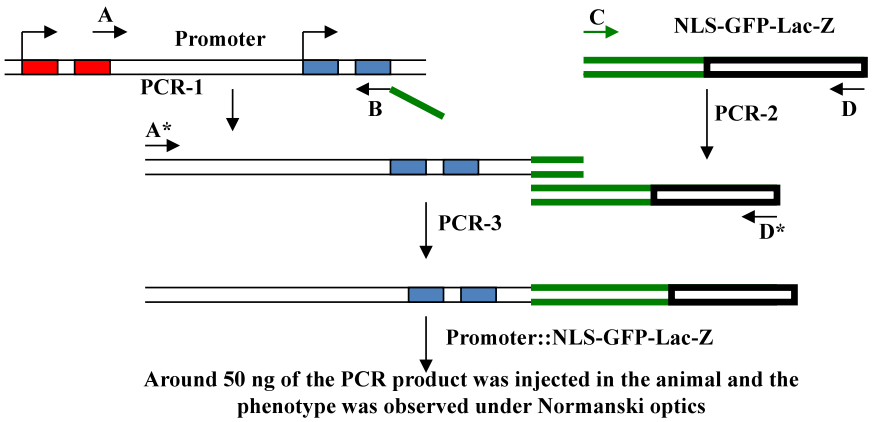

Figure 2. Fusion PCR scheme for producing transcriptional constructs for putative Notch target genes as described in materials and method.

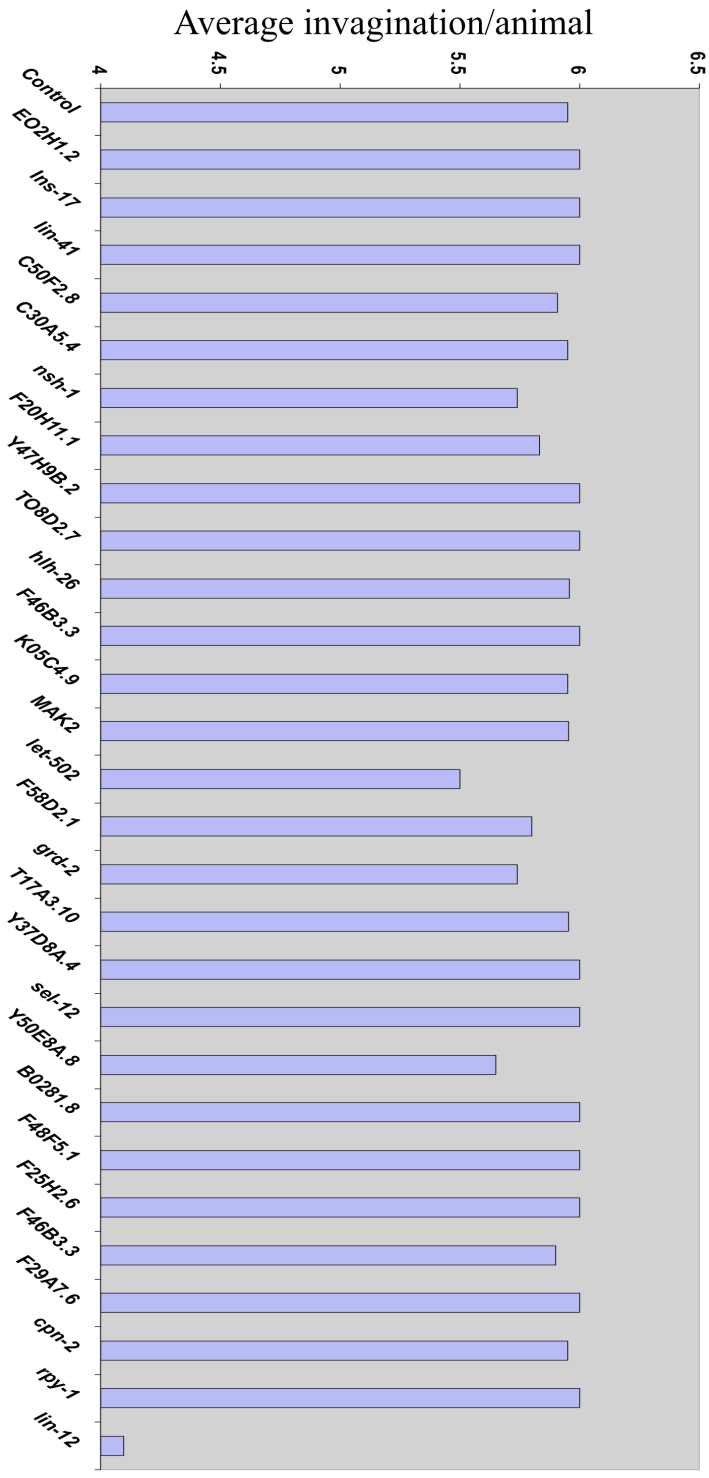

Figure 3. RNAi of the putative Notch target genes that have non-conserved CSL binding sites in Notch gain-of-function animals. X-axis represents the name of the putative Notch target gene and Y-axis represents the corresponding average vulval index (as described in materials and methods) after their RNAi mediated knockdown. For each RNAi, a minimum of 20 animals were scored. Empty vector RNAi clone was taken as negative control (vulval index=6) while, Notch (*lin-12*) RNAi was assumed as positive control (vulval index=approx 4).

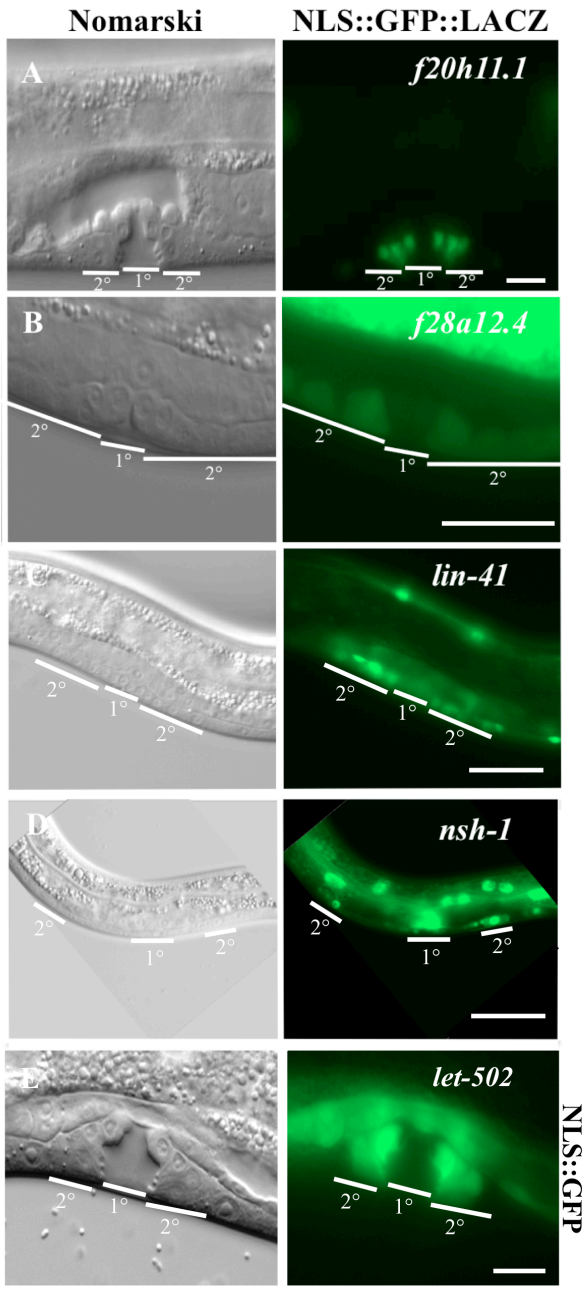

Fig.4

Expression of putative Notch target genes showing up regulation in secondary cells (2°) and down regulation in primary cells (1°) of vulva (a) Expression of f20h11.1, f28a12.4, lin-41, nsh-1 and let-502 (A',B',C',D' and E') with their corresponding Normaski images (A,B,C,D and E) at L4, late L3, late L3, early L3 and L4 stage of vulval development respectively. In all panels, anterior is to the left and ventral is to the bottom. Scale bars: 10 µ m

ORF	Gene name	Concise description	Vulval expression	2° specific
C09H6.2	*lin-10*	PDZ and PTB domain-containing protein	+	-
C10H11.9	*let-502*	Rho-kinase	+	+
C12C8.3	*lin-41*	Predicted E3 ubiquitin ligase	+	+
C18H9.7	*rpy-1*	Acetylcholine receptor-associated protein	-	-
C30A5.4	*C30A5.4*	Serine/threonine specific protein phosphatase PP1 catalytic subunit	-	-
F09C12.7	*msp-74*	Major Sperm Protein	-	-
F20G4.3	*nmy-2*	Non-muscle myosin II	+	-
F20H11.1	*F20H11.1*	Predicted protein kinase C-like and phorbol ester/diacylglycerol binding	+	+
F26A3.4	*F26A3.4*	Dual specificity phosphatase	-	-
F26D11.11	*let-413*	Basolateral epithelial marker protein	+	-
F28A12.4	*F28A12.4*	predicted aspartyl protease domain	+	+
F43D9.1	*F43D9.1*	Predicted membrane protein of the patched superfamily	-	-
F49E12.4	*ubc-24*	Ubiquitin-conjugating enzyme	-	-
H06O01.3	*ctg-1*	CRAL/TRIO and GOLD domain containing	-	-
H39E23.1	*par-1*	Serine/threonine protein kinase	+	-
R03D7.8	*R03D7.8*	Serine/threonine specific protein phosphatase PP1 domain	-	-
R06A10.4	*R06A10.4*	Ca2+/calmodulin-dependent protein kinase	-	-
T01E8.2	*ref-1*	Regulator of fusion	+	-
T24B8.6	*hlh-3*	Basic helix-loop-helix transcription factor	+	-
W07G4.3.1	*W07G4.3.1*	Predicted serine-threonine/tyrosine-protein kinase	-	-
W09D10.1	*W09D10.1*	Predicted GTPase-activating protein	+	-
Y116A8C.24	*Y116A8C.24*	Protein tyrosine kinase domain	-	-
Y65B4BR.3	*ptr-21*	Predicted membrane protein of the patched superfamily	-	-
ZK809.1	*ZK809.1*	Protein tyrosine phosphatase domain	-	-

Table 1a: Candidate NOTCH targets investigated by reporter analysis
Using a custom perl script (kindly provided by Peter Gallant), the *C. elegans* genome was screened for genes containing at least three CSL binding sites (RTGGGAA) within 2 kb upsream of the predicted translational start sites. To further narrow down the candidate gene list, we selected for genes on the basis of biological function (Pvl or Muv phenotype, genes involved in endocytosis, sorting, secretion, signaling, protein degradation, protein phosphorylation, transcriptional regulation) and conservation of the CSL motifs in the *C. briggsae* orthologs. This analysis identified the 24 candidate genes shown above, for which we generated transcriptional reporters by fusion PCR and analyzed the vulval expression pattern.

ORF	Gene name	Concise description
Y73B3A.5	*Y73B3A.5*	LIN-1 ETS paralog
F29A7.6	*F29A7.6*	M-phase phosphoprotein 6 domain
F56F3.6	*ins-17*	insulin-like peptide
F20H11.6	*let-765*	Positive regulator or RAS signaling
F41E6.4	*smk-1*	SMEK (suppressor of MEK null) proteins
Y64H9A.1	*Y64H9A.1*	Predicted unknown protein
Y60A3A.9	*Y60A3A.9*	Predicted unknown protein
F56C9.11	*F56C9.11*	Predicted unknown protein
D1069.2	*cpn-2*	calponin homolog
Y45F3A.2	*rab-30*	rab related protein
F36F2.4	*syx-7*	Syntaxin with a role for membrane fusion events in cytokinesis
Y37D8A.4	*Y37D8A.4*	Predicted unknown protein
E02H1.2	*E02H1.2*	Predicted unknown protein
T17A3.10	*T17A3.10*	Predicted unknown protein
Y47H9B.2	*Y47H9B.2*	Predicted unknown protein
F46B3.5	*grd-2*	hedgehog-like protein
Y50E8A.8	*Y50E8A.8*	Predicted unknown protein
B0281.8	*B0281.8*	Predicted unknown protein
F40G9.14	*F40G9.14*	Predicted unknown protein
F35H12.3	*sel-12*	protein orthologous to presenilins
H06O01.4	*H06O01.4*	Predicted unknown protein
K05C4.9	*K05C4.9*	Predicted unknown protein
F48F5.1	*F48F5.1*	Predicted unknown protein
T08D2.7	*T08D2.7*	Predicted unknown protein
F58D2.1	*grd-1*	Predicted unknown protein
C50F2.8	*C50F2.8*	Predicted unknown protein
F25F2.6	*F25F2.6*	Predicted unknown protein
C17C3.8	*hlh-26*	REF-1-like protein with two bHLH domains that represses lag-2 transcription
C44C8.6	*mak-2*	serine/threonine protein kinase that is orthologous to the vertebrate MAPKAPK2

Table 1b:Candidate NOTCH targets investigated by RNAi

Using a custom perl script (kindly provided by Peter Gallant), the *C. elegans* genome was screened for genes containing at least three CSL binding sites (RTGGGAA) within 2 kb upsream of the predicted translational start sites. To further narrow down the candidate gene list, we selected for genes on the basis of biological function (Pvl or Muv phenotype, genes involved in endocytosis, sorting, secretion, signaling, protein degradation, protein phosphorylation, transcriptional regulation) orthologs. This analysis identified the 29 candidate genes shown above which had non-conserved CSL sites. RNAi was performed against these genes in Notch gain-of-function animals to analyze their role in vulval fate decison (Figure 3).

NMY-2 A	CTCGTTATTGTACTTCCACAG
NMY-2 A*	ATGTCTCCATGCGTTACGAAC
NMY-2 B	AGTCGACCTGCAGGCATGCAAGCTTATCTCTGCAACCGTAGCTTC
LIN-10 A	GATCTTGCGTTCGCAGTGCC
LIN-10 A*	GCTTTCGCAACTGCATCTTGG
LIN-10 B	AGTCGACCTGCAGGCATGCAAGCTTGAGCGATGAGATGATGATGC
LET-413 A	AGCTTGAAGCCATGGAAGTC
LET-413 A*	CATCTTTGAATGGCCGTCTG
LET-413 B	AGTCGACCTGCAGGCATGCAAGCTATCAATCGAATCCACCTGACG
PAR-1 A	CCTAGTAATTCAGACTGCTGC
PAR-1 A*	GCCGAGAGCAACATCGTCAAC
PAR-1 B	AGTCGACCTGCAGGCATGCAAGCTTGGAGGCGTGTTCACATGCTC
LIN-41 A	CACCAGCGTGTGATAGGATTC
LIN-41 A*	CCAGAGATGTTGTCATCACAGG
LIN-41 B	AGTCGACCTGCAGGCATGCAAGCTTTGTGGTTGAACTGCACGGC
H06O01.3 A	ACACTATGGACGCCTCGTACC
H06O01.3 A*	AGTAGTCGAACGTTCCCATGC
H06O01.3 B	AGTCGACCTGCAGGCATGCAAGCTGAGCCAGCGGAGCACATAACC
RPY-1 A	GGAGAGCCAGGAGTCTGTGTC
RPY-1 A*	CACAGCCACGCATTCGTGCC
RPY-1 B	AGTCGACCTGCAGGCATGCAAGCTAACGTGCTTGCACCCTATCTG
MSP-74 A	GTCGGAAGTAGGATGACAAG
MSP-74 A*	CAACTGGAGGCCAGATGTCTC
MSP-74 B	AGTCGACCTGCAGGCATGCAAGCTGTCGAGGACTCCACATGGTGG
PTR-21 A	CAATTCGTCACAGGAACGTGC
PTR-21 A*	GTATCGAGCGTGTCGGCAAGG
PTR-21 B	AGTCGACCTGCAGGCATGCAAGCTGAACCTGCCAATTATCTTCCC
W09D10.1 A	GGCGGCGTTGAGTCATCGTG
W09D10.1 A*	GCAGCTCGGCGAGATGACAG
W09D10.1 B	AGTCGACCTGCAGGCATGCAAGCTCGGATCCACTTTACCTCGCAG
F43D9.1 A	AACTGTTGAAAGACGCCGAG
F43D9.1 A*	CTAGTGGAAGAGTGCATGCC
F43D9.1 B	AGTCGACCTGCAGGCATGCAAGCTCTGAAACCTGACTGCTGCAGG
F28A12.4 A	CGAGACGACGATGTCTACACC
F28A12.4 A*	CAACCCGCCTCTTTGATGC
F28A12.4 B	AGTCGACCTGCAGGCATGCAAGCTGCGGTACTCCAAATAGGCAGG
UBC-24 A	CCACAGGCTTTCTGACAATG
UBC-24 A*	TCGGTACATTCCTCCGATCG

UBC-24 B	AGTCGACCTGCAGGCATGCAAGCTAGCAGCTGCTTGAAGTGTGC
ZK809.1 A	TTCCACGACCATAACCTCCG
ZK809.1 A*	GAGCAGCAGCGACTGAGAAG
ZK809.1 B	AGTCGACCTGCAGGCATGCAAGCTCTCGGAACCTTCTTTGCAACG
F26A3.4 A	AAACGCCCTCTTCTCCGTCG
F26A3.4 A*	CGGTAGACGTGAGATCTCCTG
F26A3.4 B	AGTCGACCTGCAGGCATGCAAGCTAGCTTCACGAAGATTTCGGC
R03D7.8 A	AAACGAAGTCGGCAAGAGGG
R03D7.8 A*	GAGAATCTGGAGAGTCGAACG
R03D7.8 B	AGTCGACCTGCAGGCATGCAAGCTAAGCCGCGGATTTCGAGTAG
C30A5.4 A	TTGAAGCTGGGAGGAGACAG
C30A5.4 A*	TCCCCTATGTCTTGGTCTCC
C30A5.4 B	AGTCGACCTGCAGGCATGCAAGCTAATACAACCTGGACGCTCATCC
F20H11.1 A	TCGGTCGTCGTACTCGTACC
F20H11.1 A*	CTCTGTTCTCTCCGTTTGGC
F20H11.1 B	AGTCGACCTGCAGGCATGCAAGCTGGAACGTGTGGAAGGAGTTG
R06A10.4 A	GATGTCGGCCACGTTATAGTG
R06A10.4 A*	TGGCCGACATCTCACAGGTAC
R06A10.4 B	AGTCGACCTGCAGGCATGCAAGCTATGCGGGTCGATGTGTGCTT
Y116A8C.24 A	CATTTGCCGTTCGCCGTTTGC
Y116A8C.24 A*	CACAGCCCTGGTATGTAGCTC
Y116A8C.24 B	AGTCGACCTGCAGGCATGCAAGCTAGGATGACAACACCGATGCC
REF-1 A	TCCAGAGCTCGAATGGATCTC
REF-1 A*	CCGATGCTGCACTTCAATGTC
REF-1 B	AGTCGACCTGCAGGCATGCAAGCTTCGTCGTTTCTTCTCCTGTG
HLH-3 A	GGCATGATGGTCTTGAGTCG
HLH-3 A*	GTCGACACACGACTCTGAAGC
HLH-3 B	AGTCGACCTGCAGGCATGCAAGCTTTGTACCATGGCGCCAGAACG
W07G4.3.1 A	GAGACCTGTTGGATCGCTCCG
W07G4.3.1 A*	CTTCCGACGAGCACGACAGC
W07G4.3.1 B	AGTCGACCTGCAGGCATGCAAGCTTCGAAGATGCATGAAGAACG
PRIMER C	AGCTTGCATGCCTGCAGGTCGACT
PRIMER D	AAGGGCCCGTACGGCCGACTA
PRIMER D*	GGAAACAGTTATGTTTGGTATA

Table 2. Sequence of primers used for producing transcriptional reporters by PCR fusion as described in Materials and Methods.

References :

Amano, M., Fukata, Y. and Kaibuchi, K. (2000). Regulation and functions of Rho-associated kinase. *Exp Cell Res* **261**, 44-51.
Chen N, G. I. (2004). The lateral signal for LIN-12/Notch in C. elegans vulval development comprises redundant secreted and transmembrane DSL proteins. *Developmental Cell* **6**, 183-92.
Greenwald, I. S., Sternberg, P. W. and Horvitz, H. R. (1983). The lin-12 locus specifies cell fates in Caenorhabditis elegans. *Cell* **34**, 435-44.
Hill RJ, S. P. (1992). The gene lin-3 encodes an inductive signal for vulval development in C. elegans. *Nature* **358**, 470-6.
Hotfilder, M., Baxendale, S., Cross, M. A. and Sablitzky, F. (1999). Def-2, -3, -6 and -8, novel mouse genes differentially expressed in the haemopoietic system. *Br J Haematol* **106**, 335-44.
Ivanov, A. I., Samarin, S. N., Bachar, M., Parkos, C. A. and Nusrat, A. (2009). Protein kinase C activation disrupts epithelial apical junctions via ROCK-II dependent stimulation of actomyosin contractility. *BMC Cell Biol* **10**, 36.
Kamath, R. S., Martinez-Campos, M., Zipperlen, P., Fraser, A. G. and Ahringer, J. (2001). Effectiveness of specific RNA-mediated interference through ingested double-stranded RNA in Caenorhabditis elegans. *Genome Biol* **2**, RESEARCH0002.
Mello CC, K. J., Stinchcomb D and Ambros V. (1991). Efficient gene transfer in C.elegans: extrachromosomal maintenance and integration of transforming sequences. *EMBO* **10**, 3959-70.
Nagaraj, R. and Banerjee, U. (2007). Combinatorial signaling in the specification of primary pigment cells in the Drosophila eye. *Development* **134**, 825-31.
O, H. (2002). PCR fusion-based approach to create reporter gene constructs for expression analysis in transgenic C. elegans. *Biotechniques* **32**, 728-30.
Simms, C. L. and Baillie, D. L. (2010). A strawberry notch homolog, let-765/nsh-1, positively regulates lin-3/egf expression to promote RAS-dependent vulval induction in C. elegans. *Dev Biol* **341**, 472-85.
Slack, F. J., Basson, M., Liu, Z., Ambros, V., Horvitz, H. R. and Ruvkun, G. (2000). The lin-41 RBCC gene acts in the C. elegans heterochronic pathway between the let-7 regulatory RNA and the LIN-29 transcription factor. *Mol Cell* **5**, 659-69.
Sternberg, P. W. and Horvitz, H. R. (1989). The combined action of two intercellular signaling pathways specifies three cell fates during vulval induction in C. elegans. *Cell* **58**, 679-93.
www.wormbase.org
www.wormatlas.org
www.wormbook.org

4 Part II: Regulation morphogenesis by NOTCH/LIN-12 and ETS/LIN-1 signaling pathways via RHO-Kinase/LET-502 in *C.elegans*

4.1 Manuscript draft: Push and Pull during *C.elegans* vulval morphogenesis (under Review in Developmental Cell)

A push-pull mechanism during vulval morphogenesis in *C.elegans*

Sarfarazhussain Farooqui[1,2], Mark W. Pellegrino[1,3], Ivo Rimann[1,4], Matthias Morf[1,2], Erika Fröhli[1] and Alex Hajnal[1,5]

[1]University of Zürich, Institute of Molecular Life Sciences, Winterthurerstrasse 190, CH-8057, Switzerland

[2]Molecular Life Sciences PhD program, Uni ETH Zürich, Switzerland

[3]Present address: Memorial Sloan Kettering Cancer Centre, Rockefeller Research Laboratories, 430 East 67th street, RRL 617B New York

[4]Present address: The Scripps Research Institute, 10550 North Torrey Pines Road La Jolla, CA 92037

[5]Corresponding author: alex.hajnal@imls.uzh.ch

Phone: +41 (0)44 635 48 54 Fax: +41 (0)44 635 68 98

Key words: morphogenesis; *notch*; *ets*; epidermis; *C.elegans*; vulva

Running title: *C.elegans* NOTCH and LIN-1 control morphogenesis

Summary

Morphogenesis is a developmental phase during which cell fates are executed. Mechanical forces shaping individual cells play a key role during morphogenesis. By investigating morphogenesis of the *C.elegans* hermaphrodite vulva, we show that the force generating actomyosin network is differentially regulated by NOTCH and EGFR/RAS/MAPK signaling to shape the vulval tube. NOTCH signaling activates expression of the RHO kinase LET-502 in the secondary cell lineage through the ETS-family transcription factor LIN-1. RHO kinase induces contraction of the apical lumen in the secondary vulval toroids via actomyosin forces, thereby generating an inward pushing force. MAPK signaling in the primary lineage down-regulates Rho kinase and prevents toroid contraction, allowing the gonadal anchor cell to expand the dorsal lumen of the primary toroids, which results in an inward pulling force. The antagonistic action of the MAPK and NOTCH pathways thus controls vulval tube morphogenesis.

Introduction

Organogenesis requires the differentiation of selected cells followed by tissue morphogenesis, which involves cell shape changes, cell-cell interactions and coordinated cell movements. Tubes are the basic building blocks of most epithelial organs. Tube morphogenesis is therefore an essential process in various developmental processes such as embryonic development, tissue vascularization and the development of most epithelial organs (Andrew and Ewald, 2010; Rodriguez-Fraticelli et al., 2011). During tissue morphogenesis, mechanical forces generated between cells are necessary to determine the proper size and shape of an organ. With a high degree of mechanical coupling between cells, tissue morphogenesis could be governed by forces from a few cells pushing or pulling all other cells (Gov, 2007; Rorth, 2009). Major challenges are therefore to identify the cells that exert physical forces and the molecular pathways that control the generation of forces. *In vivo* models used to address these questions include vascular sprouting and branching in vertebrates, neuroblast migration during lateral line formation in the Zebrafish embryo, border cell migration in *Drosophila* ovaries and tracheal morphogenesis in the *Drosophila* embryo (Rodriguez-Fraticelli et al., 2011; Rorth, 2009; Schottenfeld et al., 2010). In most cases, 'leader cells' at the front of an advancing group of cells generate forces that are transmitted rearward from cell to cell, and thus act to pull along the 'follower cells' (Gov, 2007; Omelchenko et al., 2003; Poujade et al., 2007; Vaughan and Trinkaus, 1966). However, traction forces that arise predominately within follower cells and extend over several cell rows to cells at the leading edge have been observed during the collective migration of cultured MDCK cells (Xavier Trepat, 2009). Though, the contribution of forces created by lagging cells during tissue morphogenesis is unclear.

We are investigating the forces governing the morphogenesis of the *C.elegans* hermaphrodite vulva, a tubular organ that connects the uterus to the outside and permits egg-laying. While the molecular mechanisms that regulate cell fate specification during vulval induction have been characterized in great detail, much less is known about the signaling pathways controlling vulval morphogenesis (Sternberg, 2005). During vulval induction, the interplay between the EGFR/RAS/MAPK and NOTCH pathways determines the two vulval cell fates. The gonadal anchor cell (AC) induces the primary (1°) cell fate in the adjacent vulval precursor cell (VPC) P6.p by activating the EGFR/RAS/MAPK pathway. High levels of MAPK activity in P6.p result in the phosphorylation and inactivation of the LIN-1 ETS transcription factor that represses 1° cell fate specification in the remaining VPCs (Beitel et al., 1995). P6.p then induces via a lateral DELTA/NOTCH signal the neighboring VPCs P5.p

and P7.p to adopt the secondary (2°) cell fate (Greenwald, 2005). The three induced VPCs P5.p, P6.p and P7.p go through three rounds of cell divisions to generate 22 vulval cells with seven distinct sub-fates. The seven descendants of each P5.p and P7.p adopt the VulA, VulB1, VulB2, VulC and VulD sub-fates, while the eight 1° descendants of P6.p adopt the VulE and VulF sub-fates (Fig. 1 I) (Sharma-Kishore et al., 1999). During the subsequent phase of morphogenesis, the vulval cells invaginate and move inward (i.e. from the ventral midline towards the dorsal uterus) to form the vulval lumen. At the same time, the cells extend circumferentially towards the vulval midline, where they make homotypic contacts with their contralateral partner cells of the same sub-fate, thereby forming seven concentric epidermal rings called vulval toroids. In a final step, the AC expands the dorsal lumen of VulF (Estes and Hanna-Rose, 2009). Thereafter, the AC retracts and fuses with the uterine-seam cell (utse) syncytium.

We have found that NOTCH signaling in the 2° cells positively regulates via the LIN-1 transcription factor and the Rho-kinase LET-502 the formation of a contractile force on the apical surface of the 2° toroids, thereby generating an inward pushing force.

EGFR/RAS/MAPK signaling, on the other hand, prevents contraction of the 1° toroids by inhibiting LIN-1 activity, allowing the AC to expand the 1° toroid lumen, which generates an inward pulling force. We thus propose a push-pull model for vulval morphogenesis, in which antagonistic NOTCH and RAS/MAPK signaling coordinates actomyosin-induced forces that shape the toroids.

Results

LET-502 is differentially expressed in the 2° vulval cell lineage

Signaling by the LIN-12 NOTCH pathway in the 2° vulval cells activates the LAG-1 transcription factor, which is bound to **L**ag-1 **B**inding **S**ites (LBS) defined by the RTGGGAA consensus motif in the regulatory regions of its target genes (Christensen et al., 1996). In order to identify genes specifically expressed in the 2° cell lineage, we undertook an *in silico* screen for genes containing multiple conserved LBS sites in their regulatory region followed by analysis of transcriptional reporters for selected candidates. This approach identified *let-502,* which encodes a Rho-activated kinase (Wissmann et al., 1997), as one candidate gene specifically expressed in the 2° lineage (suppl. Tab. s1) .

The *let-502* enhancer/promoter region contains four conserved LBS motifs upstream of the transcription start site (dashed arrows in Fig. 1A). To further analyze the expression pattern of *let-502* during vulval development, we examined the expression of a $P_{let\text{-}502}$*::gfp*

transcriptional reporter containing 2,8 kilobase (kb) pairs upstream of the *let-502* translational start site fused to a *gfp* cassette (Dupuy et al. (2007), kind gift of the *C.elegans* gene expression consortium). $P_{let\text{-}502}$*::gfp* was expressed at equal levels in P3.p-P8.p before vulval induction in early to mid L2 larvae (Fig. 1B and data not shown). However, during vulval induction the *let-502* reporter was down-regulated in the 1° descendants of P6.p, while expression gradually increased in the P5.p and P7.p descendants that form the 2° lineage (Fig.1C,I). *let-502* expression peaked at the onset of vulval morphogenesis, when highest expression was observed in the 2° cells (Fig. 1D,I and suppl. Fig. s1A). Thus, *let-502* transcription is up-regulated in the 2° and down-regulated in the 1° cells after the vulval cell fates have been specified.

LET-502 expression is regulated by LIN-12 NOTCH signaling via LIN-1 ETS

Since the 2° lineage-specific expression of *let-502* is similar to the expression pattern of *lip-1*, which is a direct LIN-12 target gene (Berset et al., 2001), we tested if LIN-12 controls *let-502* transcription. $P_{let\text{-}502}$*::gfp* was expressed in the ectopic 2° cells induced in *lin-12(gf)* mutants, while vulval *let-502* expression was absent in *lin-12(lf)* mutants, in which P5.p and P7.p adopt the 1° or 3° instead of the 2°cell fate (Fig. 1E,F) (Greenwald et al., 1983). Thus, NOTCH signaling is necessary and sufficient to induce *let-502* transcription in 2° vulval cells. To test if LIN-12 directly regulates *let-502* transcription, we created the $P_{let\text{-}502}$ Δ*LBS::gfp* reporter in which all four LBS sites had been mutated from R**T**GGGAA to R**A**GGGAA. Surprisingly, the $P_{let\text{-}502}$Δ*LBS::gfp* mutant reporter did not show any change in the expression pattern compared to the wild-type reporter (Fig. 2A, suppl. Fig. s1B), suggesting that *let-502* is an indirect LIN-12 target. We thus performed a deletion analysis of the *let-502* regulatory region to identify the enhancer elements controlling *let-502* expression in the 2° lineage (Fig. 2A). This approach identified a 300bp region between positions -1800 and -1400 containing a cluster of four putative ETS binding sites (EBS) defined by the core motif $GGA^{A}/_{T}$ (Sementchenko and Watson, 2000; Zhang and Greenwald). The *lin-1* gene encodes an ETS family transcription factor that was originally identified as a repressor of vulval development (Beitel et al., 1995). We thus examined *let-502* expression in *lin-1(n304lf)* mutants, in which all six VPCs adopt an alternating pattern of 1° and 2° cell fates. Even though P5.p and P7.p execute a normal 2° cell lineage in *lin-1(lf)* mutants (Beitel et al., 1995), no vulval expression of the $P_{let\text{-}502}$*::gfp* reporter was observed in *lin-1(lf)* mutants (Fig. 1H). To determine the epistatic relationship between *lin-12* and *lin-1*, $P_{let\text{-}502}$*::gfp* expression was analyzed in *lin-12(gf); lin-1(lf)* double mutants, in which all VPCs adopt a 2° cell fate.

Similar to *lin-1(lf)* single mutants, no vulval $P_{let\text{-}502}$*::gfp* expression was detected in *lin-12(gf); lin-1(lf)* double mutants (Fig. 1H). Taken together, these results indicate that LIN-12 regulates *let-502* expression in the 2° vulval cells indirectly via LIN-1. Since LIN-1 activity is negatively regulated by MAPK phosphorylation in 1° cells and LIN-12 signaling blocks MAPK activation in 2° cells by inducing inhibitors of the RAS/MAPK pathway such as the MAPK phosphatase LIP-1 (Berset et al., 2001; Greenwald, 2005), we hypothesized that the non-phosphorylated form of LIN-1 may act downstream of LIN-12 as a positive regulator of *let-502* transcription in the 2° cell lineage (Fig. 1K).

The non-phosphorylated form of LIN-1 activates *let-502* transcription in the 2° vulval cells

To test the model shown in Fig. 1K, we first generated the $P_{let\text{-}502}$ *ΔEBS::gfp* reporter, in which the four putative EBS were deleted (Fig. 2A). In two out of three transgenic $P_{let\text{-}502}$ *ΔEBS::gfp* lines, no reporter expression was detected in the vulval cells, and a third line showed weak expression (Fig. 2A, suppl. Fig. s1C). We then examined whether LIN-1 directly binds to the *let-502* enhancer region by performing chromatin immunoprecipitation (ChIP) experiments (Mukhopadhyay et al., 2008). Since LIN-1 activity is negatively regulated by MPK-1-mediated phosphorylation at the C terminus, we generated a non-phosphorylatable version of LIN-1 by truncating 90 amino acids from the C-terminus, analogous to the premature stop mutation found in the *lin-1(e1790)* gain-of-function allele (Jacobs et al., 1998). This constitutively active, C-terminally truncated LIN-1 (LIN-1ΔCT) was tagged with a hemagglutinin-streptavidin tag (HA) (Glatter et al., 2009) at the N-terminus and expressed under control of the temperature-sensitive heat-shock promoter (*hs::HA::lin-1ΔCT).* In *hs::HA::lin-1ΔCT* animals that had been subjected to a brief heat-shock and analyzed 4 hours later by ChIP using anti-HA antibodies, we detected strongest binding to region B (position -1518 to -1660 bp) that spans the four EBS (Fig. 2A,B). Binding to region A located upstream of the EBS (-1640 to -1810 bp) or to region C near the translational start site (position -4 to -211 bp) was weaker than to region B but stronger than in negative control ChIPs using total IgG antiserum. In *hs::HA::lin-1ΔCT* animals that had not been subjected to a heat-shock, binding to region B was still above background levels, probably because of basal activity of the heat-shock promoter at the standard growth temperature of 20°C (Fig. 2B).

Next, we investigated whether induction of LIN-1ΔCT after cell fate specification had occurred was sufficient to induce *let-502* expression during vulval morphogenesis. In *hs::lin-*

1ΔCT; $P_{let\text{-}502}$*::gfp* animals that had been heat-shocked at the Pnp.xx or Pnp.xxx stage, *let-502* expression was up-regulated in the 1° and 2° cells at the onset of invagination (late L3) and in 2° cells of the late L4 (Pn.pxxx) stage (Fig. 2C through F). We also examined *lin-31,* which encodes a Forkhead transcription factor that represses the 1° vulval cell fate in P6.p together with LIN-1 (Tan et al., 1998). *lin-31(lf)* causes the ectopic induction of 1° and 2° vulval cell fates in the distal VPCs P3.p, P4.p and P8.p. (Miller et al., 1993). However, *let-502* continued to be expressed in *lin-31(lf)* mutants, both in the descendants of the ectopically induced distal VPCs as wells in the P5.p and P7.p descendants (Fig. 2G). Thus, LIN-1 does not require LIN-31 to induce *let-502* expression during vulval morphogenesis.

Since signaling by the MAP kinase MPK-1 results in the inactivation of LIN-1 via phosphorylation, we hyper-activated MPK-1 using a heat-shock-inducible *mpk-1* transgene (*hs::mpk-1*), which allowed us to temporally control LIN-1 activity (Lackner and Kim, 1998). Consistent with the model shown in Fig. 1K, an increase in MPK-1 activity at the Pn.px to Pnp.xx stage resulted in the loss of *let-502* expression in the P5.p and P7.p descendants at the late L4 (Pn.pxxx) stage (Fig. 2I).

Taken together, the binding of LIN-1ΔCT to a region containing EBS sites required for vulval *let-502* expression and the changes in *let-502* reporter expression after activation or inactivation of LIN-1 during morphogenesis indicate that the non-phosphorylated form of LIN-1 positively regulates *let-502* transcription in the 2° vulval cell lineage.

LET-502 is required for toroid contraction during vulval morphogenesis

To investigate the role of *LET-502* Rho kinase during vulval morphogenesis, we examined the apical cell junctions of the vulval toroids using a DLG-1::RFP reporter (Diogon et al., 2007). In addition, we visualized F-actin filaments using a transgene in which the actin-binding domain of Abp140 (first 17 amino acids) had been fused to GFP and expressed under the control of the pan-epithelial *dlg-1* promoter ($P_{dlg\text{-}1}$*::LifeAct::gfp*) (Pohl and Bao, 2010; Yang and Pon, 2002).

In the 2° VulA, VulB1 and VulB2 toroids of wild-type L4 larvae, actin microfilaments (MFs) were arranged in circumferential rings, which localized in proximity to DLG-1::RFP outlining the apical junctions on the luminal side of the toroids (Fig. 3A,C). In contrast, the MFs in the 1° VulE and VulF toroids formed a pyramidal shaped meshwork oriented along the dorso-ventral (D/V) axis, thereby connecting VulE and VulF on the dorsal side to the ventral uterus and on the ventral side to the 2° toroids. Weak LifeAct::GFP staining was also visible in the cell bodies of VulB1 and VulB2 (asterisks in Fig. 3A).

In *let-502(ok1283)* mutants at the L4 stage, we did not observe an obvious change in cell fate marker expression (suppl. Fig. s2) or number of vulval toroids, though the overall shape of the toroids appeared to be distorted (Fig. 3B,D). Specifically, the average diameter of the 2° VulA toroid lumen was increased about two-fold, while the combined height of the 2° toroids was decreased (Fig. 3F,G). The 1° VulE and VulF toroids, on the other hand, were stretched along the D/V axis, and their combined height was increased (Fig. 3B,G). Moreover, actin MFs in the 2° VulA, VulB1 and VulB2 toroids of *let-502(ok1283)* mutants appeared to be slightly disorganized, even tough they still formed circumferential rings (Fig. 3D).
Furthermore, we examined the localization of LET-502 in the vulval toroids using a translational GFP fusion reporter, which could rescue the vulval morphogenesis defects of *let-502(ok183)* mutants (Fig. 3F). LET-502::GFP was localized uniformly in the cytoplasm of 2° vulval cells (suppl. Fig. s3).
Taken together, the increased diameter and decreased height of the 2° toroids in *let-502* mutants together with the circumferential localization of actin MFs near the apical junctions of the 2° toroids suggested that actomyosin-mediated contraction on the luminal side of the 2° toroids is essential to shape the 2° vulval toroids.

LET-502 regulates 2° toroid diameter via apical actomyosin contraction

We next visualized myosin filaments either by staining L4 larvae with an antibody against non-muscle myosin NMY-2 (Guo and Kemphues, 1996) or by observing expression of a myosin light chain MLC-4::GFP reporter, in which threonine 17 and serine 18 had been changed to aspartate to create a constitutively active form (MLC-4DD::GFP) (Gally et al., 2009). Importantly, the MLC-4DD::GFP reporter shows similar expression as a wild-type MLC-4::GFP reporter in embryos (Gally et al., 2009). MLC-4DD::GFP as well as NMY-2 localized similar to actin MFs adjacent to the apical junctions (Fig. 4A,B). While NMY-2 appeared to be equally expressed near the junctions of all toroids, sub-apical expression of MLC-4DD::GFP was only observed in VulA, VulB1 and VulB2 toroids (Fig. 4B). This further differentiates the vulval toroids into two distinct types, the VulA, VulB1 and VulB2 containing actin-myosin bundles organized in circumferential rings and the VulC, VulD, VulE and VulF toroids containing lower amounts of MLC-4 and no circumferential actin MF.
Since LET-502 ROCK directly phosphorylates MLC-4 to induce actomyosin mediated contraction (Diogon et al., 2007), we examined whether expression of the constitutively active, phosphorylation-independent MLC-4DD form was able to reduce the diameter of the

2° toroids in the absence of *let-502*. Since *let-502(ok1283), [mlc-4DD::gfp]* animals were inviable for unknown reasons, we used RNAi to knock-down *let-502* function. While *let-502* RNAi caused approximately a 40% increase in 2° toroid diameter compared to the vector RNAi controls, no significant increase in lumen diameter was observed in the *[mlc-4DD::gfp]* siblings treated with *let-502* RNAi (Fig. 4C). Thus, LET-502 induces via MLC-4 actomyosin-mediated contraction of the 2° toroids.

LIN-1 regulates multiple aspects of vulval morphogenesis

Since LIN-1 directly activates *let-502* transcription in the 2° vulval cells, we examined if loss of *lin-1* function may cause similar vulval morphogenesis defects as *let-502(lf)*, in addition to the ectopic vulval induction caused by loss of the inhibitory LIN-1 function during vulval fate specification. We first examined vulval toroid formation in *lin-1(n304lf)* mutants at the L4 stage by staining apical junctions with the MH27 antibody against AJM-1. (Since the *dlg-1::rfp* reporter used for the previous experiments maps in the close vicinity of *lin-1*, this reporter could not be used.) Although P5.p, P6.p and P7.p adopt a normal 2°-1°-2° pattern of cell fates based on cell lineage analysis (Beitel et al., 1995), their descendants failed to form any ring-like structures characteristic of vulval toroids (Fig. 5B). Instead, the vulval cells retained a square shape and failed to extend the circumferential processes containing actin bundles that were observed in the wild-type (Fig. 5F). In contrast, in animals carrying a gain-of-function mutation in *let-60 ras*, P5.p, P6.p and P7.p formed toroids with a similar morphology as in the wild-type (Fig. 5C) (Sharma-Kishore et al., 1999), indicating that hyper-activation of the RAS/MAPK pathway *per se* does not disrupt vulval morphogenesis. To further investigate the role of LIN-1 during vulval morphogenesis, we inactivated LIN-1 after vulval fate specification had occurred by providing a pulse of MPK-1 activity using the *hs::mpk-1* transgene, thereby phosphorylating and inactivating LIN-1 in all vulval cells. When *hs::mpk-1* animals were heat-shocked at the Pnp.xx-Pnp.xxx stage (Fig. 5A), we observed not only a loss of *let-502* expression as shown in Fig. 2I, but also an abnormal toroid formation (Fig. 5E). Except for the VulF cells, no toroid-like structures were formed by the P5.p, P6.p and P7.p descendants at the L4 stage, similar to the constitutive *lin-1(n304)* mutants. Moreover, the diameter of the vulval lumen was increased to a similar extent as in *let-502(ok1283)* mutants (Fig. 5G).

Thus, inactivation of LIN-1 after vulval induction almost completely disrupts vulval toroid formation, suggesting that LIN-1 functions as a global regulator of vulval morphogenesis controlling additional target genes besides *let-502*.

Contraction of the 2° toroids generates an inward pushing force, while the AC pulls on the 1° cells

The increased lumen diameter and reduced height of the 2° toroids in *let-502* mutants suggested that the contraction of the 2° toroids might generate an inward (i.e. from ventral towards dorsal) pushing force during vulval invagination. To test this hypothesis, we performed cell ablation experiments in a wild-type background removing the 2° descendants of P5.p and P7.p at the Pn.pxx stage before the onset of vulval invagination. Ablation of the 2° vulval cells alone did not block invagination of the remaining 1° cells, but rather caused an increase in the height of the 1° toroids (Fig. 6B,E; n=11). The residual invagination and increased height of the 1° toroids in the absence of 2° cells suggested the existence of a pulling force acting on the 1° toroids. We therefore asked if the AC is required to induce this pulling force. Ablation of the AC before the onset of invagination caused an increase of the 1° and a simultaneous decrease of the 2° toroid height at the Pn.pxxx stage (Fig. 6C,E; n=10), suggesting that the AC indeed generates an inward pulling force on the 1° toroids. Interestingly, AC ablation increased the height of the 1° VulF but not the VulE toroid, while ablation of the 2° cells increased the height of both the VulF and VulE toroids (Fig. 6F). Finally, simultaneous ablation of the AC and the 2° cells resulted in the formation of a very small vulval lumen without a connection between the uterus and the cuticle (Fig. 6D; n=10). The height of the remaining toroids could not be reliably quantified due to their small size and severely distorted morphology. Taken together, the inward pushing force from the 2° toroids and the inward pulling force exerted by the AC on the 1° toroids are both required during vulval invagination.

To characterize the dynamic shape changes of the toroids in more detail, we followed vulval morphogenesis in wild-type L4 larvae expressing the apical junction marker AJM-1::GFP (Koppen et al., 2001) by time-lapse (4D) microscopy and quantified the changes in toroid diameter and height over time. As the diameter of the ventral-most VulA toroid lumen decreased to its final size of less than 15µm, the height of the 2° toroids increased (Fig.7A,D,E, supplementary movie s1, quantification of one out of three similar recordings is shown). During this first phase of 2° toroid contraction, the height of the 1° toroids did not change significantly (Fig.7E). After the 2° toroids had fully contracted in mid L4 larvae, we observed an increase in the diameter of the dorsal toroid lumen (Fig. 7B,F, supplementary movie s2, quantification of one out of five similar recordings is shown). Even though 1° toroid height remained constant, the combined height of all toroids further increased during

this final phase of dorsal (VulF) toroid lumen expansion (Fig. 7G). In AC ablated animals, on the other hand, dorsal toroid lumen did not expand and the 1° toroid lumen thus remained small (Fig. 6C).

Finally, we tested whether the vulval lumen in L4 larvae represents a closed compartment to which pressure is being applied during morphogenesis. For this purpose, we punctured the ventral epidermis separating the vulval lumen from the outside using a cell ablation laser. This microsurgery caused a rapid efflux of fluids and collapse of the vulval lumen (Fig. 7C, suppl. movie s3; n=5). The appearance of the vulva after this induced collapse of the lumen was remarkably similar to the vulva in young adult animals after vulval eversion had occurred.

Based on the changes in 1° toroid height and diameter induced by 2° cell or AC ablation and the increase in toroid height during 2° toroid contraction and 1° toroid expansion, we propose a push-pull mechanism underlying vulval morphogenesis (Fig. 7H). Actomyosin driven contraction of the 2° toroids first generates an inward pushing force, while AC induced dorsal toroid lumen expansion in a subsequent step produces an inward pulling force (Fig. 7H).

Discussion

LIN-1 links cell fate specification and morphogenesis

The actomyosin network is a universal force-generating mechanism used in many developmental processes to control the shape of individual cells and thereby the morphogenesis of entire organs or embryos (Marston and Goldstein, 2006). In this process, Rho kinase-mediated phosphorylation of the regulatory myosin light chain (rMLC) is a key regulatory step that induces actomyosin contraction (Gally et al., 2009). We have discovered a direct link between the cell fate specification pathways determining the 1° and 2° vulval fates and the force generating actomyosin network used during vulval morphogenesis. Rho kinase *let-502* transcription is directly induced by the ETS-family transcription factor LIN-1 (Fig. 1K). High levels of NOTCH signaling in the 2° vulval cells prevent activation of the MAPK and thus keep LIN-1 in its active, un-phosphorylated state, while high levels of MAPK signaling in the 1° cells result in the phosphorylation and inactivation of LIN-1. In this manner, a differential expression of Rho kinase *LET-502* is established during the subsequent phase of vulval morphogenesis, such that high levels of *LET-502* are maintained in the 2° cells, whereas *LET-502* expression gradually fades in the 1° cells. In contrast to

LET-502, the RHO-1 GTPase and the RHO guanine exchange factor ECT-2 are uniformly expressed in 1° and 2° vulval cells (S. Canevascini and A. Hajnal, unpublished results), suggesting that the control of *LET-502* expression may be key to regulate actomyosin activity. Our results also indicate that continuous RAS/MAPK and NOTCH signaling is required to maintain this differential *LET-502* expression, as activation and inactivation of LIN-1 after vulval fate specification altered *LET-502* expression levels and perturbed vulval morphogenesis. Hence, expression of both the EGFR ligand by the AC and the NOTCH ligands by the 1° vulval cells are maintained until the final stage of vulval development.
It has recently been reported that RAS and NOTCH signaling regulate the different steps in the development of the *C.elegans* excretory system (Abdus-Saboor et al., 2011). Also in this organ, RAS and NOTCH signaling do not only control the specification of the different cell fates, but at a later time point are also involved in the morphogenesis of the excretory tube. Though, if and how LIN-1 directly regulates excretory tube morphogenesis is not known. Interestingly, LIN-1 appears to control multiple aspects of vulval morphogenesis besides regulating *LET-502* expression and independently of its earlier inhibitory role during VPC fate specification. Even though the VPCs in *lin-1(lf)* mutants adopt an alternating pattern of 1° and 2° cell fates (Beitel et al., 1995), vulval toroids are largely absent and actin filaments do not organize in circumferential bundles in the 2° toroids. Therefore, LIN-1 in addition appears to be necessary for the formation of circumferential cell extensions and homotypic cell contacts during vulval toroid formation by regulating distinct target genes. The opposing effects of the NOTCH and RAS/MAPK signaling pathways on LIN-1 activity thus orchestrate the cell shape changes necessary for vulval tube formation.

Contraction of the 2° toroids generates an inward pushing force

The 2° vulval toroids differ from the 1° toroids not only by higher *LET-502* expression levels but also by a fundamentally different orientation of the actomyosin network (Fig. 7H). While actin filaments are organized in circumferential bundles near the apical surface of the 2° VulA, VulB1 and VulB2 toroids, actin filaments in the 1° VulE and VulF toroids are aligned along the dorso-ventral axis and connected dorsally to the junctions between VulF and the uterus and ventrally to the junction between VulD and VulE. Ishiuchi and Takeichi (2011) proposed that actomyosin contraction is activated by inducing the redistribution of Rho-kinases from the cytoplasm to apical junctions. However, we observed a uniform cytoplasmic localization of a functional *LET-502*::GFP protein in the 2° toroids, and loss of *let-502* function did not change the overall orientation or organization of actin filaments. In contrast,

expression of the regulatory myosin light chain MLC-4 was restricted to the subapical domain near the adherens junctions of the VulA, VulB1 and VulB2 toroids. Thus, only the three ventral-most toroids are capable of contracting in response to *LET-502* activation, while actin filaments in the 1° toroids may serve to transmit mechanical forces from the AC to the toroids. It is not known how the different orientation of the actin fibers in 1° and 2° toroids is established.

The generation of an inward pushing force by 2° toroid contraction requires that the vulval lumen represents a closed compartment to which pressure can be applied. Indeed, when the vulval lumen was punctured in L4 larvae, this resulted in an almost instantaneous collapse of the vulval lumen and vulval eversion, indicating that the luminal space indeed represents a closed compartment that is under pressure. Moreover, mutations in the *sqv* genes, which encode proteins required for the biosynthesis or secretion of glycoproteins, cause a drastic reduction in the size of the vulval lumen (Herman et al., 1999; Herman and Horvitz, 1999; Hwang et al., 2003). It was therefore proposed that hygroscopic proteoglycans secreted into the vulval lumen cause fluids to fill up the vulval lumen and build up osmotic pressure. A reduction in the radius of the lumen on the ventral side will therefore cause an elongation of the lumen dorsally and thereby generate an inward pushing force (Fig. 7H).

The AC induces an inward pulling force in the 1° toroids

Ablation of the 2° vulval cells alone did not prevent invagination of the 1° cells. However, simultaneous ablation of the 2° cells and the AC almost completely blocked vulval lumen formation. Thus, the AC induces an inward pulling force that acts cooperatively with the inward pushing force generated by 2° toroid contraction. It is possible, that the AC serves -as its name indicates- to anchor the vulval toroids to the uterus, which might generate a mechanical pulling force. However, at a later stage of vulval morphogenesis, after the 2° toroids had contracted ventrally , we observed a dorsal expansion of the 1° toroid lumen, which is induced by the AC. It has previously been reported that invasion of the AC into the vulval tissue is necessary for dorsal lumen morphogenesis, after which the AC retracts again and fuses with the utse (Estes and Hanna-Rose, 2009). Accordingly, when we ablated the AC after invasion but before the onset of invagination, this resulted in a reduced size of the 1° vulval lumen and increased height of VulF (Fig. 6C). Thus, the AC is required for proper VulF morphogenesis through direct cell-cell contact and to expand the dorsal, 1° toroid lumen. The AC may increase the diameter of the 1° lumen by secretion of hygroscopic proteins, it may mechanically stretch the VulF toroid or induce remodeling of the cytoskeleton in VulF through direct cell-cell interaction. In either case, dorsal lumen

expansion by the AC is accompanied by a further increase in total toroid height. We thus propose that the dorsal expansion of the 1° toroids by the AC generates an inward pulling force, which promotes vulval invagination together with the ventral contraction of the 2° toroids.

Leaders and followers cooperate

Tissue morphogenesis depends on collective cell movements and the transmission of mechanical forces between different cell types. In many examples of collective cell migration, specific leader cells have been identified that generate a mechanical force, which is transmitted to follower cells (Caussinus et al., 2008; Rorth, 2009; Schottenfeld et al., 2010). However, to what extent the follower cells also contribute forces has remained largely unknown. In analogy to branching morphogenesis in the *Drosophila* tracheal system or to vertebrate angiogenesis, the 1° vulval cells may be regarded as the leader cells, while the 2° cells act as followers (Caussinus et al., 2008; Schottenfeld et al., 2010). NOTCH signaling and an ETS transcription factor are also used during *Drosophila* tracheal development. But in contrast to the *Drosophila* trachea, we find that both 1° leaders and 2° followers produce cooperative forces necessary to form an invagination during *C.elegans* vulval morphogenesis. Finally, we show that the same signaling pathways first used to specify the vulval cell fates are again employed during vulval morphogenesis to differentially regulate actomyosin activity. Vulval fate specification and morphogenesis are therefore tightly coupled processes.

Material and Methods

General methods and strains

C.elegans strains were maintained at 20°C on standard nematode growth media as described previously (Brenner, 1974). The wild-type strain of *C.elegans* used was Bristol N2. Strains used were as follows: LGI: *dpy-5(e907), let-502(ok1283)/hT2[bli-4(e937) let(q782) qIs48] (I;III),* LGIII*: dpy-19(e1259), lin-12(n137)/unc-32(e189) lin-12(n137n720), lin-1(n304), lin-31(n301),* LGIV: *let-60(n1046).* Extrachromosomal and integrated arrays: *gaIs36[hs::mpk-1(+), Dmek-2(wt)]* (Lackner and Kim, 1998)*, swIs79[ajm-1::gfp,*$P_{scm\text{-}1}$*::gfp, unc-119(+)]* (Walser et al., 2006)*, mcIs46[dlg-1::rfp, unc-119(+)]* (Diogon et al., 2007)*, sIs10781[rcesC10H11.9::gfp, pCeh361]* (Dupuy et al., 2007)*, zhEx401[*$P_{let\text{-}502}$*::nls::gfp::lacz::unc-54 3'utr,* $P_{lin\text{-}48}$*::gfp], zhEx402[*$P_{let\text{-}502}$ *LBS Δ1-4::nls::gfp::lacz::unc-54 3'utr,* $P_{lin\text{-}48}$*::gfp], zhEx399[-1.1*$P_{let\text{-}502}$*::nls::gfp::lacz::unc-54 3'utr,* $P_{lin\text{-}48}$*::gfp],*

zhEx403[-2.8P$_{let-502}$ Δ1.1-1.4 kb::nls::gfp::lacz::unc-54 3'utr, P$_{lin-48}$::gfp], zhEx404[-2.8P$_{let-502}$ Δ1.1-1.8 kb::nls::gfp::lacz::unc-54 3'utr, P$_{lin-48}$::gfp], zhEx405[-2.8P$_{let-502}$ Δ1.1-2.2 kb::nls::gfp::lacz::unc-54 3'utr, P$_{lin-48}$::gfp], zhEx393[-2.8P$_{let-502}$ ΔEBS::nls::gfp::lacz::unc-54 3'utr, P$_{lin-48}$::gfp], zhEx395[hs::lin-1ΔCT, P$_{lin-48}$::gfp], zhEx394[hs::3xHA::strep::lin-1ΔCT, P$_{lin-48}$::gfp], zhIs396[P$_{dlg-1}$::lifeact::gfp::unc-54 3'utr, P$_{lin-48}$::gfp], mcEx402[P$_{mlc-4}$::gfp::mlc-4(DD) + P$_{pie-1}$::gfp::mlc-4(wt), rol-6(gf)] (Gally et al., 2009)*, zhEx398[let-502 genomic::gfp::unc-54 3'utr, P$_{lin-48}$::gfp]*.

All constructs were microinjected into the gonad arms of adult worms at concentrations between 2 and 50 ng/µl along with the co-injection marker *P$_{lin-48}$::gfp* at 50 ng/µl and pBluescript added to a final concentration of 150 to 200 ng/µl to generate stable transgenic lines (Mello et al., 1991).

Reporter constructs

For the *P$_{let-502}$::gfp* transcriptional reporter, a 2.8 kb fragment from the 5'-region was PCR amplified with the primers OSF205 and OSF130 containing SalI and BamHI restriction sites and subcloned into pPD96.04. Constructs for the *let-502* promoter deletion analysis (Fig. 2A) were generated by fusion PCR (Hobert, 2002) using primers listed in suppl. Tab. s2. For the *P$_{let-502}$ ΔEBS::nls::gfp::lacz::unc-54 3'utr* reporter, the 4 EBS were deleted by fusion PCR with primers OSF225 and OSF226 and subcloning into pPD96.04 was done as described above for the wild-type reporter. For the *P$_{let-502}$ ΔLBS::nls::gfp::lacz::unc-54 3'utr* reporter, the 4 RTGGGAA motifs were mutated to RAGGGAA using a QuikChange Multi Site-Directed Mutagenesis Kit (Stratagene) with primers OSF132-OSF135. For the *P$_{dlg-1}$::lifeact::gfp::unc-54 3'utr* reporter, a 5.2kb *dlg-1* promoter fragment was amplified with primers OSF278 containing a PstI site and OSF272 containing the *lifeact* coding sequence and a BamHI restriction site and cloned into PstI/ BamHI digested pPD95.75.

For the *P$_{mlc-4}$::mlc-4DD::gfp::unc-54 3'utr* construct, a 2.8kb *mlc-4* promoter fragment was amplified with primers OSF302 and OSF297 and fused with a second second fragment amplified with OSF298 and OSF304 using OSF302 and OSF304. The fusion fragment was digested with PstI and SalI and cloned into pPD95.75. For the *hs::lin-1ΔCT* construct, a 1kb *lin-1* cDNA fragment spanning codons 1-351 followed by a stop codon was amplified with primers OSF185 containing an NheI restriction site and OSF186 containing a KpnI site and cloned into pJK465. For *hs::3xHA::strepIII::lin-1ΔCT*, a 153 bp fragment containing the *3xHA::strep* tag (Glatter et al., 2009) was amplified using OSF223 and OSF224 and inserted

into the NheI site of *hs::lin-1ΔCT*. For the *let-502 genomic::gfp::unc-54 3'utr* rescue construct, a fragment containing -2.8kb upstream to +14.8kbp downstream of the translational start site was amplified using primers OSF196 and OSF253 and fused with GFP amplified from pPD95.75 using primers C' and D'.

RNA interference

RNA interference (RNAi) was performed using the feeding method as described (Kamath et al., 2001). Worms were synchronized at the L1 stage, transferred to nematode growth media plates containing 3 mM IPTG and 50ng/ml ampicillin, seeded with the desired RNAi bacteria and allowed to grow for 3-5 days at 20°C. The first generation progeny was analyzed.

Immunostaining and microscopy

Immunostaining was performed as described previously (Miller and Shakes, 1995). In brief, worms were permeabilized using the freeze-crack method and immediately fixed in methanol at −20 °C. Samples were blocked with 3% BSA, first incubated with primary antibody (1:25 MH27 and 1:1000 anti NMY-2) for 2 h at room temperature, then incubated with secondary antibody (1:100 anti-mouse TRITC and anti-rabbit CY-5), washed and mounted in Mowiol. Fluorescent images were obtained using a Leica DMRA wide-field microscope, equipped with a cooled CCD camera (Hamamatsu ORCA-ER). Images were analyzed using Openlab 3.0 software package (Improvision). For three-dimensional (3D) reconstructions, GFP and RFP images of larvae animals were recorded with an Olympus FV1000 confocal microscope with a stack size of 0.3 to 0.5 µm. For 4D recordings of vulval toroid morphogenesis, animals were mounted on 4% agarose pads containing 2.5 mM tetramisole and immobilized with 100nm latex beads (Polysciences Inc.). Images were recorded on an Olympus BX61 DSU spinning disc microscope at 10 minutes time intervals taking 30 to 40 z-stacks of 0.4 µm per time point.

Image analysis

3D reconstructions were made using Imaris software (7.1.) and 4D movies were analyzed using Image J. Measurements of toroid height and diameters were done on mid-sagittal sections through the toroids of late L4 larvae, after the VulF lumen had expanded and the AC had fused with the utse. For each parameter, the distances shown in suppl. Fig. s4 were measured, and the averages and standard deviations were calculated.

Chromatin immunoprecipitation (ChIP) analysis

For ChIP analysis, chromatin was prepared from *hs::HA::lin-1ΔCT* animals and precipitated with anti HA antibodies (Roche) as described (Mukhopadhyay et al., 2008). As negative control, a mock precipitation using IgG as primary antibody was performed in parallel. In each experiment, samples were processed in triplicates. Binding was quantified by Q-PCR with the probes shown in Fig. 2A. The primers used for probes are shown in suppl. Tab. s2. For each sample, the signal was normalized to the input DNA (Δct) and the % of bound DNA relative to 5% of the input signal was plotted.

ACKNOWLEDGEMENTS

We thank Juan Escobar, Stefan Luschnig and Michael Walser for comments on the manuscript, all present and past group members for critical discussion and Dr. Oleg Georgiev for technical help during cloning. We are also grateful to the *C.elegans* genetics centre, S. Mitani (Japan Knockout Consortium), Gene expression consortium for providing strains, and to Andrew Fire for vectors. S. F. was the recipient of a Forschungskredit grant from the University of Zürich, and travel grants from the Julius Klaus Stiftung and Molecular Life Science PhD program, Zürich. This research was also supported by the Kanton Zürich and by grants from Swiss National Science Foundation to A.H..

Figure legends

Fig. 1 LIN-12 NOTCH induces *LET-502* expression in the 2° vulval lineage via LIN-1 ETS

(A) Structure of the transcriptional $P_{let\text{-}502}$::*gfp* reporter. The locations of the predicted LBS and EBS sites are indicated. (B through D) Time-course analysis of $P_{let\text{-}502}$::*gfp* expression from the L2 until the L4 stage with (B' through D') the corresponding Nomarski images. (E) $P_{let\text{-}502}$::*gfp* expression and (E') the corresponding Nomarski image in *lin-12(lf),* (F and F') *lin-12(gf),* (G and G') *lin-1(lf)* and (H and H') *lin-12(gf); lin-1(lf)* mutans. In all panels, anterior is to the left and ventral is to the bottom, and the dotted lines represent the uterine-vulval boundary. The scale bar is 5 μm. (I) Summary of the *let-502* expression pattern in the vulval cell lineage. The VulA through VulF subfates are indicated. (K) Model for the transcriptional regulation of *let-502* by LIN-12, LET-23 EGFR, MPK-1 MAPK and LIN-1. Alleles used: *lin-12(n137gf), lin-12(n137gf n720lf), lin-1(n301), sIs10781.*

Fig. 2 Non-phosphorylated LIN-1 induces *let-502* transcription in the 2° vulval cells

(A) Structure of reporter constructs used to assay *let-502* promoter activity. Three independent lines were analyzed for each construct. Arrows indicate the positions of the putative ETS binding sites (EBS) and arrowheads the LAG-2 binding sites (LBS). Gray arrowheads in the ΔLBS construct indicate the point-mutations changing the LBS from RTGGGAA to RAGGGAA. Grey arrows in the ΔEBS construct indicate the deletions of the EBS and the deleted nucleotides are shaded in gray. The double headed arrows indicate regions A, B and C used as probes for ChIP. (B) Binding of LIN-1ΔCT to the *let-502* 5' regulatory region detected by ChIP followed by Q-PCR. A, B and C refer to the probe regions shown in (A) and 3' to a probe at the 3' end of the gene. Error bars indicate the standard deviations of three experiments. (C) $P_{let\text{-}502}$*::gfp* expression and the (C') corresponding Nomarski image in a *hs::lin-1ΔCT* larva at the onset of invagination (late Pn.pxx to early Pn.pxxx stage) without heat-shock, and (D, D') the same stage after heat-shock at the Pn.px stage. (E, E') and (F, F') $P_{let\text{-}502}$*::gfp* expression in a *hs::lin-1ΔCT* larva at the late L4 (Pn.pxxx) stage without and after heat-shock at the Pn.pxx stage, respectively. (G, G') $P_{let\text{-}502}$*::gfp* expression in a *lin-31(lf)* L4 larva. Note that expression was detected in the P.5 and P7.p descendant (arrows) as well as in the ectopically induced P3.p and P4.p descendants (underlined). (H, H') $P_{let\text{-}502}$*::gfp* expression in a *hs::mpk-1* larva without and (I, I') after heat-shock at the Pn.pxx stage. In all panels, anterior is to the left and ventral is to the bottom, and the dotted lines represent the uterine-vulval boundary. Scale bars are 5 μm.

Alleles used in (A): *zhEx393, 398, 399, 401-405*,(B): *zhEx394* (C through I): *lin-31(n301), gaIs36, zhEx395, sIs10781*.

Fig. 3 *LET-502* is required for toroid contraction during vulval morphogenesis

(A) 3D reconstructions of LifeAct::GFP expression to visualize polymerized actin, (A') DLG-1::RFP to visualize the apical junctions and (A'') the merged images in the toroids of a wild-type L4 and (B through B'') a *let-502(lf)* L4 larva. (C) through (D'') show ventro-lateral projections of the same animals. The dashed lines in all panels indicate the uterine-vulval boundary. The double arrows in (A) and (B) indicate the height of 1° toroids, and in (A') and (B') the 2° toroid height between the dotted lines. The dashed bracket indicates the VulA lumen diameter. The dashed boxes in (A) and (D) indicate the regions magnified in the insets showing mid-sagittal sections. The asterisks in (A), (B), (C) and (D) indicate LifeAct staining in the cell bodies. The arrowheads in (C) through (D'') indicate the vulval lumen. (F) Average VulA lumen diameter in wild-type, *let-502(lf)* and *let-502(lf)* mutants rescued with the *let-502::gfp* translational fusion. For details on the measurement points used to quantify each parameter, see suppl. Fig. s4. (G) Average 1° and 2° toroid heights in wild-type and *let-502(lf)* mutants. The numbers in brackets indicate the number of animals analyzed and the error bars the standard deviations. The scale bar is 5 µm. Alleles used: *let-502(ok1283), mcIs46, zhIs396.*

Fig. 4 Sub-apical localization of NMY-2 and MLC-4 in the vulval toroids

(A) 3D reconstructions of NMY-2 antibody staining, (A') AJM-1 antibody staining using MH27 monoclonal antibodies and (A'') the merged images in the toroids of an L4 larva. (B) A mid-sagittal confocal section showing MLC-4DD::GFP expression, (B') DLG-1::RFP and (B'') the merged images. NMY-2 localized near the apical junctions of all toroids, while sub-apical MLC-4DD::GFP localization was detected only in VulA, VulB1 and VulB2 toroids. Scale bar is 5µm. (C) Average diameter of the VulA toroid lumen in wild-type and MLC-4DD::GFP L4 larvae treated with *let-502* RNAi or empty vector control. The numbers in brackets indicate the number of animals analyzed and the error bars the standard deviations. Alleles used: *mcIs46, mcEx402.*

Fig. 5 LIN-1 regulates multiple aspects of vulval morphogenesis

(A) Lineage diagram showing the timing of *mpk-1* induction by heat-shock and observation by 3D microscopy. (B) Vulval toroid junctions visualized by MH27 antibody staining in a

lin-1(lf) and (C) *let-60(gf)* mutant L4 larva. (D) Vulval toroid junctions at the L4 stage visualized by DLG-1::RFP expression without and (E) after heat-shock induction of MPK-1 at the Pn.pxx stage. (D') and (E') show mid-sagittal sections of the animals shown in (D) and (E), respectively. (F) Polymerized actin visualized with LifeAct::GFP expression in a *lin-1(lf)* L4 larva. Note the absence of circumferential actin rings formed in 2° cells as shown for the wild-type in Fig. 3A. The dashed lines indicate the vulval-uterine boundary and the dashed brackets the diameters of the multiple invaginations. Scale bars are 5µm. (G) Average VulA diameter without and after heat-shock induction of MPK-1 measured as described in suppl. Fig. s4. Alleles used: *lin-1(n301)*, *mcIs46, gaIs36, zhIs96*

Fig. 6 The 2° cells push and the AC pulls the 1° cell inwards

(A through A''') Nomarski image, DLG-1::RFP labelled junctions, polymerized actin visualized with LifeAct::GFP and merged images in a wild-type L4 larva at the Pn.pxxx stage without ablation, (B through B''') after ablation of the 2° P5.p and P7.p descendants at the Pn.pxx stage, (C through C''') after ablation of the AC at the Pn.pxx stage and (D through D''') after simultaneous ablation of the AC and the 2° P5.p and P7.p descendants. Double headed arrows and the dotted lines indicate the height of the 1° and 2° toroids. Dashed curved lines indicate the junction between VulD and VulE or in (B) and (D) the ventral epidermis and VulE. The scale bar is 5 µm. (E) Average height of the 1° and 2° toroids and (F) VulF and VulE after the different ablations. Measurements were performed as described in suppl. Fig. s4. Alleles used: *mcIs46, zhIs396.*

Fig. 7 Quantitative analysis of vulval toroid morphogenesis.

(A) Mid-sagittal optical sections of individual time frames from a 4D time lapse recording of 2° toroid contraction in an early L4 larva using the AJM-1::GFP marker. (suppl. movie s1) (B) Time-lapse recording of 1° toroid expansion in an L4 larva after the 2° toroids had contracted (see also suppl. movie s2). Each panel shows a z-projection. (C) Puncturing of the vulval lumen in L4 larvae results in a rapid lumen collapse and vulval eversion. The arrow in the first frame indicates the site in the ventral epidermis where the lumen was punctured with an ablation laser. The animals were mounted in a suspension of 100nm latex beads to visualize the efflux of fluids. Measurements on the recordings shown in (A) and (B) were performed on one out of three to five movies obtained for each stage. (D) Quantification of the reduction in VulA lumen diameter and (E) toroid height during 2° toroid contraction in the larva shown in panel (A). (F) Quantification of the increase in VulF lumen diameter and

(G) VulF and total toroid height during dorsal toroid lumen expansion in the animal shown in panel (B). Measurements were performed as described in suppl. Fig. s4. The scale bars are 5 µm. Allele used: *swIs79.*

(H) Push-pull model for vulval morphogenesis. Cell bodies of 1° VulF and VulE toroids are shown in light red, cell bodies of 2° VulD and VulC toroids in light green and of VulB2, VulB1 and VulA in dark green. Green lines indicate actomyosin filaments and black and gray lines the apical cell junctions. *LET-502*-mediated apical contraction of VulA, VulB1 and VulB2 toroids result in an inward pushing force (red arrows), while invasion of the AC (blue cell) into the 1° toroids expands the dorsal toroid lumen and thus generates an inward pulling force (blue arrows).

Figure 1

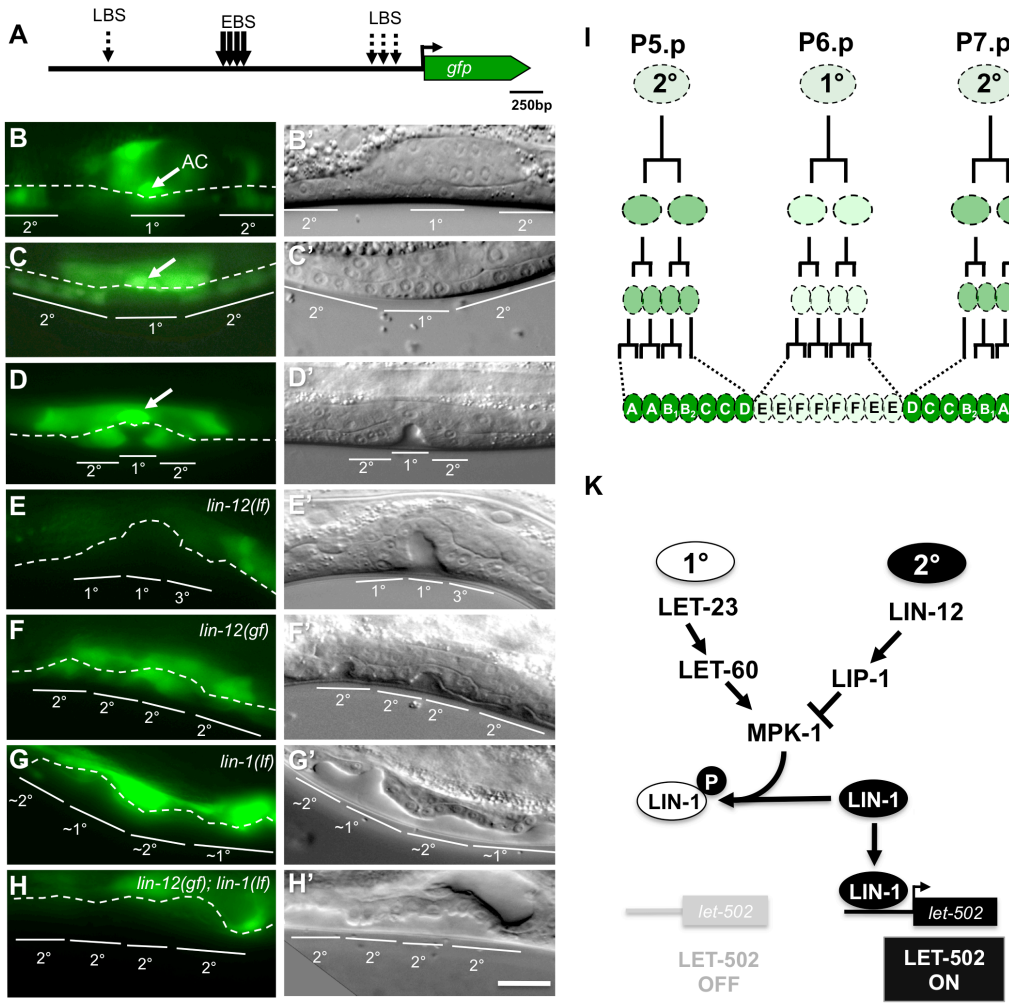
A
LBS
EBS
LBS
gfp
250bp
B
AC
B'
C
C'
D
D'
E
lin-12(lf)
E'
F
lin-12(gf)
F'
G
lin-1(lf)
G'
H
lin-12(gf); lin-1(lf)
H'
I
P5.p
P6.p
P7.p
K
1°
2°
LET-23
LIN-12
LET-60
LIP-1
MPK-1
LIN-1
P
LIN-1
LIN-1
let-502
let-502
LET-502 OFF
LET-502 ON

Figure 2

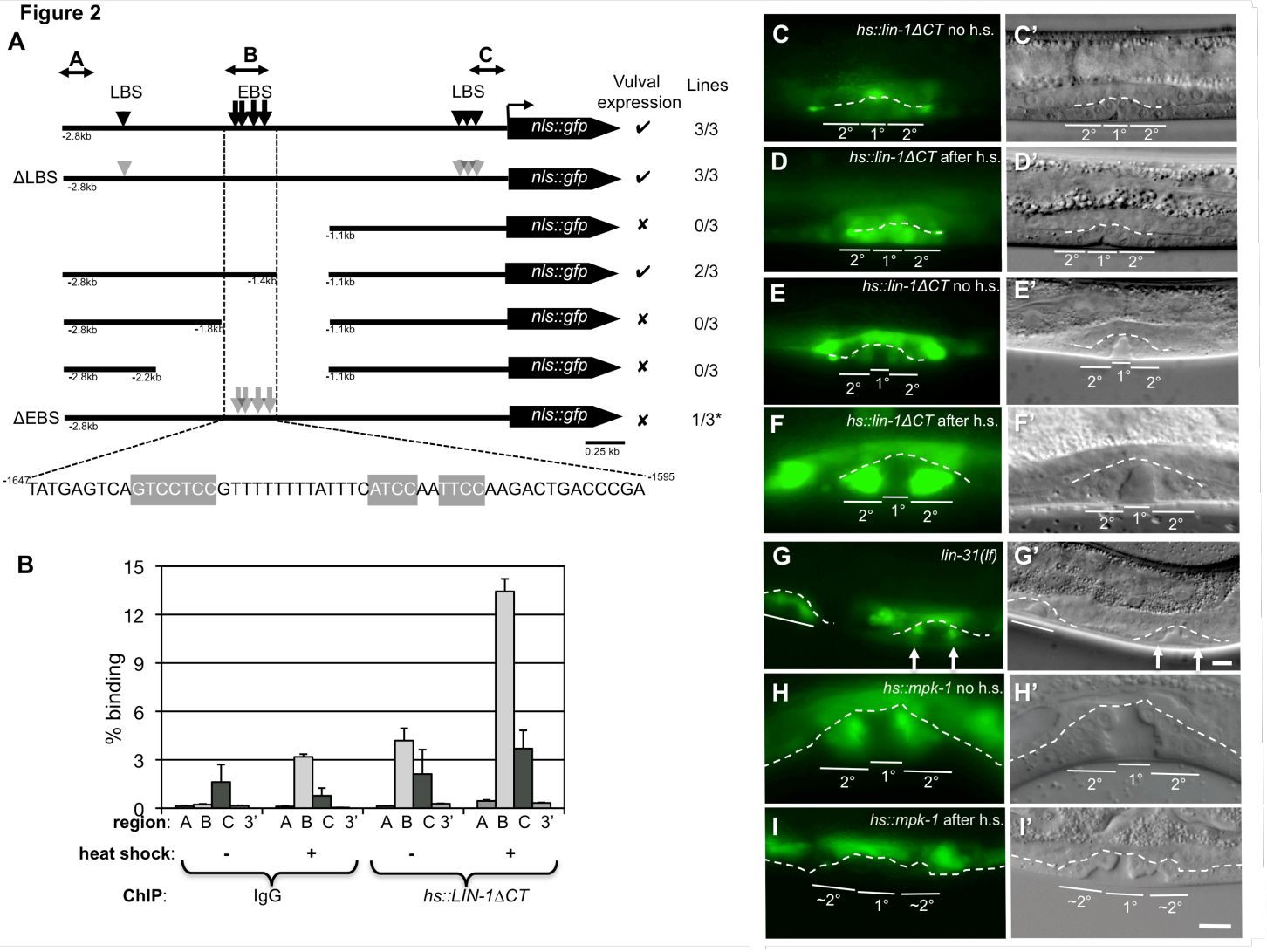
A
A
B
C
LBS
EBS
LBS
Vulval expression
Lines
nls::gfp
-2.8kb
✔
3/3
ΔLBS
✔
3/3
-1.1kb
✘
0/3
-1.4kb
✔
2/3
-1.8kb
✘
0/3
-2.2kb
✘
0/3
ΔEBS
✘
1/3*
0.25 kb
-1647
TATGAGTCAGTCCTCCGTTTTTTTTATTTCATCCAATTCCAAGACTGACCCGA
-1595
B
% binding
15
12
9
6
3
0
region: A B C 3' A B C 3' A B C 3' A B C 3'
heat shock: - + - +
ChIP: IgG hs::LIN-1ΔCT
C hs::lin-1ΔCT no h.s.
C'
D hs::lin-1ΔCT after h.s.
D'
E hs::lin-1ΔCT no h.s.
E'
F hs::lin-1ΔCT after h.s.
F'
G lin-31(lf)
G'
H hs::mpk-1 no h.s.
H'
I hs::mpk-1 after h.s.
I'
2° 1° 2°
~2° 1° ~2°

Figure 3

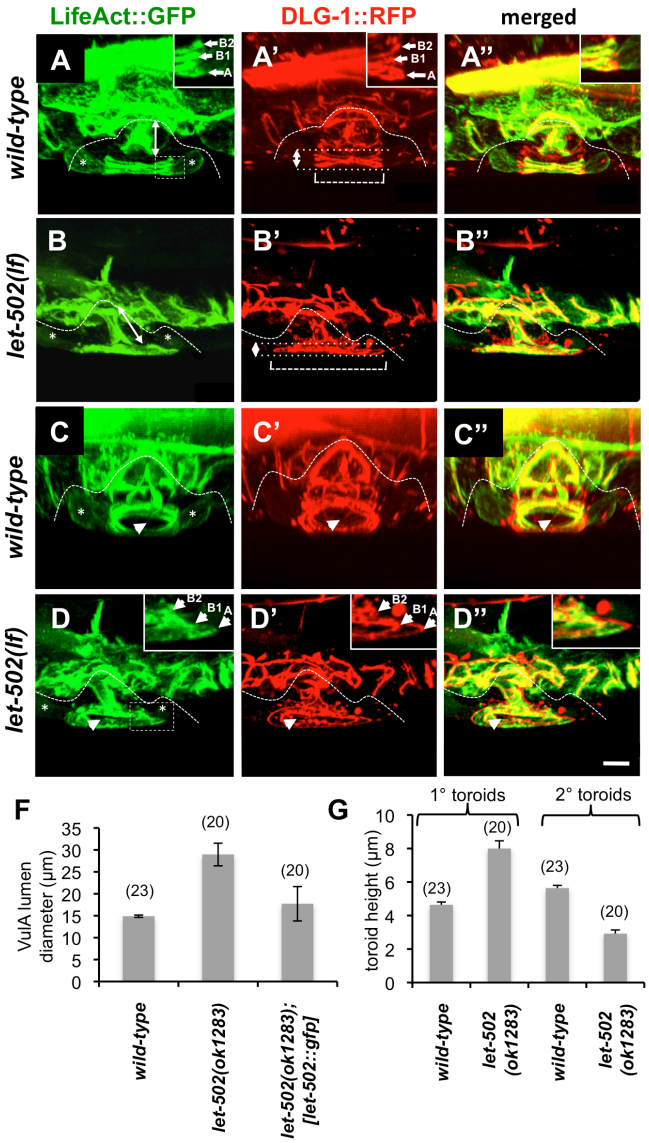
LifeAct::GFP
DLG-1::RFP
merged
wild-type
let-502(lf)
wild-type
let-502(lf)
A
A'
A''
B
B'
B''
C
C'
C''
D
D'
D''
B2
B1
A
F
VulA lumen diameter (µm)
(23)
(20)
(20)
wild-type
let-502(ok1283)
let-502(ok1283); [let-502::gfp]
G
1° toroids
2° toroids
toroid height (µm)
(23)
(20)
(23)
(20)
wild-type
let-502 (ok1283)
wild-type
let-502 (ok1283)

Figure 4

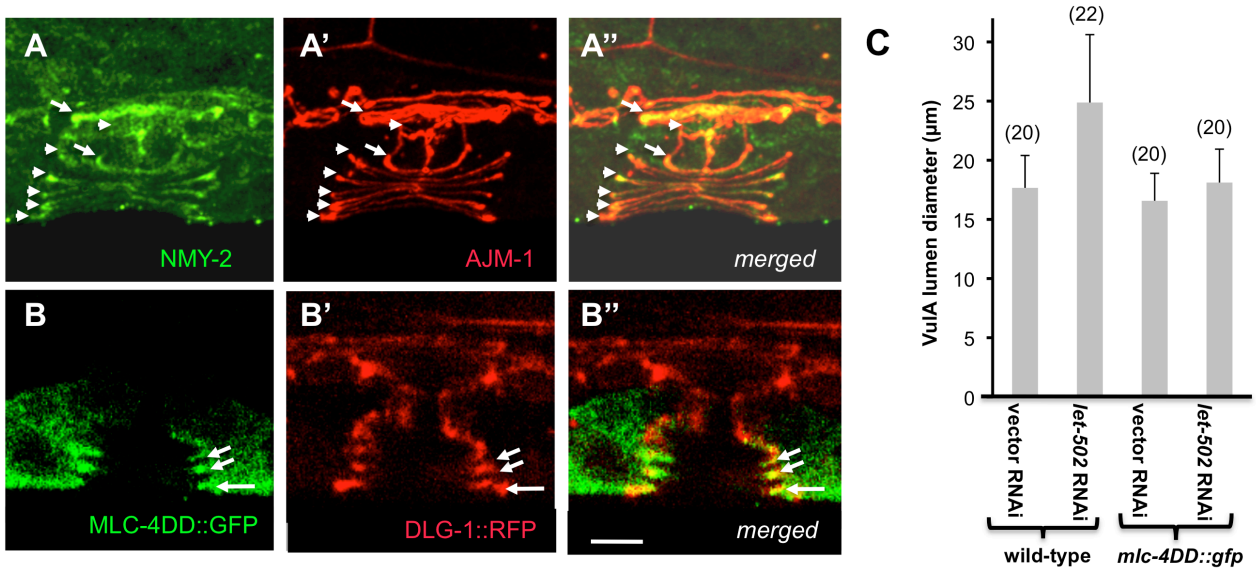
A
NMY-2
A'
AJM-1
A''
merged
B
MLC-4DD::GFP
B'
DLG-1::RFP
B''
merged
C
VulA lumen diameter (µm)
0
5
10
15
20
25
30
(20)
(22)
(20)
(20)
vector RNAi
let-502 RNAi
vector RNAi
let-502 RNAi
wild-type
mlc-4DD::gfp

Figure 5

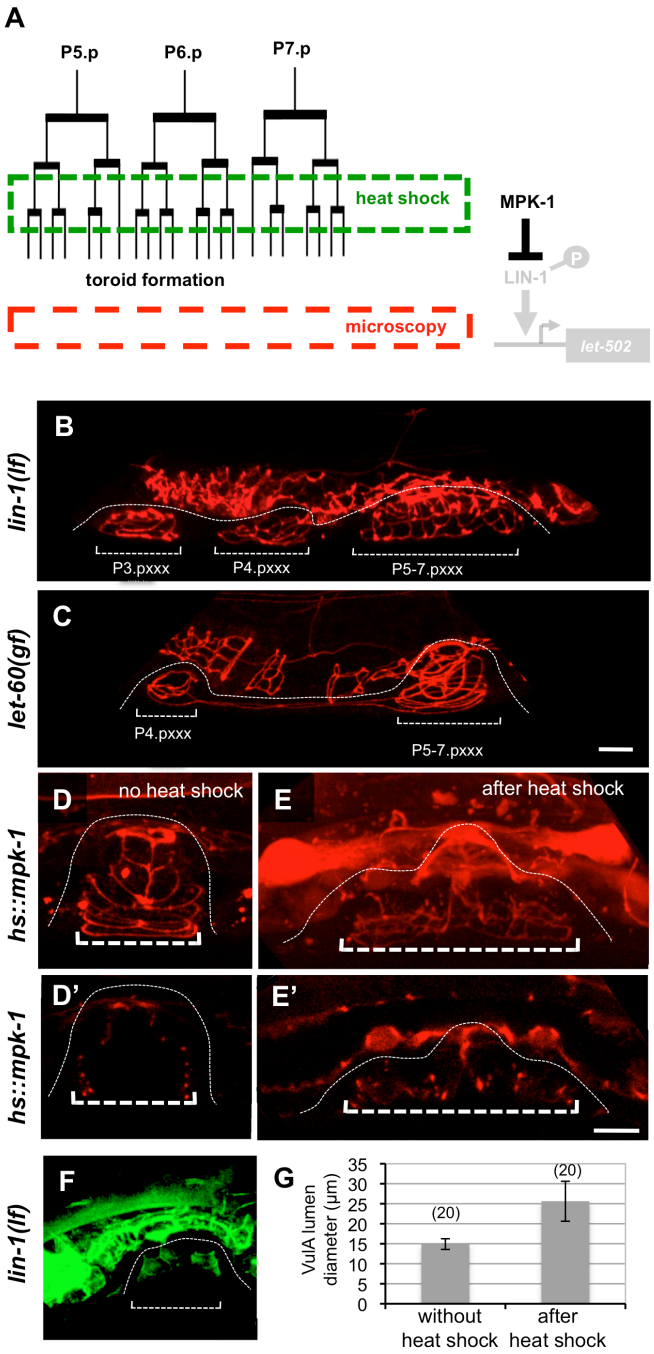
A
P5.p
P6.p
P7.p
heat shock
toroid formation
microscopy
MPK-1
LIN-1
P
let-502
lin-1(lf)
B
P3.pxxx
P4.pxxx
P5-7.pxxx
let-60(gf)
C
P4.pxxx
P5-7.pxxx
hs::mpk-1
D
no heat shock
E
after heat shock
hs::mpk-1
D'
E'
lin-1(lf)
F
G
VulA lumen diameter (µm)
35
30
25
20
15
10
5
0
(20)
(20)
without heat shock
after heat shock

Figure 6

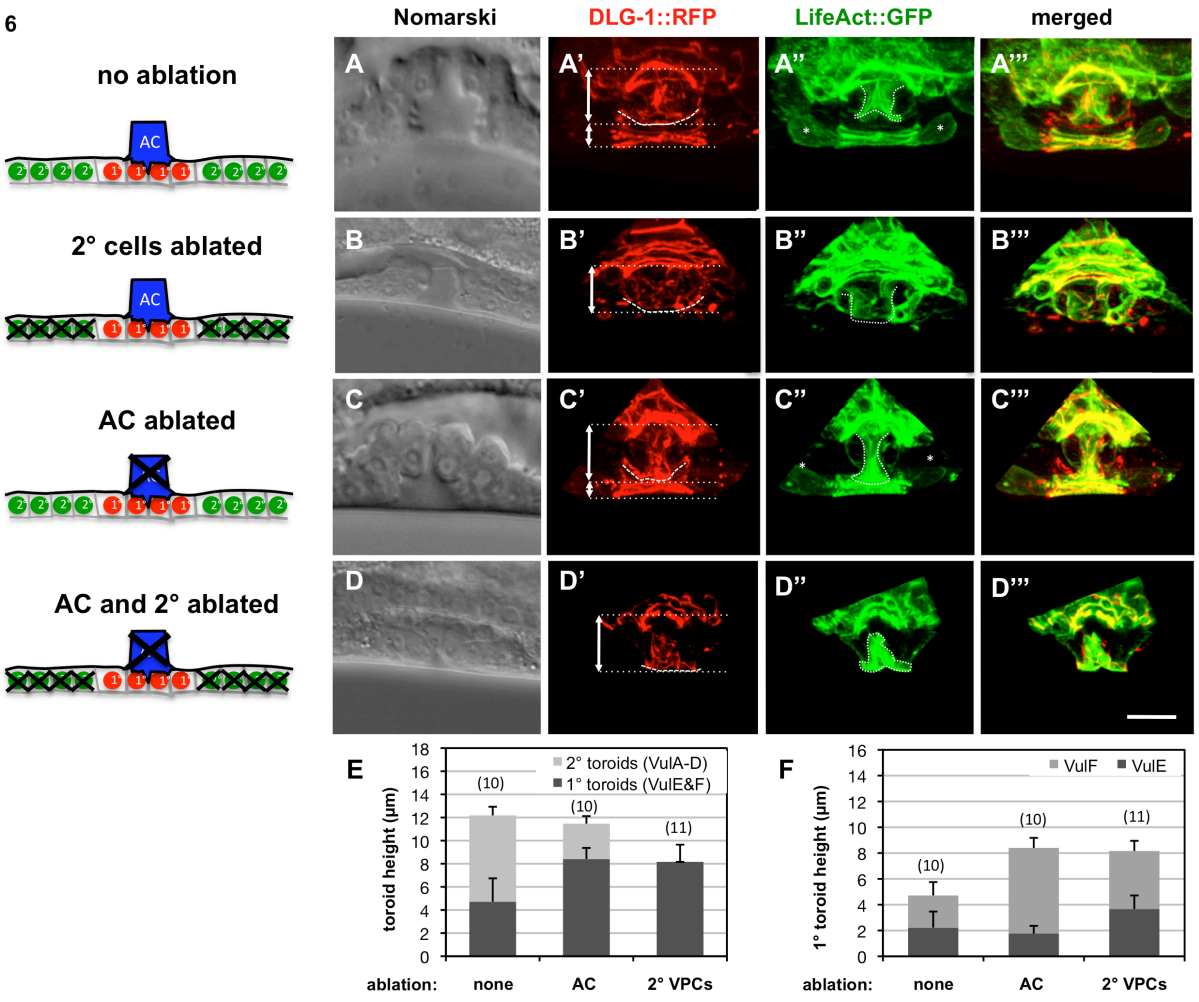
Nomarski
DLG-1::RFP
LifeAct::GFP
merged
no ablation
2° cells ablated
AC ablated
AC and 2° ablated
AC
A
A'
A''
A'''
B
B'
B''
B'''
C
C'
C''
C'''
D
D'
D''
D'''
E
2° toroids (VulA-D)
1° toroids (VulE&F)
toroid height (µm)
(10)
(10)
(11)
ablation:
none
AC
2° VPCs
F
VulF
VulE
1° toroid height (µm)
(10)
(10)
(11)
ablation:
none
AC
2° VPCs

Figure 7

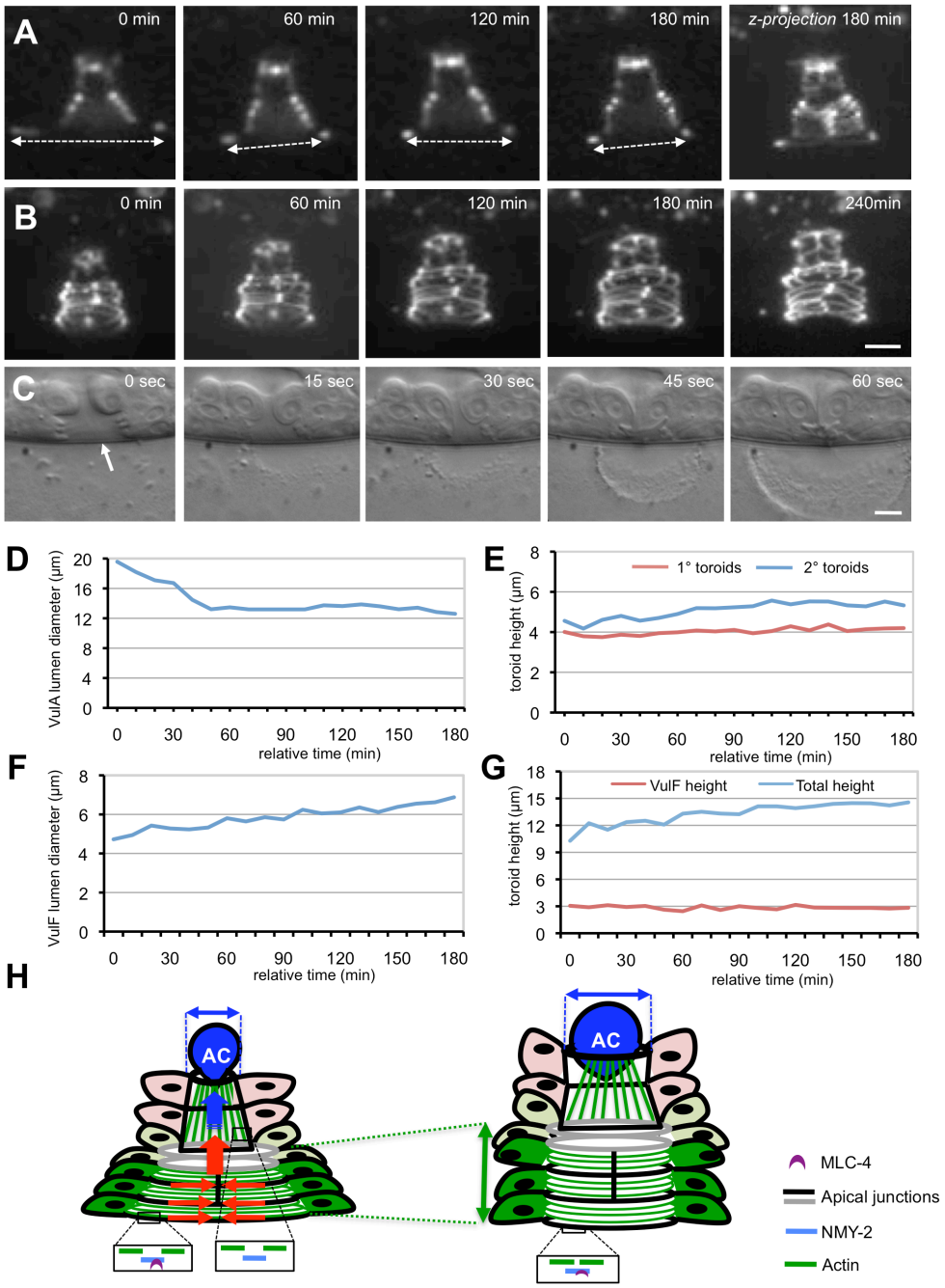
A
0 min
60 min
120 min
180 min
z-projection 180 min
B
0 min
60 min
120 min
180 min
240min
C
0 sec
15 sec
30 sec
45 sec
60 sec
D
VulA lumen diameter (µm)
relative time (min)
E
1° toroids
2° toroids
toroid height (µm)
relative time (min)
F
VulF lumen diameter (µm)
relative time (min)
G
VulF height
Total height
toroid height (µm)
relative time (min)
H
AC
AC
MLC-4
Apical junctions
NMY-2
Actin

suppl. figure 1

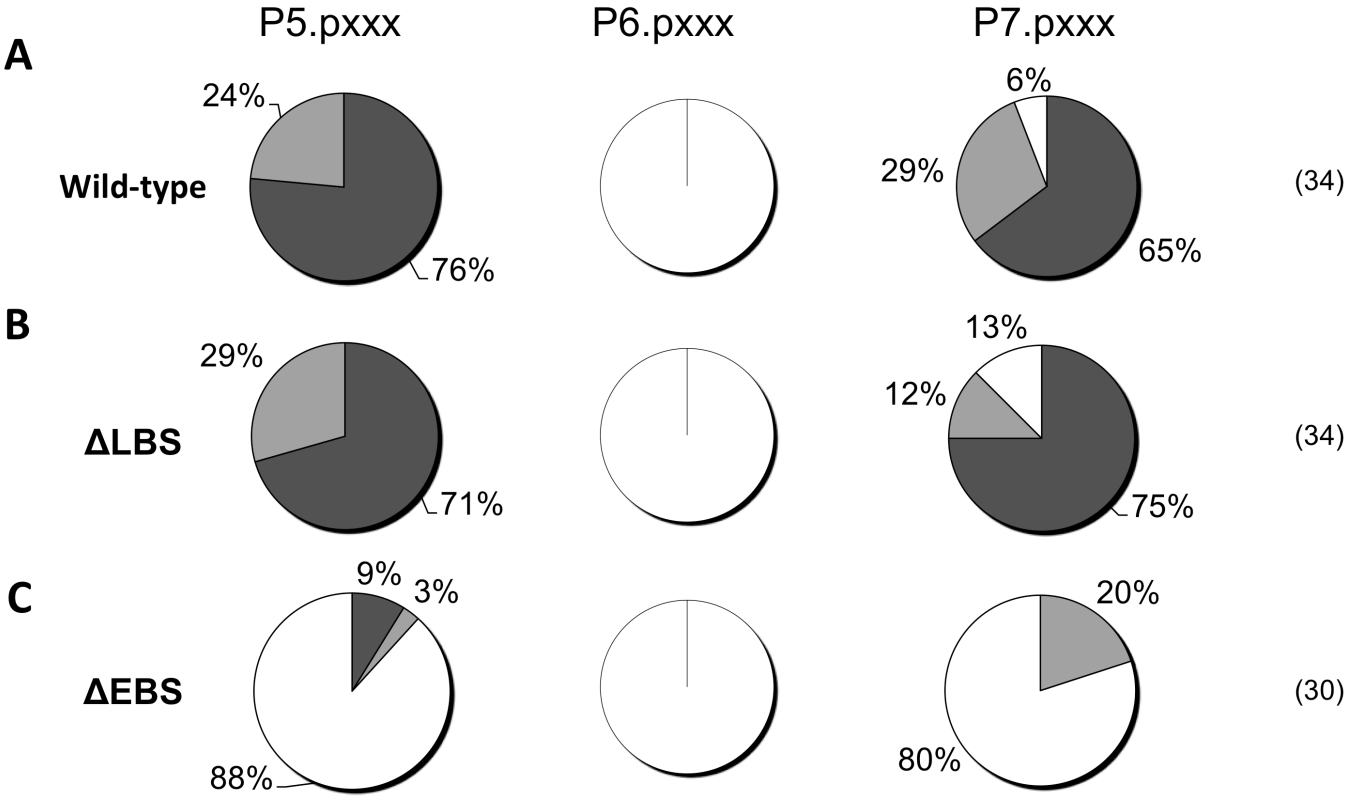

Suppl. fig. s1. Quantification of the *let-502* expression pattern. (A) Expression of the wild-type *let-502p::nls::gfp reporter*, (B) the *ΔLBS* and (C) the ΔEBS mutants (see Fig.2A). Quantification of the expression patterns was performed with synchronized populations of worms at the L4 stage (see materials and methods). The expression intensities were classified as follows: black: maximal expression (e.g. P5.pxxx in fig 1 E), grey: intermediate expression (e.g. P5.pxx in fig. 1 D), white: low or undetectable expression (e.g. P5.pxx in fig. 1 F). The numbers of animals analyzed are indicated in brackets to the right.

suppl. figure s2

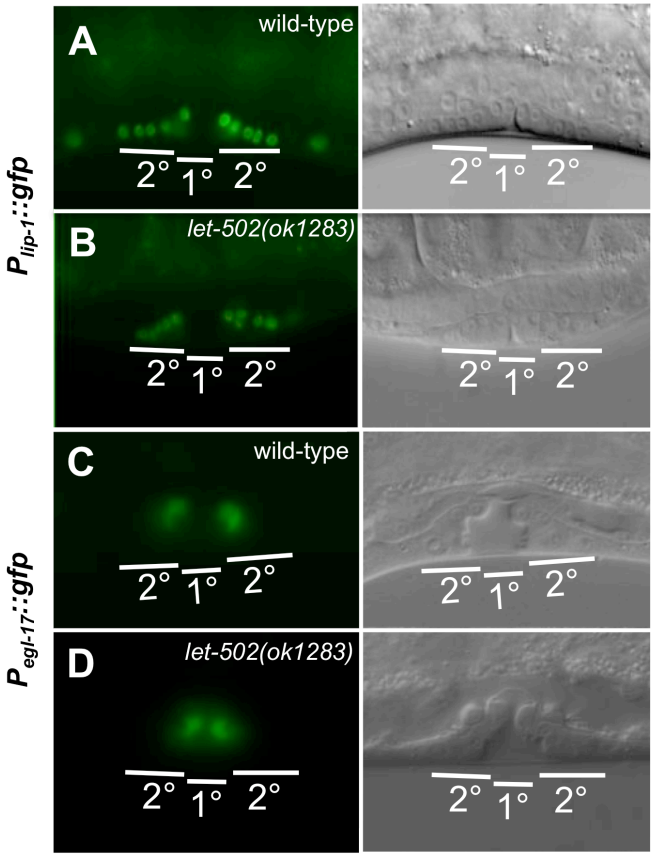

Suppl. fig. s2. 1° and 2° cell fate marker expression in *let-502(ok1283)* mutants. (A) Expression of the early 2° fate marker $P_{lip\text{-}1}$*::gfp (zhIs4)* in a wild-type and (B) *let-502(ok1283)* larva at the Pn.pxx to Pn.pxxx stage. (C) Expression of the late 2° fate marker $P_{egl\text{-}17}$*::gfp (ayIs4)* in a wild-type and (D) *let-502(ok1283)* L4 larva at the 'Christmas tree' stage. Corresponding Nomarski images are shown in the right panels.

suppl. figure s3

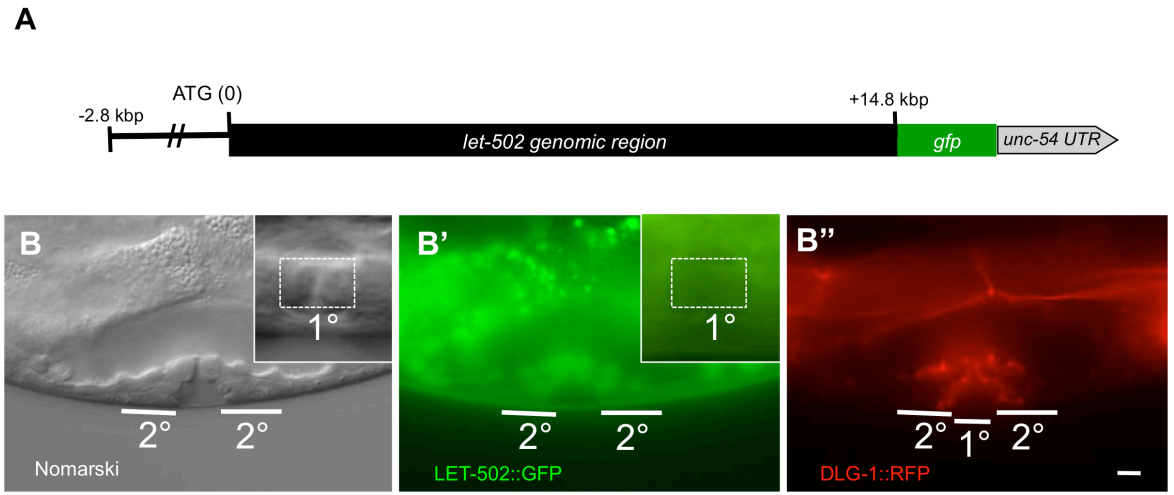

Suppl. fig. s3. Vulval expression of the rescuing LET-502::GFP reporter. (A) Structure of the translational LET-502::GFP reporter used for the rescue experiment shown in Fig. 3F. (B) Nomarski image, (B') LET-502::GFP expression and (B'') apical junctions labeled with DLG-1::RFP in an L4 larva. The insets in (B) and (B') show and upper focal plane where four of the eight 1° cell nuclei are located. Scale bar is 5µm.

suppl. figure s4

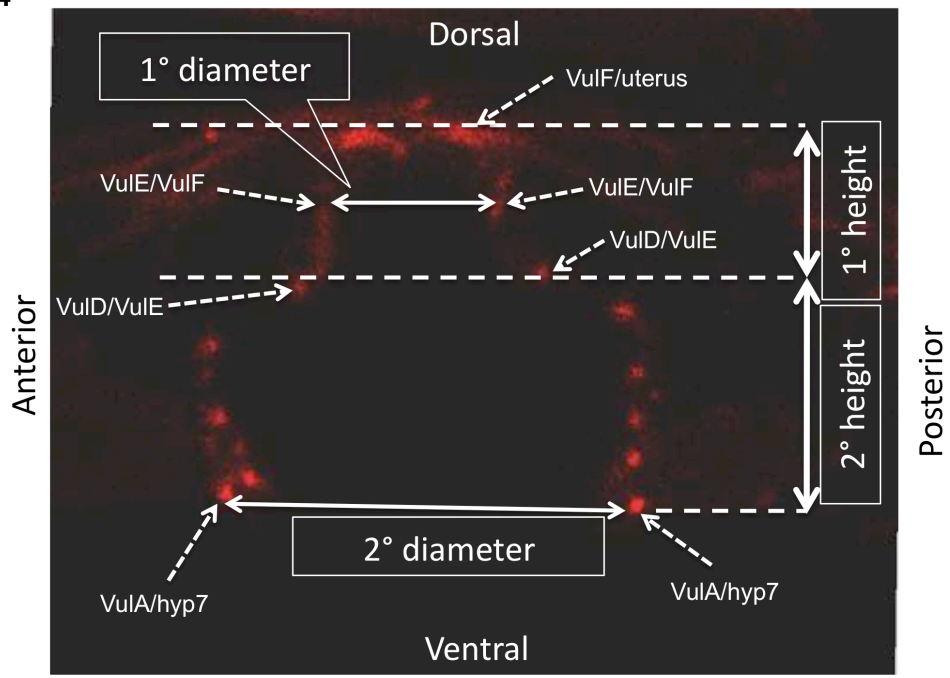

Suppl. fig. s4. Quantification of toroid diameter and height. A mid-sagittal optical section through the toroids labelled with DLG-1::RFP is shown. The distances measured to quantify 1° and 2° toroid height and diameter at the indicated junction points are indicated with solid arrows. L4 larvae were analyzed after the 1° lumen had expanded and the AC fused with the utse (Fig. 3-5) or for Fig. 7 in the individual time frames.

ORF	Gene name	Concise description	Vulval expression	2° specific
C09H6.2	*lin-10*	PDZ and PTB domain-containing protein	+	-
C10H11.9	*let-502*	Rho-kinase	+	+
C12C8.3	*lin-41*	Predicted E3 ubiquitin ligase	+	+
C18H9.7	*rpy-1*	Acetylcholine receptor-associated protein	-	-
C30A5.4	*C30A5.4*	Serine/threonine specific protein phosphatase PP1 catalytic subunit	-	-
F09C12.7	*msp-74*	Major Sperm Protein	-	-
F20G4.3	*nmy-2*	Non-muscle myosin II	+	-
F20H11.1	*F20H11.1*	Predicted protein kinase C-like and phorbol ester/diacylglycerol binding	+	+
F26A3.4	*F26A3.4*	Dual specificity phosphatase	-	-
F26D11.11	*let-413*	Basolateral epithelial marker protein	+	-
F28A12.4	*F28A12.4*	predicted aspartyl protease domain	+	+
F43D9.1	*F43D9.1*	Predicted membrane protein of the patched superfamily	-	-
F49E12.4	*ubc-24*	Ubiquitin-conjugating enzyme	-	-
H06O01.3	*ctg-1*	CRAL/TRIO and GOLD domain containing	-	-
H39E23.1	*par-1*	Serine/threonine protein kinase	+	-
R03D7.8	*R03D7.8*	Serine/threonine specific protein phosphatase PP1 domain	-	-
R06A10.4	*R06A10.4*	Ca2+/calmodulin-dependent protein kinase	-	-
T01E8.2	*ref-1*	Regulator of fusion	+	-
T24B8.6	*hlh-3*	Basic helix-loop-helix transcription factor	+	-
W07G4.3.1	*W07G4.3.1*	Predicted serine-threonine/tyrosine-protein kinase	-	-
W09D10.1	*W09D10.1*	Predicted GTPase-activating protein	+	-
Y116A8C.24	*Y116A8C.24*	Protein tyrosine kinase domain	-	-
Y65B4BR.3	*ptr-21*	Predicted membrane protein of the patched superfamily	-	-
ZK809.1	*ZK809.1*	Protein tyrosine phosphatase domain	-	-

suppl. table s1. Candidate NOTCH targets investigated by reporter analysis
Using a custom perl script (kindly provided by Peter Gallant), the *C. elegans* genome was screened for genes containing at least three CSL binding sites (RTGGGAA) within 2 kb upstream of the predicted translational start sites. To further narrow down the candidate gene list, we selected for genes on the basis of biological function (Pvl or Muv phenotype, genes involved in endocytosis, sorting, secretion, signaling, protein degradation, protein phosphorylation, transcriptional regulation) and conservation of the CSL motifs in the *C. briggsae* orthologs. This analysis identified the 24 candidate genes shown above, for which we generated transcriptional reporters by fusion PCR and analyzed their vulval expression pattern.

Primer	Sequence (5'-3')	Used for
OSF130	CGCGGATCCACCAGCTGATCACG	*zhEx401, zhEx403, zhEx399, zhEx401, zhEx405*
OSF132	CAGTGCTCACTTCCCTCCGGAAGAAACAAAAAA GTCG	*zhEx402*
OSF133	GCGAAAGTTTAGAGCTGAGGGAATGCGAATAAAATGAAAAC	*zhEx402*
OSF134	GATAAGAAAAATAAAAGGGAAATTCCATTACAATCATATGGG	*zhEx402*
OSF135	GCTGTACTATTTGAGAAAGAGAACCAAAGTAGTCAAGC	*zhEx402*
OSF185	CTAGCTAGCATGAATCACATTGACCTTTTGAAGG	*zhEx394*
OSF186	CGGGGTACCTCAGAACGGTGACTGGGACGCC	*zhEx394*
OSF196	CCACCAGATGAGCAATTTTGTTG	*zhEx398*
OSF205	TTTGTCGACCCACCAGATGAGCAATTTTGT	*zhEx401, zhEx403, zhEx401, zhEx405, zhEx393*
OSF206	GCTCTCATGAGTGGAGCGGTG	*zhEx399, zhEx403, zhEx401, zhEx405*
OSF207	CACCGCTCCACTCATGAGAGCGTACTATGGGGTCTGCTGACCG	*zhEx403,*
OSF208	GTGACTTGTGATTATCTTAG	*zhEx401*
OSF209	CACCGCTCCACTCATGAGAGCGAAAAGGTAAACGGAGAGAGG	*zhEx405*
OSF223	TTTTACTAGTATGTACCCATACGATGTTCCTG	*zhEx394*
OSF224	TTTTACTAGTATCGGCCGCTTTTTCGAACTGC	*zhEx394*
OSF225	CAGTCTTTTGAAATAAAAAAAACTGACTCATAGTTAGCCTTGAATG	*zhEx393*
OSF226	AGTTTTTTTTATTTCAAAAGACTGACCCGACCGCATAAATTGTC	*zhEx393*
OSF230	TTCGCGGATCCTTGATAGATTGTGGAAGAGTTTGACG	*zhEx403, zhEx401, zhEx405, zhEx393*
OSF253	GTGAAAAGTTCTTCTCCTTTACTCATAGGCGGAGGTGTTGGTCCG	*zhEx398*
OSF262	GGCCCACAATATGTGTAGAATCAGTC	ChIP probe '3''
OSF265	CATTCAAGGCTAACTATGAGTC	ChIP probe 'B'
OSF266	GTACTATGGGGTCTGCTGACCG	ChIP probe 'B'
OSF269	GACTCATAGTTAGCCTTGAATG	ChIP probe 'A'
OSF270	CTAAGATAATCACAAGTCAC	ChIP probe 'A'
OSF272	CTCCTTGGAGATGGACTCGAACTTCTTGATAAGGTCAGCGACTCCCATGCTT CCTTCCTTCGGTGAGGCG	*zhEx396*
OSF278	TTTTCTGCAGCTGTACGACAGTTGCACATTCGG	*zhEx396*
OSF281	AACGGACCAACACCTCCGCC	ChIP probe '3''
OSF282	CTGCAGCTCGATTTTCGTC	ChIP probe 'C'
OSF283	TCCGGTGGGAAGTGAGCACTG	ChIP probe 'C'
'C'	AGCTTGCATGCCTGCAGGTCGACT	*zhEx398*
'D'	AAGGGCCCGTACGGCCGACTAGTAGG	*zhEx398*

Supplementary table s2. Sequence of primers used for constructs and ChIP experiments described in Materials and Methods.

Bibliography

Abdus-Saboor, I., Mancuso, V.P., Murray, J.I., Palozola, K., Norris, C., Hall, D.H., Howell, K., Huang, K., and Sundaram, M.V. (2011). Notch and Ras promote sequential steps of excretory tube development in *C.elegans*. Development *138*, 3545-3555.

Andrew, D.J., and Ewald, A.J. (2010). Morphogenesis of epithelial tubes: Insights into tube formation, elongation, and elaboration. Dev Biol *341*, 34-55.

Beitel, G.J., Tuck, S., Greenwald, I., and Horvitz, H.R. (1995). The Caenorhabditis elegans gene lin-1 encodes an ETS-domain protein and defines a branch of the vulval induction pathway. Genes Dev *9*, 3149-3162.

Berset, T., Hoier, E.F., Battu, G., Canevascini, S., and Hajnal, A. (2001). Notch inhibition of RAS signaling through MAP kinase phosphatase LIP-1 during *C.elegans* vulval development. Science *291*, 1055-1058.

Brenner, S. (1974). The genetics of Caenorhabditis elegans. Genetics *77*, 71-94.

Caussinus, E., Colombelli, J., and Affolter, M. (2008). Tip-cell migration controls stalk-cell intercalation during Drosophila tracheal tube elongation. Curr Biol *18*, 1727-1734.

Christensen, S., Kodoyianni, V., Bosenberg, M., Friedman, L., and Kimble, J. (1996). lag-1, a gene required for lin-12 and glp-1 signaling in Caenorhabditis elegans, is homologous to human CBF1 and Drosophila Su(H). Development *122*, 1373-1383.

Diogon, M., Wissler, F., Quintin, S., Nagamatsu, Y., Sookhareea, S., Landmann, F., Hutter, H., Vitale, N., and Labouesse, M. (2007). The RhoGAP RGA-2 and *LET-502*/ROCK achieve a balance of actomyosin-dependent forces in *C.elegans* epidermis to control morphogenesis. Development *134*, 2469-2479.

Dupuy, D., Bertin, N., Hidalgo, C.A., Venkatesan, K., Tu, D., Lee, D., Rosenberg, J., Svrzikapa, N., Blanc, A., Carnec, A.*, et al.* (2007). Genome-scale analysis of in vivo spatiotemporal promoter activity in Caenorhabditis elegans. Nat Biotechnol *25*, 663-668.

Estes, K.A., and Hanna-Rose, W. (2009). The anchor cell initiates dorsal lumen formation during *C.elegans* vulval tubulogenesis. Dev Biol *328*, 297-304.

Gally, C., Wissler, F., Zahreddine, H., Quintin, S., Landmann, F., and Labouesse, M. (2009). Myosin II regulation during *C.elegans* embryonic elongation: *LET-502*/ROCK, MRCK-1 and PAK-1, three kinases with different roles. Development *136*, 3109-3119.

Glatter, T., Wepf, A., Aebersold, R., and Gstaiger, M. (2009). An integrated workflow for charting the human interaction proteome: insights into the PP2A system. Mol Syst Biol *5*, 237.

Gov, N.S. (2007). Collective cell migration patterns: follow the leader. Proc Natl Acad Sci U S A *104*, 15970-15971.

Greenwald, I. (2005). LIN-12/Notch signaling in *C.elegans*. WormBook, 1-16.

Greenwald, I.S., Sternberg, P.W., and Horvitz, H.R. (1983). The lin-12 locus specifies cell fates in Caenorhabditis elegans. Cell *34*, 435-444.

Guo, S., and Kemphues, K.J. (1996). A non-muscle myosin required for embryonic polarity in Caenorhabditis elegans. Nature *382*, 455-458.

Herman, T., Hartwieg, E., and Horvitz, H.R. (1999). sqv mutants of Caenorhabditis elegans are defective in vulval epithelial invagination. Proc Natl Acad Sci U S A *96*, 968-973.

Herman, T., and Horvitz, H.R. (1999). Three proteins involved in Caenorhabditis elegans vulval invagination are similar to components of a glycosylation pathway. Proc Natl Acad Sci U S A *96*, 974-979.

Hobert, O. (2002). PCR fusion-based approach to create reporter gene constructs for expression analysis in transgenic *C.elegans*. Biotechniques *32*, 728-730.

Hwang, H.Y., Olson, S.K., Esko, J.D., and Horvitz, H.R. (2003). Caenorhabditis elegans early embryogenesis and vulval morphogenesis require chondroitin biosynthesis. Nature *423*, 439-443.

Ishiuchi, T., and Takeichi, M. (2011). Willin and Par3 cooperatively regulate epithelial apical constriction through aPKC-mediated ROCK phosphorylation. Nat Cell Biol.

Jacobs, D., Beitel, G.J., Clark, S.G., Horvitz, H.R., and Kornfeld, K. (1998). Gain-of-function mutations in the Caenorhabditis elegans lin-1 ETS gene identify a C-terminal regulatory domain phosphorylated by ERK MAP kinase. Genetics *149*, 1809-1822.

Kamath, R.S., Martinez-Campos, M., Zipperlen, P., Fraser, A.G., and Ahringer, J. (2001). Effectiveness of specific RNA-mediated interference through ingested double-stranded RNA in Caenorhabditis elegans. Genome Biol *2*, RESEARCH0002.

Koppen, M., Simske, J.S., Sims, P.A., Firestein, B.L., Hall, D.H., Radice, A.D., Rongo, C., and Hardin, J.D. (2001). Cooperative regulation of AJM-1 controls junctional integrity in Caenorhabditis elegans epithelia. Nat Cell Biol *3*, 983-991.

Lackner, M.R., and Kim, S.K. (1998). Genetic analysis of the Caenorhabditis elegans MAP kinase gene mpk-1. Genetics *150*, 103-117.

Marston, D.J., and Goldstein, B. (2006). Actin-based forces driving embryonic morphogenesis in Caenorhabditis elegans. Curr Opin Genet Dev *16*, 392-398.

Mello, C.C., Kramer, J.M., Stinchcomb, D., and Ambros, V. (1991). Efficient gene transfer in C.elegans: extrachromosomal maintenance and integration of transforming sequences. EMBO J *10*, 3959-3970.

Miller, D.M., and Shakes, D.C. (1995). Immunofluorescence microscopy. Methods Cell Biol *48*, 365-394.

Miller, L.M., Gallegos, M.E., Morisseau, B.A., and Kim, S.K. (1993). lin-31, a Caenorhabditis elegans HNF-3/fork head transcription factor homolog, specifies three alternative cell fates in vulval development. Genes Dev *7*, 933-947.

Mukhopadhyay, A., Deplancke, B., Walhout, A.J., and Tissenbaum, H.A. (2008). Chromatin immunoprecipitation (ChIP) coupled to detection by quantitative real-time PCR to study transcription factor binding to DNA in Caenorhabditis elegans. Nat Protoc *3*, 698-709.

Omelchenko, T., Vasiliev, J.M., Gelfand, I.M., Feder, H.H., and Bonder, E.M. (2003). Rho-dependent formation of epithelial "leader" cells during wound healing. Proc Natl Acad Sci U S A *100*, 10788-10793.

Pohl, C., and Bao, Z. (2010). Chiral forces organize left-right patterning in *C.elegans* by uncoupling midline and anteroposterior axis. Dev Cell *19*, 402-412.

Poujade, M., Grasland-Mongrain, E., Hertzog, A., Jouanneau, J., Chavrier, P., Ladoux, B., Buguin, A., and Silberzan, P. (2007). Collective migration of an epithelial monolayer in response to a model wound. Proc Natl Acad Sci U S A *104*, 15988-15993.

Rodriguez-Fraticelli, A.E., Galvez-Santisteban, M., and Martin-Belmonte, F. (2011). Divide and polarize: recent advances in the molecular mechanism regulating epithelial tubulogenesis. Curr Opin Cell Biol.

Rorth, P. (2009). Collective cell migration. Annu Rev Cell Dev Biol *25*, 407-429.

Schottenfeld, J., Song, Y., and Ghabrial, A.S. (2010). Tube continued: morphogenesis of the Drosophila tracheal system. Curr Opin Cell Biol *22*, 633-639.

Sementchenko, V.I., and Watson, D.K. (2000). Ets target genes: past, present and future. Oncogene *19*, 6533-6548.

Sharma-Kishore, R., White, J.G., Southgate, E., and Podbilewicz, B. (1999). Formation of the vulva in Caenorhabditis elegans: a paradigm for organogenesis. Development *126*, 691-699.

Sternberg, P.W. (2005). Vulval development. WormBook, 1-28.

Tan, P.B., Lackner, M.R., and Kim, S.K. (1998). MAP kinase signaling specificity mediated by the LIN-1 Ets/LIN-31 WH transcription factor complex during *C.elegans* vulval induction. Cell *93*, 569-580.

Vaughan, R.B., and Trinkaus, J.P. (1966). Movements of epithelial cell sheets in vitro. J Cell Sci *1*, 407-413.

Walser, C.B., Battu, G., Hoier, E.F., and Hajnal, A. (2006). Distinct roles of the Pumilio and FBF translational repressors during *C.elegans* vulval development. Development *133*, 3461-3471.

Wissmann, A., Ingles, J., McGhee, J.D., and Mains, P.E. (1997). Caenorhabditis elegans *LET-502* is related to Rho-binding kinases and human myotonic dystrophy kinase and interacts genetically with a homolog of the regulatory subunit of smooth muscle myosin phosphatase to affect cell shape. Genes Dev *11*, 409-422.

Xavier Trepat, M.R.W., Thomas E. Angelini, Emil Millet, David A. Weitz, James P. Butler and Jeffrey J. Fredberg (2009). Physical forces during collective cell migration. Nature Physics *5*, 426-430.

Yang, H.C., and Pon, L.A. (2002). Actin cable dynamics in budding yeast. Proc Natl Acad Sci U S A *99*, 751-756.

Zhang, X., and Greenwald, I. Spatial Regulation of lag-2 Transcription During Vulval Precursor Cell Fate Patterning in Caenorhabditis eleganslag-2. Genetics *188*, 847-858.

4.2 Additional experiments

4.2.1. *let-502* acts in parallel with the *mig-2* and possibly also the *smp-1/unc-73* signaling pathway

Vulval morphogenesis involves several interdependent processes including the migration and guidance of the extending vulval cells towards the vulval midline, allowing contralateral pairs of cells with the same subfates to contact each other at the midline. Genetic approaches have identified two parallel pathways regulating vulval cell migration and guidance. The first pathway involves the SMP-1 Semaphorin ligand, the PLX-1 Plexin receptor and the CED-10 Rac small GTPase (Dalpe et al., 2005). A second pathway utilizes the MIG-2 Rac small GTPase and its activator UNC-73 GEF (Kishore RS, 2002). To investigate the interaction between *let-502* and the *smp-1/plx-1/ced-10* and the *unc-73/mig-2* signaling pathways, *let-502* expression was knocked-down by feeding *let-502* dsRNA to mutants of the components of these two pathways and separately scored defects in vulval migration and toroid formation (Fig 4I). An abnormal shape of the vulval toroids and an enlarged diameter of the vulval lumen was observed in 95% of *let-502(ok1283)* single mutants (n=20) and also in 5% of *let-502* RNAi treated wild-type animals (Fig. 4B and I). On the other hand, *let-502(ok1283)* mutants only rarely (5%, n=20) showed defects in the migration of cells towards the midline, resulting in a second, ectopic invagination (Fig. 4E and I). *let-502* RNAi in the *mig-2(mu28)* or the *unc-73(e936)* background resulted in a penetrant cell migration defect reflected by ectopic invaginations (Fig. 4D, H, I). Moreover, *let-502* RNAi enhanced the defects in toroid formation in the *unc-73(e936)* and the *ced-10(e1993)* background (Fig. 4F and I). Unexpectedly, *let-502* RNAi in the *plx-1(ev724)* or the *smp-1(ev715)* background caused penetrant embryonic lethality with only few escapers that were likely not affected by *let-502*

RNAi, making it impossible to study their interaction during vulval morphogenesis (data not shown).

The enhancement of mutants in both the SMP-1/PLX-1/CED-10 and the UNC-73/MIG-2 signaling pathways suggests that LET-502 acts in a parallel, partially independent pathway to regulate vulval morphogenesis (Fig. 4J).

4.3 Materials and methods for additional experiments

Strains used

C.elegans strains were maintained at 20 °C on standard nematode growth media as described previously (Brenner, 1974). The wild-type strain of *C.elegans* used was Bristol N2. Other strains used were as follows *unc-73(e936), ced-10(1993), mig-2(mu28)*

RNA interference

RNA interference (RNAi) was performed using the feeding method as described (Kamath et al., 2001). Worms were synchronized at the L1 stage, transferred to nematode growth media plates (with 3 mM IPTG and 50ng/ml ampicillin) containing the desired RNAi bacteria and allowed to grow for 3-5 days at 20°C. The first generation progeny was analyzed.

4.4 Further discussion and future experiments

Recently, genetic approaches have revealed that two parallel pathways regulate vulval cell migration and morphogenesis. The first pathway requires the SMP-1 Semaphorin ligand, the PLX-1 Plexin receptor and the CED-10 Rac small GTPase, while the second pathway utilizes the MIG-2 Rac small GTPase and its activator UNC-73 GEF (Dalpe et al., 2005; Kishore RS, 2002). They predicted presence of another pathway parallel to above-mentioned pathways. By performing *let-502* RNAi in different mutant backgrounds of these two parallel

pathways, we demonstrated that Rho-Rho-kinase signaling could be the third pathway (Figure 4j), which interacts with them. Also, the lethality of *smp-1* and *plx-1* loss of function mutants in *let-502* RNAi background indicate that they act in parallel to regulate embryonic lethality which has not been established so far. This phenotype should be probed further by analyzing it closely in terms of fate determination defect and morphogenesis defects.

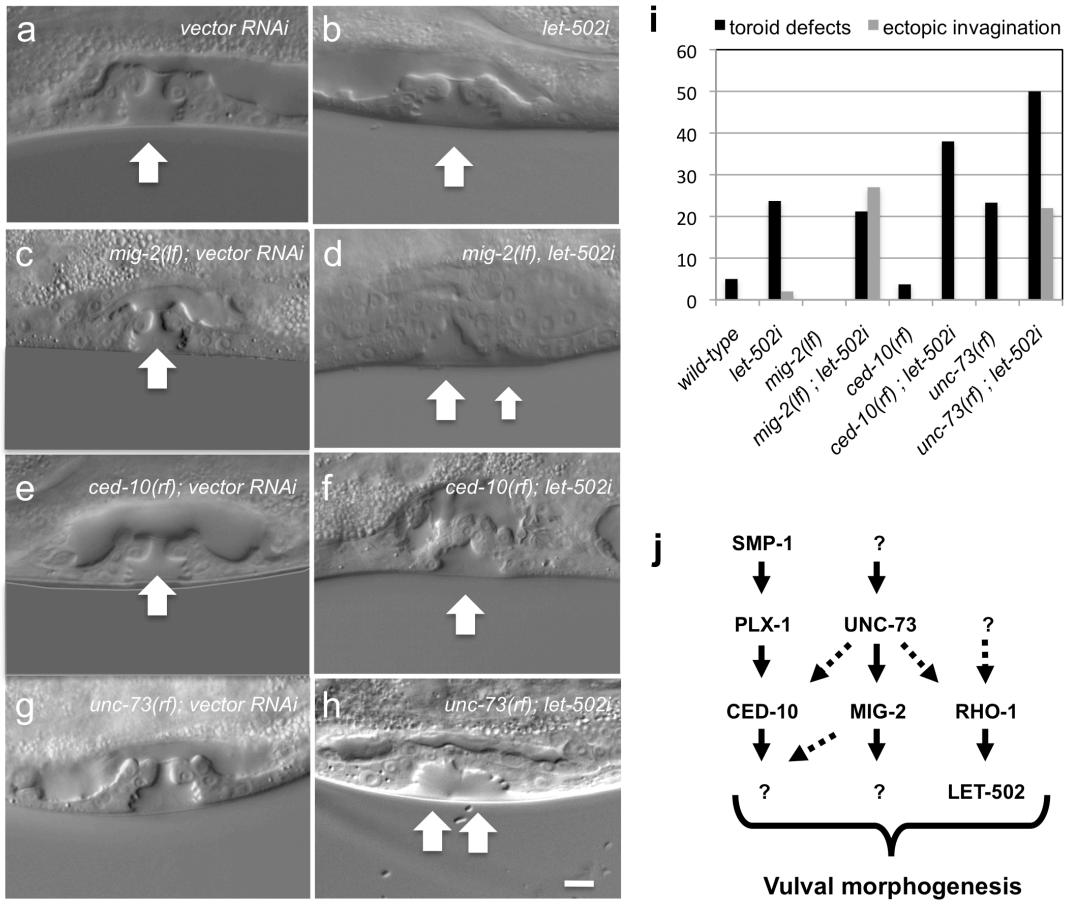

Figure 4. *let-502* acts in parallel with *mig-2* and possibly also *smp-1/unc-73* signaling pathway. Normaski optics of vulva at L4 stage of the animals grown on empty vector (a,c,e,g) (negative control) RNAi and *let-502* RNAi (b,d,f,h). (i) Graph showing percentage of animals showing defective vulva phenotype (b.d.f.h) (Y axis) in different genetic backgrounds (X-axis) mentioned. (j) model for interaction of *let-502* with *smp-1/unc-73* signaling pathway during vulval morphogenesis. Two phenotypes, toroid and ectopic invagination were scored. *Let-502* is in the same pathway as mig-2 while possibly parallel to *ced-10* and *unc-73* signaling for regulating toroid defects. *let-502* is in parallel to *mig-2* and possibly *unc-73* while possibly in the same pathway as ced-10 for regulating ectopic invagination defects.

Reference:

Brenner, S. (1974). The genetics of Caenorhabditis elegans. *Genetics* **77**, 71-94.
Dalpe, G., Brown, L. and Culotti, J. G. (2005). Vulva morphogenesis involves attraction of plexin 1-expressing primordial vulva cells to semaphorin 1a sequentially expressed at the vulva midline. *Development* **132**, 1387-400.
Kishore RS, S. M. (2002). ced-10 Rac and mig-2 function redundantly and act with unc-73 trio to control the orientation of vulval cell divisions and migrations in Caenorhabditis elegans. *Developmental Biology* **241**, 339-348.

5 Part III: LIN-39 HOX and THE EGFR/RAS/MAPK pathway regulate *C.elegans* vulval morphogenesis via the VAB-23 ZINC FINGER protein. (In collaboration with Dr. Mark Watson Pellegrino)

5.1 Publication: LIN-39 HOX and THE EGFR/RAS/MAPK pathway regulate *C.elegans* vulval morphogenesis via the VAB-23 ZINC FINGER protein.

Development 138, 4649-4660 (2011) doi:10.1242/dev.071951

LIN-39 and the EGFR/RAS/MAPK pathway regulate *C. elegans* vulval morphogenesis via the VAB-23 zinc finger protein

Mark W. Pellegrino[1,2,*], Sarfarazhussain Farooqui[2,3], Erika Fröhli[2], Hubert Rehrauer[4], Stéphanie Kaeser-Pebernard[5], Fritz Müller[5], Robin B. Gasser[1,†] and Alex Hajnal[2,†]

SUMMARY

Morphogenesis represents a phase of development during which cell fates are executed. The conserved hox genes are key cell fate determinants during metazoan development, but their role in controlling organ morphogenesis is less understood. Here, we show that the *C. elegans* hox gene *lin-39* regulates epidermal morphogenesis via its novel target, the essential zinc finger protein VAB-23. During the development of the vulva, the egg-laying organ of the hermaphrodite, the EGFR/RAS/MAPK signaling pathway activates, together with LIN-39 HOX, the expression of VAB-23 in the primary cell lineage to control the formation of the seven vulval toroids. VAB-23 regulates the formation of homotypic contacts between contralateral pairs of cells with the same sub-fates at the vulval midline by inducing *smp-1* (*semaphorin*) transcription. In addition, VAB-23 prevents ectopic vulval cell fusions by negatively regulating expression of the fusogen *eff-1*. Thus, LIN-39 and the EGFR/RAS/MAPK signaling pathway, which specify cell fates earlier during vulval induction, continue to act during the subsequent phase of cell fate execution by regulating various aspects of epidermal morphogenesis. Vulval cell fate specification and execution are, therefore, tightly coupled processes.

KEY WORDS: Morphogenesis, *hox*, *ras*, *C. elegans*, Vulva

INTRODUCTION

Morphogenesis is the phase in development that occurs after cells have adopted their cell fates. A pivotal condition for proper morphogenesis is the proper specification of cell fates by the hox genes, which encode homeodomain-containing transcription factors that typically control anterior-posterior cell fate decisions during embryogenesis and the axial patterning of the limbs (Hombria and Lovegrove, 2003; McGinnis and Krumlauf, 1992).

The nematode *Caenorhabditis elegans*, which contains a single non-redundant hox gene cluster, has been used extensively to characterize hox gene functions. Six *C. elegans* hox genes have been identified: the *labial*-like gene *ceh-13* (Brunschwig et al., 1999); the *Antp* class genes *lin-39* (Clark et al., 1993) and *mab-5* (Kenyon, 1986); and the posterior *Abd-b*-like genes *egl-5*, *nob-1* and *php-3* (Chisholm, 1991; Van Auken et al., 2000). A central role for *lin-39* and its co-factors has been observed during vulval development in the hermaphrodite larva (Clark et al., 1993; Yang et al., 2005). The vulva forms a connection between the uterus and the outside, through which the fertilized eggs are laid. Composed of only 22 cells generated in a relatively simple and invariant cell lineage, the vulva serves as an excellent model to study cell fate determination (Sternberg, 2005). During the second larval stage, three out of six equipotent vulval precursor cells (VPCs) are induced by an epidermal growth factor (EGF) signal from the uterine anchor cell (AC) to adopt a vulval cell fate (Hill and Sternberg, 1992). The EGF receptor, encoded by *let-23*, transduces the inductive signal in the VPCs via the RAS/MAPK pathway (Aroian and Sternberg, 1991; Beitel et al., 1990; Lackner and Kim, 1998). In response to the inductive signal, a lateral signal from P6.p activates LIN-12 NOTCH in P5.p and P7.p, which represses EGFR/RAS/MAPK signaling in these cells (Berset et al., 2001; Greenwald, 2005). Thus, high MAPK activity in P6.p results in the primary (1°) fate, whereas strong LIN-12 signaling in P5.p and P7.p specifies the secondary (2°) fate (Greenwald, 2005). Once the cell fates have been determined, P5.p-P7.p undergo three rounds of divisions to generate 22 vulval cells that are further divided into seven sub-fates. VulA, VulB1, VulB2, VulC and VulD are generated by the seven 2° descendants each of P5.p and P7.p, and VulE and VulF are formed by the eight 1° descendants of P6.p (Fig. 1A) (Shemer et al., 2000). During the subsequent phase of morphogenesis, cells migrate and form extensions towards the vulval midline, where they make homotypic contacts with their contralateral partner cells of the same sub-fates, thereby forming seven symmetric rings called toroids. With the exception of VulB1 and VulB2, cells within a toroid fuse, thus generating a stack of syncytial toroids arranged in a pyramidal manner.

LIN-39, which is activated through the combined actions of the EGFR/RAS/MAPK and WNT signaling pathways, performs at least two distinct functions during vulval development (Eisenmann et al., 1998; Maloof and Kenyon, 1998). First, LIN-39 prevents the fusion of the VPCs with hyp7 at the early L2 stage (Clark et al., 1993). Second, during cell fate execution and morphogenesis, LIN-39 is required for cell proliferation and toroid formation (Shemer and Podbilewicz, 2002). The HOX co-factors CEH-20 PBX and UNC-62 MEIS play similar roles during vulval morphogenesis by regulating cell fusion and migration (Yang et al., 2005). Previous work has indicated that *let-60 ras* is also involved in controlling vulval morphogenesis (Shemer et al., 2000), though the exact role of EGFR/RAS/MAPK signaling during vulval cell fate execution is not well understood.

[1]The University of Melbourne, Department of Veterinary Science, Werribee, Victoria, Australia 3030. [2]University of Zürich, Institute of Molecular Life Sciences, Winterthurerstrasse 190, CH-8057 Zürich, Switzerland. [3]PhD Program in Molecular Life Sciences UNI ETH Zürich, Winterthurerstrasse 190, CH-8057 Zürich, Switzerland. [4]The Functional Genomics Center, UNI ETH Zürich, Winterthurerstrasse 190, CH-8057 Zürich, Switzerland. [5]Department of Biology, Chemin du Musée 10, CH-1700 Fribourg, Switzerland.

*Present address: Memorial Sloan Kettering Cancer Centre, Rockefeller Research Laboratories, 430 East 67th street, RRL 617B New York, NY 10065, USA
†Authors for correspondence (alex.hajnal@imls.uzh.ch; robinbg@unimelb.edu.au)

Accepted 16 August 2011

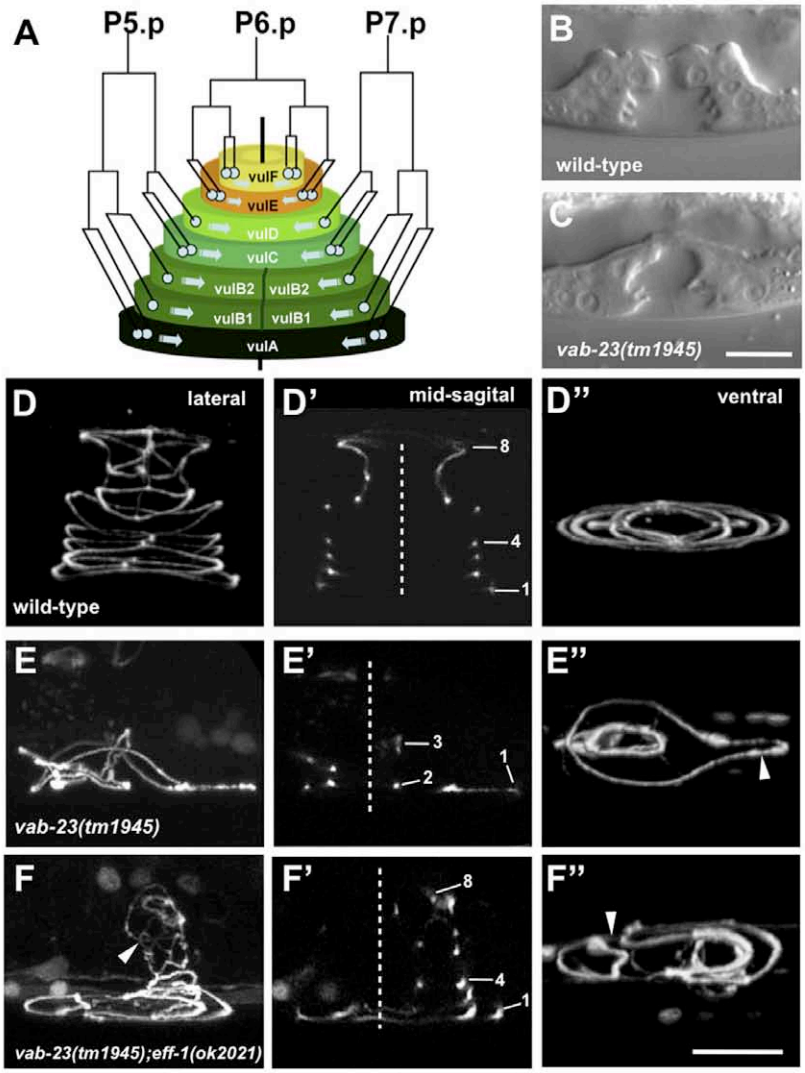

Fig. 1. VAB-23 regulates toroid formation and blocks cell fusion during morphogenesis in *C. elegans*. (**A**) A stack of seven concentric toroids forms the vulva. The cell lineages are indicated on the sides. The thick black line in the center marks the vulval midline. Arrows represent the cell movement towards the midline, where cells of the same sub-fates attach and fuse to each other (except for VulB1 and VulB2) to form toroids. (**B**,**C**) Nomarski images of the vulva in wild-type (B) and *vab-23(tm1945)* (C) L4 larva. (**D-F″**) Toroids visualized by AJM-1::GFP in wild-type (D-D″), *vab-23(tm1945)* (E-E″) and *vab-23(tm1945); eff-1(ok1021)* (F-F″) L4 larvae. D-F show lateral views of 3D confocal reconstructions, D′-F′ are single mid-sagittal optical sections showing the junctions between toroids, and D″-F″ are ventral views of the 3D reconstructions. Dashed lines indicate the vulval midline. The arrowhead in F points at a site where cells formed aberrant contacts on one side of the midline, and the arrowheads in E″ and F″ indicate defective migration of VulA to the midline. Anterior is left. Scale bars: 10 μm.

We have previously identified the *vab-23* gene as an essential regulator of morphogenesis that controls the movements of ventral epidermal cells in the embryo (Pellegrino et al., 2009). VAB-23 is the first characterized member of a family of nuclear proteins containing a strongly conserved C4H2-type zinc finger domain at the C-terminus. All metazoans genomes encode a single VAB-23 homolog, and the human protein HCA127 (ZC4H2 – Human Gene Nomenclature Database) was found to be an auto-antigen in hepatocellular carcinomas (Wang et al., 2002). Here, we describe the functions of VAB-23 during vulval morphogenesis. The LIN-39 and RAS/MAPK target VAB-23 guides cell interactions during toroid formation. VAB-23 positively regulates, among others, the transcription of *smp-1* to allow proper interactions to occur between cells of the same sub-fates. In addition, VAB-23 inhibits EFF-1-dependent cell fusion during toroid formation. Thus, *vab-23* is an essential factor linking LIN-39 and the EGFR/RAS/MAPK pathway, which are first used during vulval fate specification, to the subsequent phase of morphogenesis.

MATERIALS AND METHODS

Strains

C. elegans strains were maintained at 20°C as described (Brenner, 1974) unless noted otherwise. Wild type refers to the Bristol N2 strain. Transgenic lines were generated by microinjection of the indicated constructs at 10-20 ng/μl together with transformation markers at 50-75 ng/μl and bluescript carrier to a total DNA concentration of 150 ng/μl. Strains used are as follows: LGII: *vab-23(tm1945)/mIn1[mIs14 dpy-10(e128)]* (this study), *lin-7(e1413)*, *eff-1(ok1021)*. LGIII: *lin-39(n1760)*. LGIV: *lin-3(e1417)*, *let-60(n1046)*. LGV: *sos-1(cs41)*. Integrated arrays: LGII: *kuIs36[P_{egl-26}::gfp,unc-119(+)]* (Hanna-Rose and Han, 2002). LGIII: *syIs90[P_{egl-17}::yfp,unc-119]*, *syIs107[unc-119(+),P_{lin-3}::Δpes-10::gfp]* (Chang et al., 1999). LGIV: *jcIs1[ajm-1::gfp]* (Mohler et al., 1998), *zhIs1[lin-39::gfp]* (Szabo et al., 2009), *swIs79[ajm-1::gfp,unc-119]*, *mcIs46[dlg-1:dsred;unc119(+)]*. LGV: *syIs51[P_{cdh-3}::gfp,unc-119]* (Inoue et al., 2002), *gaIs36[hs-mpk-1(+),D-mek(gf)]* (Lackner and Kim, 1998), *zzIs16[P_{eff-1}::gfp,rol-6(gf)]* (Fernandes and Sternberg, 2007). Extra-chromosomal arrays: *zhEx229[vab-23::gfp,lin-48::gfp]* (Pellegrino et al., 2009), *zhEx271[$P_{unc-119}$-vab-23a::gfp,lin-48::gfp]* (Pellegrino et al., 2009), *zhEx275[vab-23::gfp,rol-6(d)]*, *zhEx276[vab-23::gfp,P_{sur-5}::dsred]*, *zhEx277[vab-23a::gfp,lin-48::gfp]*, *zhEx286[vab-23Hox(+),lin-48::gfp]*, *zhEx287[vab-23 HoxΔ1,lin-48::gfp]*, *zhEx288[vab-23HoxΔ2,lin-48::gfp]*, *zhEx294[vab-23Hox-mut,lin-48::gfp]*, *zhEx295[vab-23,P_{sur-5}::dsred]*, *zhEx317[$P_{unc-119}$-vab-23a::gfp,smp-1::gfp,plin-48::gfp]*, *zhEx372 [$P_{smp-1-2256-2987}$::nls::gfp::lacZ,myo-2::mcherry]*, *zhEx373[$P_{smp-1-2256-1}$:: nls::gfp::lacZ,myo-2::mcherry]*, *zhEx371[$P_{smp-1-2256-2987Δ486-2497}$::nls:: gfp::lacZ,myo-2::mcherry]*, *zhEx375[$P_{smp-1\ 2494-2987}$::nls::gfp::lacZ,myo-2::mcherry]*, *zhEx391[$P_{smp-1-2604-2987}$::nls::gfp::lacZ,myo-2::mcherry]*, *zhEx390[$P_{smp-1-2701-2987}$::nls::gfp::lacZ,myo-2::mcherry]*, *zhEx388 [$P_{smp-1-2803-2987}$::nls::gfp::lacZ,myo-2::mcherry]*, *zhEx389[$P_{smp-1-2903-2987}$:: nls::gfp::lacZ,myo-2::mcherry]*, *zhEx400[$P_{smp-1-2604-2987Δ2790-2809}$:: nls::gfp::lacZ,myo-2::mcherry]*.

RNA interference

RNA interference (RNAi) was performed using the feeding method (Kamath et al., 2001). Worms were synchronized at the L1 stage, transferred to nematode growth media plates containing 3 mM IPTG, 50 μg/ml ampicillin and RNAi bacteria, and allowed to grow for 3-5 days at 25°C. The F1 progeny were analyzed.

Microscopy and 3D reconstructions of vulval toroids

Images were recorded of anesthetized larvae using a Leica DMRA wide-field microscope equipped with a cooled CCD camera (Hamamatsu ORCA-ER) as described (Pellegrino et al., 2009) and analyzed using the Openlab 5.0 software package (Improvision/Perkin Elmer). To quantify signal intensities (Figs 5, 6), images were recorded under identical conditions and the mean fluorescence intensity subtracted by the background fluorescence was determined using the Openlab measurement tool. To create 3D reconstructions of vulval toroids (Figs 1, 7), confocal sections through the larvae were recorded with an Olympus FV1000 confocal microscope and processed with the Volocity 2.0 software package (Improvision/Perkin Elmer).

vab-23 and *smp-1* promoter and chromatin immunoprecipitation (ChIP) analysis

vab-23 promoter deletion analysis was performed by PCR using the *vab-23::gfp* plasmid as template. The upstream region of the *vab-23* promoter for each PCR product is as follows: 3372 bp for *vab-23Hox(+)*, 1363 bp for *vab-23 HoxΔ1*, 1203 bp for *vab-23 HoxΔ2*. Point mutations in both conserved PBX sites (*vab-23 Hox mut*) were introduced using a combination of the QuikChange Multi Site-Directed Mutagenesis Kit (Stratagene) and overlap PCR (Hobert, 2002). *smp-1* promoter analysis was performed by PCR amplification of the fragments indicated in Fig. 4E subcloned into the *Pst*I and *Sal*I sites of the Fire vector pPD96.04.

For ChIP analysis, chromatin prepared from animals carrying a functional LIN-39::GFP reporter was precipitated with GFP antibodies (Roche) as described by Mukhopadhyay et al. (Mukhopadhyay et al., 2008). As negative control, a mock precipitation omitting the primary antibody was performed in parallel. Binding was quantified by Q-PCR with the probes shown in Fig. 6B. For each sample, the signal was first normalized to the input DNA (Δct) and then to the signal obtained with a probe in the 3′UTR of *vab-23* (ΔΔct) as internal reference to calculate relative binding. Primers used for Q-PCR analysis were: CTCAAAGTGGTCCCAAAAA and AGAGAAGAAAGAAGGAGG for region I; TACTTCCCCTCTTGCACT and CGGACCACTATCAAA-ACAC for region II; CCCATTGACATTTCCTAC and GACAAGATTG-ATTCGGCG for region III; and CAATTACTTTGTGATCTCCC and TCCCATATACACTCCGCA for the 3′ region. For ChIPseq analysis, 20 ng of immunoprecipitated DNA was used as template for the SOLiD 4 whole-genome sequencing platform yielding around 4×10^7 reads of 50 bp each. DNAs isolated from the input chromatin fraction and from a ChIP experiment using an unrelated GFP fusion protein were subjected to the same sequence analysis and used as background controls. Sequence alignment to the *C. elegans* reference sequence (WS192) was performed with the CLC genomics workbench software using default parameters. Peak detection was performed with a custom R script described in the legend to Table S1 in the supplementary material.

RESULTS

VAB-23 is essential for toroid formation during vulval morphogenesis

The function of *vab-23* was analyzed using the *vab-23(tm1945)* deletion allele (kindly provided by S. Mitani, Tokyo Women's University School of Medicine, Japan) that is likely to represent a null mutation (Pellegrino et al., 2009). The *vab-23(tm1945)* deletion results in a completely penetrant embryonic or early larval lethal phenotype due to defects in epidermal morphogenesis. The lethality could be rescued by expression of *vab-23a* cDNA with *gfp* fused at the C-terminus under control of the pan-neuronal *unc-119* promoter ($P_{unc\text{-}119}$*::vab-23::gfp*) (Pellegrino et al., 2009). This neuron-specific rescue allowed us to study the function of *vab-23* during post-embryonic development. Homozygous *vab-23(tm1945)* mutants carrying the $P_{unc\text{-}119}$*::vab-23::gfp* transgene developed into fertile adults with a completely penetrant protruding vulva (Pvl) phenotype. At low penetrance (<15%), $P_{unc\text{-}119}$*::vab-23::gfp* was weakly expressed in the 1° vulval lineage, which we attribute to the leaky nature of the *unc-119* promoter. However, the low level of epidermal *vab-23* expression was insufficient to rescue the Pvl phenotype. For the remainder of this study, we refer to *vab-23(tm1945)* larvae rescued by $P_{unc\text{-}119}$*::vab-23::gfp* as *vab-23(tm1945)* mutants.

We first investigated whether the vulval defects of *vab-23(tm1945)* were caused by an abnormal pattern of cell division. For this purpose, we directly followed the vulval lineage of *vab-23(tm1945)* animals, but observed no change in the cell division pattern or the orientations of the cleavage axes (n=4). In addition, we counted the number of vulval cells at the early L4 stage and found the normal number of 22 cells in all cases (n=20; data not shown). However, all *vab-23(tm1945)* L4 larvae displayed penetrant defects in vulval morphogenesis. The wild-type vulva is made of a stack of seven concentric toroid rings that are formed by the circumferential migration and subsequent fusion of contralateral pairs of cells of the same sub-fates (Fig. 1A,B). By contrast, the vulvae of *vab-23(tm1945)* larvae were asymmetric in configuration and abnormal in shape (Fig. 1C). These defects could be phenocopied by *vab-23* RNAi (see Fig. S1 in the supplementary material) and rescued by introducing the entire genomic *vab-23* locus into *vab-23(tm1945)* mutants (Fig. 8A, in this particular experiment in the absence of $P_{unc\text{-}119}$*::vab-23::gfp*). Thus, the observed vulval morphogenesis defects are caused by a loss of *vab-23* function.

Next, we used the AJM-1::GFP adherens junction marker to examine the shape of the vulval toroids in L4 larvae (Mohler et al., 1998). In the wild type, AJM-1::GFP appeared as a stack of eight concentric rings delineating the seven toroids (Fig. 1D). A mid-sagittal cross-section revealed eight dots representing the cell junctions of the toroids (Fig. 1D′). *vab-23(tm1945)* animals displayed two characteristic defects. First, fewer abnormally shaped toroids were formed with an average of 4.3±0.2 vulval toroid junctions per animal (n=43; Fig. 1E,E′). The absent toroids were predominantly those normally formed by the 2° VulC, VulD and the 1° VulE and VulF cells. Second, cells failed to migrate towards the vulval midline in 45% (n=64) of *vab-23(tm1945)* L4 larvae (arrowhead in Fig. 1E″). Thus, *vab-23* is not necessary for the execution of the vulval cell lineage, but rather controls toroid formation during morphogenesis.

vab-23 represses *eff-1*-mediated vulval cell fusions

Next, we examined whether the reduced toroid number in *vab-23(tm1945)* mutants might be due to ectopic cell fusions resulting from inter-toroid fusion between cells of different sub-fates or from fusion with the surrounding hyp7. The fusogen EFF-1 is necessary for most somatic cell fusions, including those between vulval cells and hyp7 and between vulval cells within toroids (Mohler et al., 2002). We used a transcriptional $P_{eff\text{-}1}$*::gfp* reporter to examine whether ectopic *eff-1* expression might be responsible for the loss of toroids. In control RNAi animals, $P_{eff\text{-}1}$*::gfp* was expressed at the L4 stage in VulA, VulC and less frequently in VulF (21%, n=43) (Fig. 2A). Reduction of *vab-23* function by RNAi caused an increased expression of $P_{eff\text{-}1}$*::gfp* in VulF (65%, n=34) and additional expression in VulE (38%, n=34), where no expression was observed in control animals (n=43) (Fig. 2B). We then investigated whether loss of *eff-1* function suppresses the reduced toroid number in *vab-*

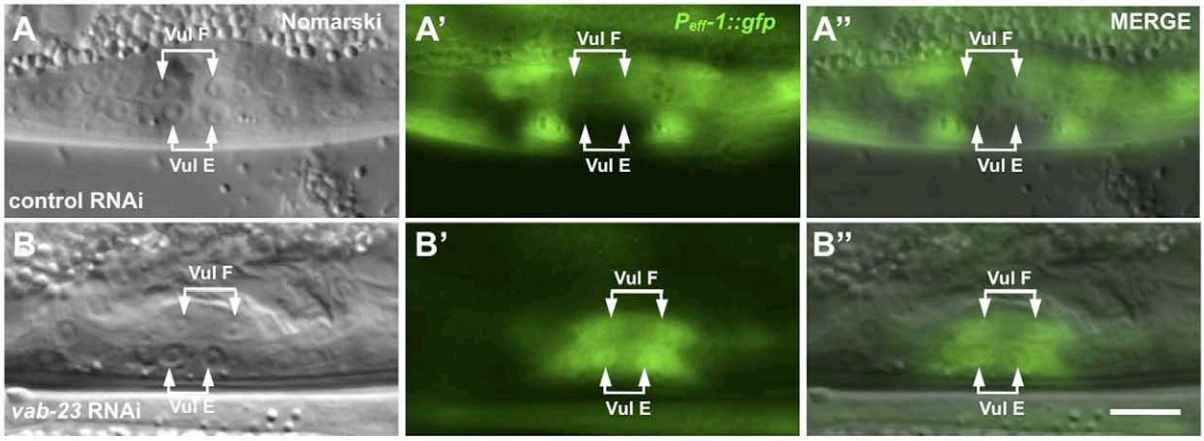

Fig. 2. VAB-23 represses the fusogen *eff-1* in VulE and VulF. (**A-B″**) Nomarski (A,B), GFP (A′,B′) and merged (A″-B″) images of control (A-A″) and *vab-23* RNAi-treated (B-B″) larvae carrying an *eff-1::gfp* reporter. The positions of the VulE and VulF nuclei are indicated by arrows. Anterior is left. Scale bar: 10 μm.

23(tm1945) mutants. Vulval morphogenesis was still abnormal and toroids were malformed in *eff-1(ok1021); vab-23(tm1945)* double mutants, although the number of cell junctions was increased from 4.3±0.2 to an average of 6.4±0.2 per animal (n=24; Fig. 1F). Taken together, loss of VAB-23 function results in the ectopic expression of EFF-1, which is partially responsible for the reduced toroid number. However, as the toroids that formed in *eff-1(ok1021); vab-23(tm1945)* double mutants were still abnormally shaped, VAB-23 is not only required to repress EFF-1-mediated vulval cell fusions but also to mediate proper toroid formation.

VAB-23 represses the formation of ectopic cell contacts

VAB-23 regulates the formation of contacts between contralateral pairs of epidermal cells during morphogenesis of the embryo (Pellegrino et al., 2009). To assess whether VAB-23 plays a similar function during vulval morphogenesis, we followed cell junctions formed between adjacent vulval cells during larval development (Fig. 3). Cell contacts in *vab-23(tm1945)* worms appeared normal at the early L3 stage (Pn.p to Pn.px stage, n=33). However, beginning at the Pn.pxx stage, abnormal cell extensions between adjacent vulval cells formed in 59% of *vab-23(tm1945)* animals (n=41; Fig. 3D), and at the onset of vulval invagination (Pn.pxxx stage) ectopic contacts between 1° and 2° vulval cells were observed in 88% of the cases (n=33; Fig. 3F). Finally, in *eff-1(ok1021); vab-23(tm1945)* double mutants at the L4 stage, 1° and 2° cells failed to reach their contralateral partner cells across the midline (Fig. 1F), suggesting that the vulval morphogenesis defects are similar to the defects observed during ventral epidermal enclosure of the embryo (Pellegrino et al., 2009). Thus, besides repressing cell fusions, VAB-23 is also required for the proper interaction between vulval cells of the same sub-fates.

VAB-23 regulates *smp-1* transcription during vulval morphogenesis

The abnormal vulval cell migrations and cell contacts in *vab-23(tm1945)* mutants are reminiscent of mutations in *smp-1*, which encodes a transmembrane Semaphorin 1a homolog, or in *plx-1*, which encodes the putative SMP-1 receptor Plexin-A4 (Dalpe et al., 2005). We therefore examined whether *smp-1* and/or *plx-1* expression might be regulated by VAB-23, as we previously found that the zinc finger domain of VAB-23 is essential for its nuclear function (Pellegrino et al., 2009). Using a translational SMP-1::GFP reporter (kind gift of Joseph Culotti, The Samuel Lumenfeld Research Institute, Ontario, Canada), for which expression and localization at the vulval midline has been previously described (Dalpe et al., 2005), we found that 59% of *vab-23(tm1945)* larvae (n=29) lacked SMP-1::GFP expression at the onset of vulval invagination, whereas SMP-1::GFP expression was absent in only 9% of wild-type animals at this stage (n=34) (Fig. 4A′,B′). We verified that the loss of SMP-1 expression was not due to excess cell fusions by analyzing the adherens junction marker DLG-1::dsRED (Fig. 4A″,B″) (Bossinger et al., 2001). Despite the abnormal shape of the vulval invagination, no reduction in DLG-1::dsRED expression was detected in *vab-23(tm1945)* mutants at this stage, indicating that the ectopic cell fusions occur at a later stage and are therefore unlikely to be the cause of the lost SMP-1::GFP expression.

To determine whether VAB-23 controls *smp-1* expression at the transcriptional or post-transcriptional level and to identify the cis-regulatory elements, we generated a series of transcriptional *smp-1* reporters (Fig. 4E). A construct in which an *nls::gfp::lacZ* reporter cassette was fused in frame within exon II to include 2256 bb of the 5′ *smp-1* promoter/enhancer region and the entire intron I yielded specific expression in the VulF, VulE and VulD cells ($P_{smp\text{-}1\text{-}2256\text{-}2987}$ in Fig. 4E and data not shown). However, a construct consisting only of the 2256 bb of the 5′ promoter/enhancer region upstream of exon I did not show any detectable expression in the vulval cells but showed strong ectopic expression in body wall muscles and hypodermal cells ($P_{smp\text{-}1\text{-}2256\text{-}1}$ in Fig. 4E and data not shown). Thus, intron I must contain the regulatory elements required for vulva-specific transcription of *smp-1* mRNA. We further narrowed down the region that is sufficient for vulval expression to a 493 bp fragment at the end of intron I (Fig. 4C,C′ and $P_{smp\text{-}1\text{-}2494\text{-}2987}$ in 4E). When the $P_{smp\text{-}1\text{-}2494\text{-}2987}$ reporter was introduced into the *vab-23(tm1945)* mutant background, expression was strongly reduced but not eliminated (Fig. 4D). Specifically, 30% (n=30) of *vab-23(tm1945)* L4 larvae showed detectable NLS::GFP expression in the vulval cells, whereas strong expression was observed in 85% (n=20) of wild-type larvae. Further deletion analysis identified a 102 bp region (between positions 2701 and

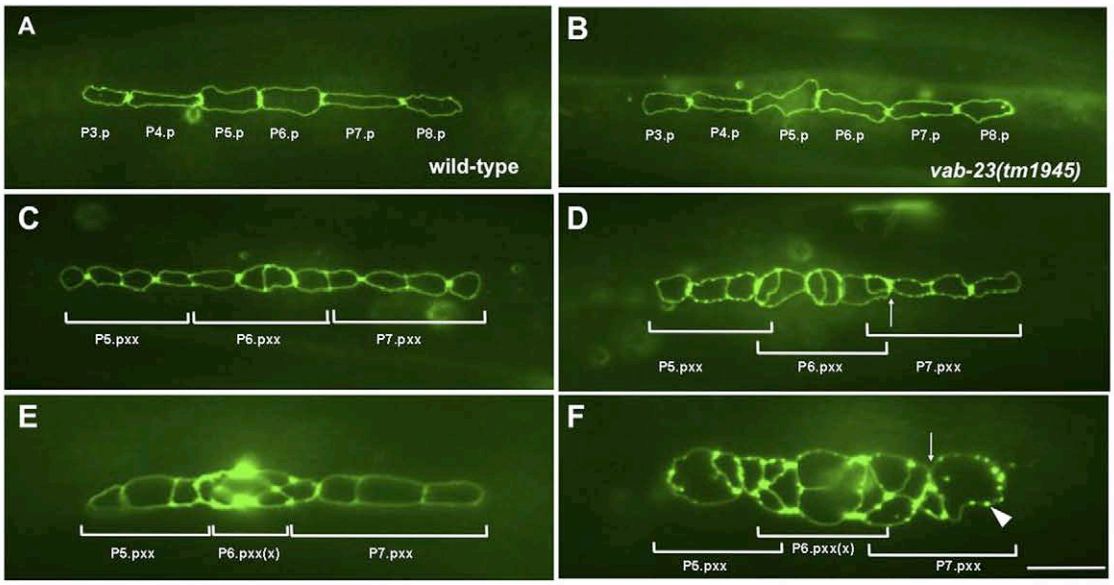

Fig. 3. VAB-23 regulates the formation of proper vulval cell contacts. (**A-F**) Ventral views of AJM-1::GFP in wild-type (A,C,E) and *vab-23(tm1945)* (B,D,F) larvae at the Pn.p, Pn.pxx to Pn.pxxx stages. Arrows in D and F indicate abnormal cell contacts, and the arrowhead in F shows punctate AJM-1::GFP expression. Scale bar: 10 μm.

2803) that is absolutely required for expression of *smp-1* as no NLS::GFP expression was detectable in animals carrying the $P_{smp\text{-}1\text{-}2803\text{-}2987}$ reporter. Possibly, this minimal region in intron I defines an alternative, vulva-specific promoter generating an *smp-1* mRNA that uses an alternative translational start codon present at the beginning of exon II (position 2884) or a further downstream start codon within exon II. This essential 102 bp region contains a stretch of 20 bp (positions 2790 to 2809) that are strongly conserved between the four closely related nematode species *C. elegans*, *C. briggsae*, *C. remanei* and *C. brenneri* (Fig. 4F). When this conserved 20 bp element was deleted in the minimal reporter ($P_{smp\text{-}1\text{-}2604\text{-}2987\Delta 2790\text{-}2809}$ in Fig. 4E), vulval expression was strongly reduced but not eliminated, similar to the reduction observed in *vab-23(tm1945)* mutants. Specifically, 22% of $P_{smp\text{-}1\text{-}2604\text{-}2987\Delta 2790\text{-}2809}$ L4 larvae showed NLS::GFP expression, whereas no expression was detected in 52% and asymmetric expression on one side of the vulval invagination in the remaining 25% of the cases (n=36).

To test whether the VAB-23 protein interacts directly with the *smp-1* locus, we performed chromatin immunoprecipitation of VAB-23 followed by deep sequencing of the bound DNA fragments (ChIPseq). For this purpose, we used the translational *vab-23::gfp* fusion construct described previously (Pellegrino et al., 2009) and isolated the VAB-23::GFP protein-chromatin complexes with anti-GFP antibodies. Importantly, the *vab-23::gfp* transgene efficiently rescued the embryonic and vulval morphogenesis defects of *vab-23(tm1945)* mutants (Fig. 8A). The ChIPseq analysis detected strong binding of VAB-23::GFP to the *smp-1* locus over a relatively large region with a peak (i.e. region of the highest read coverage) in the same region that had been identified by *smp-1* promoter analysis (left-right arrow in Fig. 4E; see Fig. S2A in the supplementary material).

Taken together, our promoter and ChIPseq analysis indicated that VAB-23 directly activates transcription of *smp-1* in the VulF, VulE and VulD cells. In addition to *smp-1*, we identified another 455 specific binding VAB-23 binding sites throughout the *C. elegans* genome, suggesting that VAB-23 controls the transcription of a large number of target genes (see Table S1 in the supplementary material and Materials and methods).

VAB-23 regulates the expression of late VulE and VulF sub-fate-specific genes

Next, we used various markers to determine whether early or late steps during cell fate specification are affected in *vab-23(tm1945)* mutants (Fig. 5). We examined the 1° fate specification using a $P_{egl\text{-}17}$*::yfp* reporter, which is predominantly expressed in the 1° cell lineage until the 4-cell stage (Pn.pxx). This early, 1°-specific expression of $P_{egl\text{-}17}$*::yfp* was unchanged or even slightly elevated in *vab-23(tm1945)* larvae, indicating proper 1° fate specification (Fig. 5A,B). To examine the VulE and VulF sub-fates, we used transcriptional $P_{egl\text{-}26}$*::gfp* and $P_{lin\text{-}3}$*::gfp* reporters, respectively (Chang et al., 1999; Hanna-Rose and Han, 2002). In *vab-23(tm1945)* mutants, 75% of L4 larvae (n=61) lacked $P_{lin\text{-}3}$*::gfp* expression in VulF cells, compared with 9% of wild-type larvae showing no expression at this stage (n=23; Fig. 5C,D). Similarly, a reduction of *vab-23* function by RNAi caused a loss of $P_{egl\text{-}26}$*::gfp* expression in VulE in 61% of the animals (n=54; Fig. 5E,F). Moreover, VAB-23::GFP ChIPseq analysis detected a small but significant peak in the *egl-26* 5′ regulatory region contained within the $P_{egl\text{-}26}$*::gfp* reporter (see Fig. S2B in the supplementary material), whereas no binding to the *lin-3* locus was detected (data not shown).

LIN-3 EGF expression in VulF cells is necessary to specify the uv1 cell fate in the ventral uterine cells (Chang et al., 1999). Accordingly, *vab-23(tm1945)* mutants or RNAi-treated animals often had thick tissue blocking the connection between the vulval lumen and the uterus, suggesting a defect in uterine development (see Fig. S1B in the supplementary material). Finally, we examined the $P_{egl\text{-}17}$*::yfp* and $P_{cdh\text{-}3}$*::gfp* reporters in L4 larvae to assay the specification of the 2° VulC and VulD sub-fates (Burdine et al., 1998; Inoue et al., 2002), but observed no obvious changes in their expression patterns (Fig. 5G-J). Thus, VAB-23 is not necessary for

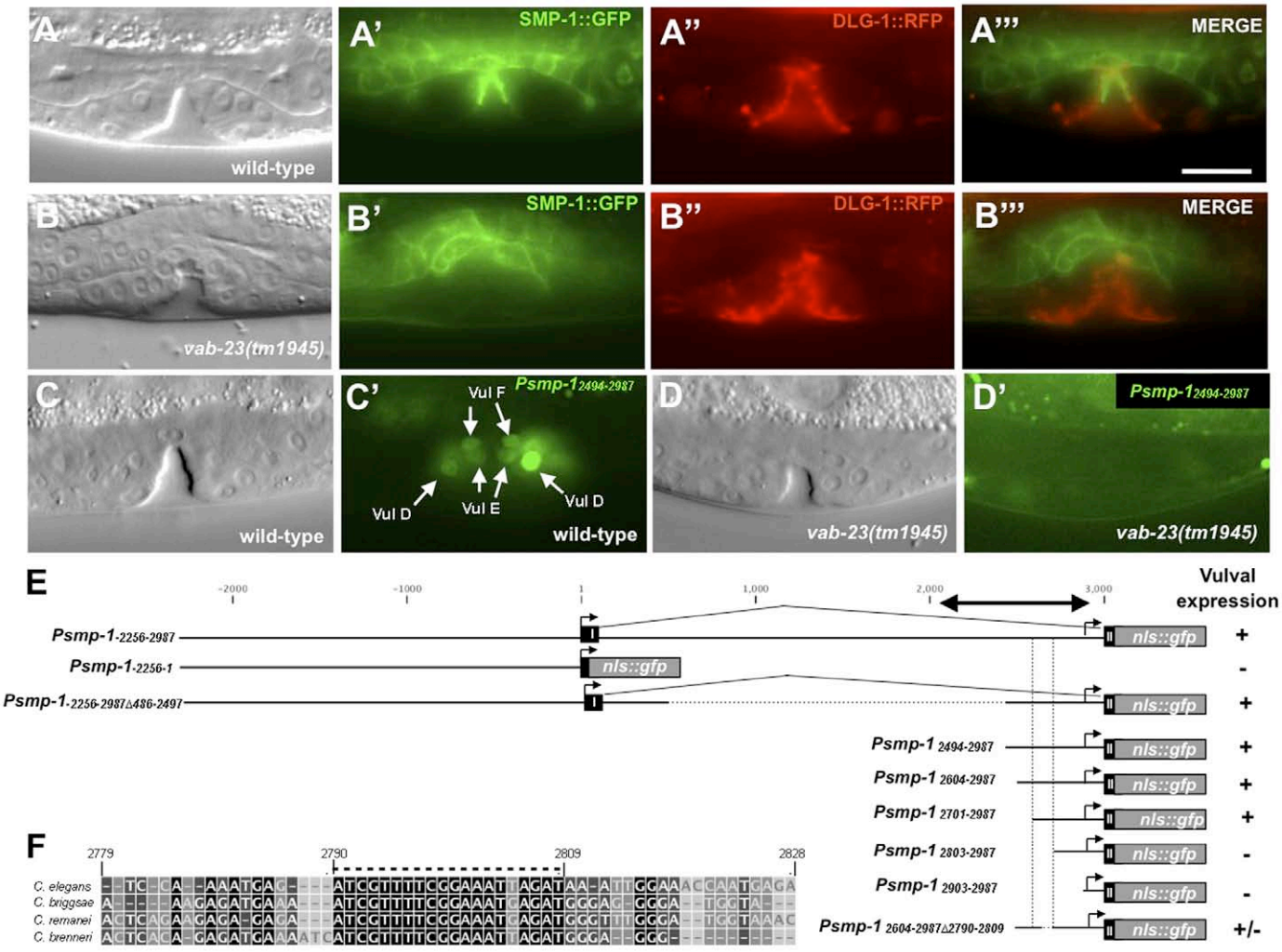

Fig. 4. VAB-23 induces *smp-1* transcription in VulF, VulE and VulD. (**A-B‴**) Nomarski images (A,B), expression of the translational SMP-1::GFP reporter (A′,B′), expression of the DLG-1::dsRED reporter (A″,B″) and merged images (A‴,B‴) in wild-type (A-A‴) and *vab-23(tm1945)* (B-B‴) L4 larvae at the onset of toroid formation. (**C-D′**) Nomarski images (C,D) and expression of the transcriptional $P_{smp\text{-}1\text{-}2494\text{-}2987}$ reporter (C′,D′) in wild-type (C,C′) and *vab-23(tm1945)* (D,D′) L4 larvae. Anterior is left. Scale bar: 10 μm. (**E**) Structures of the *smp-1* transcriptional reporters used for promoter analysis. The numbers indicate the positions relative to the translational start site. For each construct, three independent lines were analyzed except for $P_{smp\text{-}1\text{-}2803\text{-}2987}$ which yielded only two lines. +, strong vulval expression; –, no detectable expression; +/–, reduced expression (see text). (**F**) Sequence alignment of the conserved element in the vulva-specific element in intron I. The dashed line indicates the 20 nucleotides deleted in reporter $P_{smp\text{-}1\text{-}2604\text{-}2987\Delta2790\text{-}2809}$.

the specification of the 1° or 2° cell fates during vulval induction, but rather controls the patterning of the 1° VulF and VulE cells. Regulation of *egl-26* transcription by VAB-23 might be direct, whereas regulation of *lin-3* expression appears to be indirect.

VAB-23 expression is regulated by EGFR/RAS/MAPK signaling during vulval induction and morphogenesis

We analyzed the post-embryonic VAB-23 expression pattern using the translational VAB-23::GFP reporter described previously (Pellegrino et al., 2009). VAB-23::GFP was expressed in the AC, the vulval cells, in the ventral and dorsal uterine cells, the seam cells, the vulval muscle cells, a small cluster of unidentified tail cells, and some ventral cord neurons (Fig. 6 and data not shown). Vulval expression of VAB-23::GFP was observed predominantly in the 1° lineage beginning at the time of induction and persisting until adulthood (Fig. 6A-D and data not shown). Even though VAB-23::GFP was initially expressed at low levels in all VPCs, expression was downregulated in the 2° lineage during induction and persisted at low levels in the tertiary (3°) cells. VAB-23::GFP continued to be strongly expressed in the VulE and VulF cells of L4 larvae during vulval morphogenesis, although relatively weaker expression was also observed in VulC and VulD at this later stage (Fig. 6D, VulC and VulD nuclei are out of focus).

The upregulation of VAB-23 in the 1° cell and simultaneous downregulation in the 2° lineage suggested that *vab-23* might be a target of the EGFR/RAS/MAPK signaling pathway. We therefore analyzed VAB-23::GFP expression in various mutants in which the activity of the EGFR/RAS/MAPK signaling pathway is changed. Diminished activation of LET-23 EGFR by a mutation in *lin-3* (Hill and Sternberg, 1992) or through mislocalization via a *lin-7* mutation (Simske et al., 1996) had two effects on VAB-23::GFP expression. First, expression in P6.p and its descendants was strongly reduced, and second, equally weak expression was observed in P5.p to P7.p

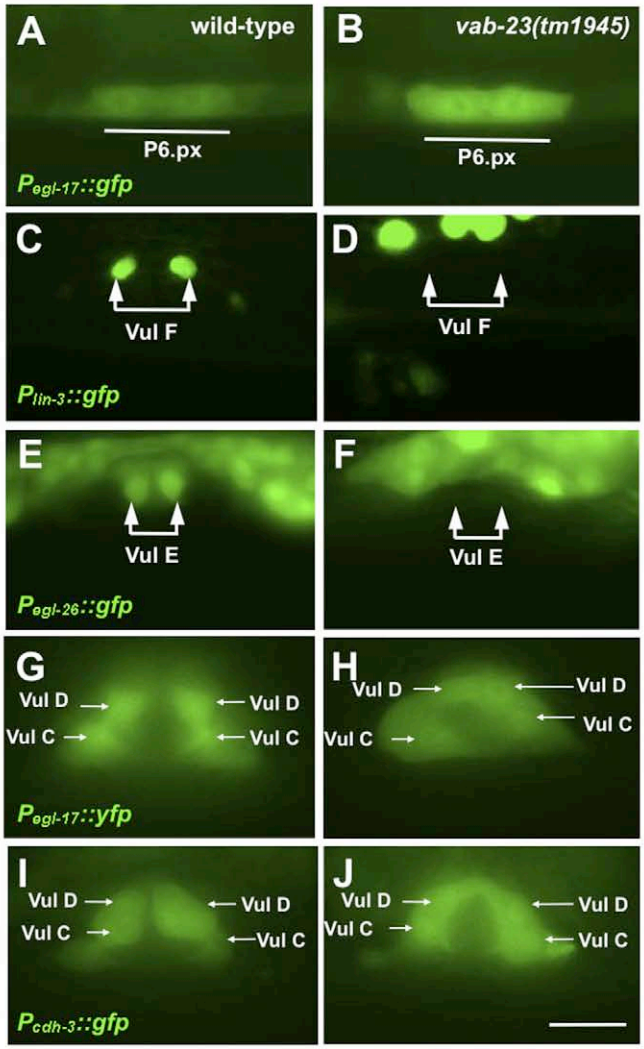

Fig. 5. VAB-23 controls the expression of late 1° cell fate markers. (**A**,**B**) Expression of EGL-17::YFP in wild-type (A) and *vab-23(tm1945)* (B) L3 larvae at the Pn.px stage, (**C-J**) LIN-3::GFP (C,D), EGL-26::GFP (E,F), EGL-17::YFP (G,H) and CDH-3::GFP (I,J) expression in wild-type (C,E,G,I) and *vab-23(tm1945)* (D,F,H,J) L4 larvae. Arrows indicate the nuclei of the indicated sub-fates on one side. Anterior is to left. Scale bar: 10 μm.

and their descendants, probably owing to the loss of lateral inhibition from P6.p (Fig. 6E,F). By contrast, ectopic expression of VAB-23::GFP was induced in the pseudovulvae formed by P3.p, P4.p or P8.p descendants in animals carrying a constitutively active *let-60* allele or by overexpressing the MAP kinase MPK-1 along with MEK-2 (Fig. 6G,H) (Beitel et al., 1990; Lackner and Kim, 1998). Lastly, we examined whether EGFR/RAS/MAPK signaling continues to regulate VAB-23::GFP expression after vulval induction. For this purpose, we used a temperature-sensitive allele of *sos-1*, which encodes the major guanine nucleotide exchange factor for LET-60 (Chang et al., 2000). We observed a reduced or absent expression of VAB-23::GFP in ~80% of *sos-1(ts)* worms that had been shifted to the restrictive temperature after vulval induction had occurred (Fig. 6I,J; see Fig. S2 in the supplementary material). We conclude that EGFR/RAS/MAPK signaling is first required to upregulate *vab-23* expression during induction and later to maintain expression in the 1° lineage during morphogenesis.

vab-23 is a direct target of LIN-39 and CEH-20

LIN-39 performs at least two distinct functions during vulval development (Clark et al., 1993; Maloof and Kenyon, 1998; Shemer and Podbilewicz, 2002). First, LIN-39 represses the expression of the fusogen *eff-1* to prevent the fusion of VPCs with the surrounding hypodermis. Second, *lin-39* is required for the execution of the vulval cell lineage after the fates have been specified, because in *eff-1(0); lin-39(0)* double mutants the vulval cells fail to divide (Shemer and Podbilewicz, 2002). Because *lin-39* expression is positively regulated by EGFR/RAS/MAPK signaling and *vab-23* prevents *eff-1*-mediated cell fusions, we investigated whether *vab-23* might function downstream of LIN-39 during vulval morphogenesis (Guerry et al., 2007; Maloof and Kenyon, 1998). For this purpose, the loss-of-function allele *lin-39(n1760)* was examined together with the *eff-1(ok1021)* mutation, which suppresses the early VPC fusions. VAB-23::GFP expression was strongly reduced in the *eff-1(ok1021); lin-39(n1760)* double mutants, but unchanged in *eff-1(ok1021)* single mutants (Fig. 6K,L and data not shown). In early L3 larvae at the Pn.px cell stage, VAB-23::GFP was absent or barely detectable in 89% of *eff-1(ok1021); lin-39(n1760)* double mutants and strongly reduced in the remaining cases (n=26; Fig. 6K). Also, at the time of toroid formation, *eff-1(ok1021); lin-39(n1760)* animals showed, on average, a fourfold decrease in the intensity of VAB-23::GFP expression with 63% of the animals showing no or strongly reduced expression (n=27; Fig. 6L). In the remaining 37% of cases, VAB-23::GFP expression persisted albeit at a reduced level, indicating that late VAB-23 expression is partially regulated by a LIN-39-independent pathway. Similarly, a reduction-of-function mutation in *ceh-20*, which encodes a LIN-39 co-factor of the Extradenticle/PBX family (Yang et al., 2005), resulted in reduced VAB-23::GFP expression during the early (Pn.p to Pn.pxx) stages of vulval development, whereas the late (Pn.pxxx stage) expression was not affected by *ceh-20* (Fig, 6M,N).

Next, we determined whether *vab-23* is a transcriptional target of LIN-39. We aligned the *vab-23* 5′ regulatory regions from *C. elegans* and the closely related nematodes *C. briggsae* and *C. remanei* and searched for conserved HOX/PBX consensus binding motifs, such as TGATNNAT (Cui and Han, 2003; Koh et al., 2002). Two conserved putative HOX/PBX binding sites were present in a 72 bp region located 1.3 kb upstream of the *vab-23* translation initiation site (Fig. 7A, region II in 7B). By performing a promoter deletion and mutation analysis, we found that the early (Pn.px stage) vulval expression of VAB-23::GFP depends on the 72 bp region, whereas a smaller deletion leaving the 72 bp region intact (HoxΔ1) had no significant effect (Fig. 7B,C). By contrast, deletion of the two HOX/PBX sites had only moderate effects on the late VAB-23::GFP expression in L4 larvae (HoxΔ2 in Fig. 7D). Moreover, point mutations in both conserved HOX/PBX sites (Hox-mut) eliminated the early but not the late VAB-23::GFP expression, suggesting that early on *vab-23* is a direct LIN-39 and CEH-20 target (Fig. 7C,D). Thus, LIN-39 regulates VAB-23 expression until the Pn.px stage together with CEH-20 and from the Pn.pxx stage onwards, in conjunction with another, unidentified co-factor.

Finally, we observed a direct interaction between LIN-39 and the region containing the HOX/PBX sites in ChIP experiments. Using a functional LIN-39::GFP reporter (Szabo et al., 2009), we detected strongest binding to region II, which contains the HOX/PBX sites, whereas regions I and III showed weaker binding relative a probe in the 3′UTR used as internal reference (Fig. 7B,E) (see Materials and methods). It should be noted that the ChIPseq experiments performed by the modENCODE consortium (Celniker et al., 2009)

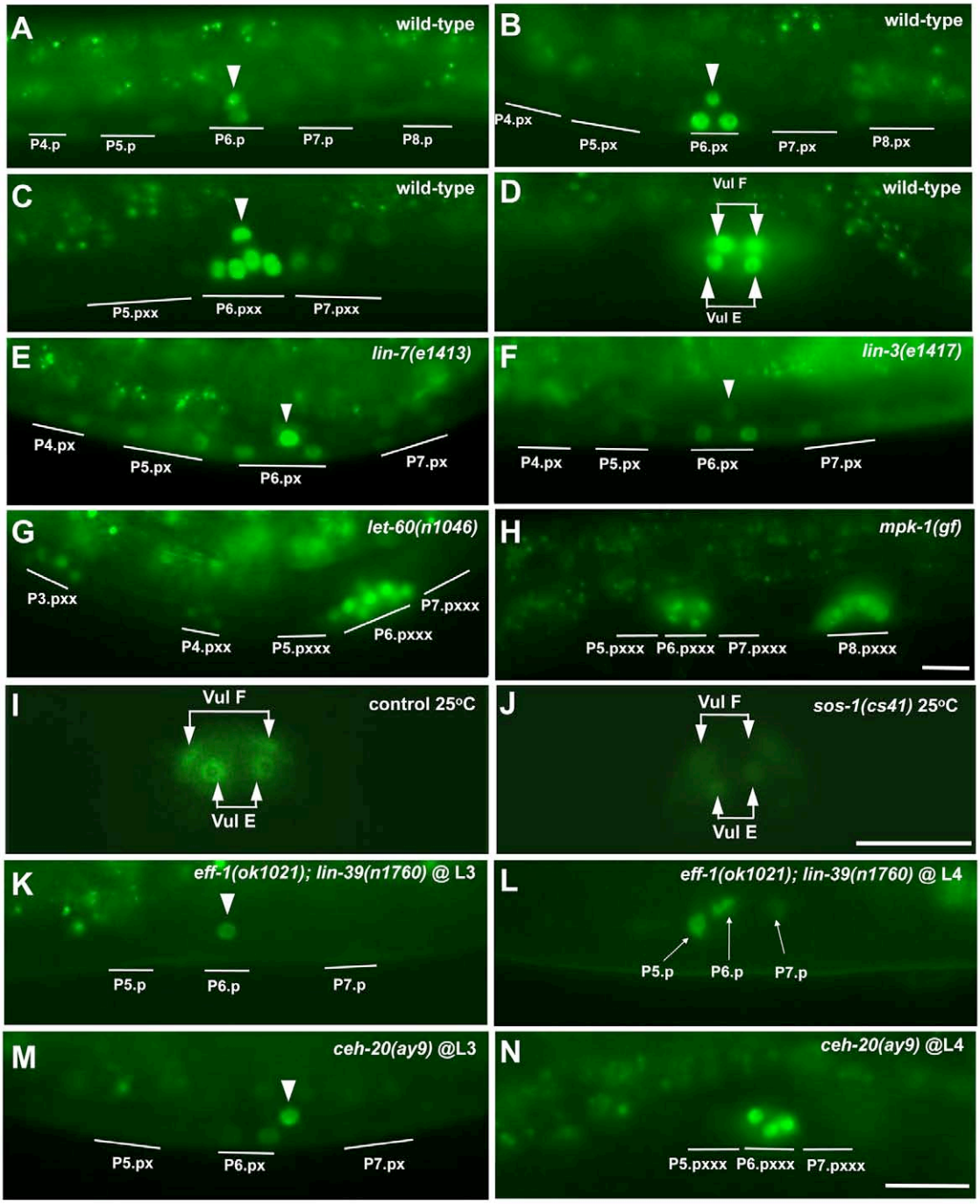

Fig. 6. VAB-23::GFP expression pattern and its regulation by EGFR/RAS/MAPK and LIN-39. (**A-D**) VAB-23::GFP expression in wild-type larvae from the Pn.p to the Pn.pxxx stages. (**E-H**) VAB-23::GFP expression in *lin-7(e1413)* (E) and *lin-3(e1417)* (F) L3 larvae at the Pn.px stage, and in *let-60(n1046)* (G) and *gaIs36[hs::mpk-1, dmek(gf)]* (H) L4 larvae. (**I**,**J**) VAB-23::GFP expression in wild-type control (I) and *sos-1(cs41ts)* (J) larvae, which had been up-shifted to 25°C in the L3 stage after induction and developed at 25°C until the L4 (Pn.pxxx) stage (see also Fig. S3 in the supplementary material). (**K**,**L**) VAB-23::GFP expression in the undivided VPCs of *lin-39(n1760); eff-1(ok1021)* mid-L3 (K) and L4 (L) larvae. (**M**,**N**) VAB-23::GFP expression in *ceh-20(ay9)* larvae at the L3 (M) and L4 (N) stages. Arrowheads indicate the position of the AC, which also expressed VAB-23::GFP. Anterior is left. Scale bars: 10 μm.

detected binding of LIN-39::GFP to the same region in the *vab-23* gene that we identified in our analysis. Taken together, our data indicate that LIN-39 directly regulates *vab-23* expression by interacting with the conserved HOX/PBX sites in the 5′ regulatory region.

LIN-39-induced expression of VAB-23 is required for toroid formation

Finally, we examined whether the early *vab-23* expression induced by LIN-39 and CEH-20 is necessary for toroid formation during the subsequent morphogenesis. For this purpose, we investigated

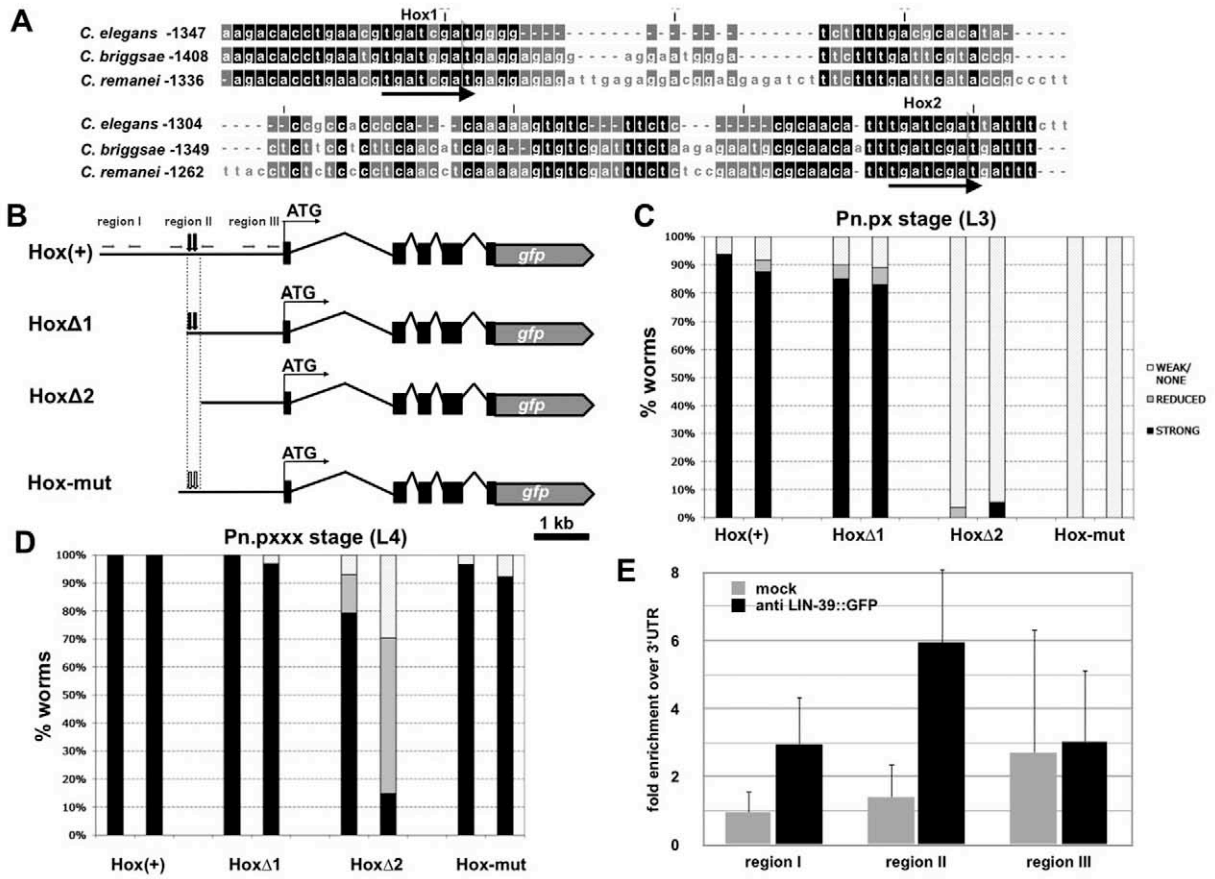

Fig. 7. *vab-23* is a transcriptional target of LIN-39 and CEH-20. (**A**) Sequence alignments of the *C. elegans*, *C. briggsae* and *C. remanei vab-23* enhancer regions containing the CEH-20 (PBX) binding sites TGATNNAT underlined with arrows. (**B**) Reporter constructs used to assay *vab-23* promoter activity. Black arrows indicate the positions of the PBX sites. The gray arrows in the Hox-mut construct indicate the two point-mutations changing the PBX consensus sequence from TGATNNAT to TCTCGAGT. The primers used as probes for regions I to III in the ChIP experiments are indicated with small horizontal arrows. (**C**,**D**) Early (C; Pn.px stage) and late (D; Pnp.pxxx stage) expression of the reporter constructs shown in B. Two independent lines were analyzed for each construct. Expression was scored as 'strong' (black bars) if it was more than twice the background signal, 'reduced' (gray bars) if less than twice the background and 'weak/none' (light bars) if approximately at background levels. (**E**) Binding of LIN-39::GFP to the *vab-23* 5′ regulatory region detected by ChIP. 'Mock' refers to a control precipitation performed in parallel and omitting the primary antibody. The average of three independent experiments with each quantification done in triplicate is shown. Signals were normalized to a probe in the 3′UTR used as internal reference. Error bars indicate the s.d.

toroid formation in *vab-23(tm1945)* mutants carrying the *vab-23* Hox-mut transgene to eliminate the early but not the late VAB-23::GFP expression (Fig. 7C). The *vab-23* Hox-mut transgene rescued the embryonic lethality of *vab-23*, allowing 36% of *tm1945* homozygotes to survive to adulthood (n=359), which is comparable to the rescue obtained with wild-type *vab-23* transgenes (Pellegrino et al., 2009). *vab-23(tm1945); [vab-23 Hox-mut]* animals displayed a highly penetrant Pvl phenotype due to abnormal morphogenesis (Fig. 8A-C), but contained on average 7.2±0.1 toroid junctions (n=45), indicating nearly complete rescue of the toroid hyperfusion defect of *vab-23(tm1945)* mutants (Fig. 7E′). However, the toroids in *vab-23(tm1945); [vab-23 Hox-mut]* animals were abnormally shaped, as the cells failed to establish contacts with their contralateral partner cells, similar to the phenotype described above for *vab-23(tm1945); eff-1(0)* double mutants (Fig. 8E and Fig. 1F). In addition, 31% of *vab-23(tm1945); [vab-23 Hox-mut]* animals displayed cell migration defects (arrow in Fig. 8E). Thus, the early VAB-23 expression controlled by LIN-39 and CEH-20 is only necessary for proper cell migration and cell recognition.

DISCUSSION

VAB-23 is essential for multiple aspects of vulval morphogenesis

We propose the following model for the regulation of toroid formation by VAB-23 (Fig. 9). At the time of vulval induction, inductive signaling induces LIN-39 expression via inactivation of the LIN-1 ETS transcriptional repressor (Guerry et al., 2007; Tan et al., 1998; Wagmaister et al., 2006). LIN-39 and its co-factor CEH-20 then activate *vab-23* transcription in the 1° lineage, and VAB-23 upregulates SMP-1 expression to guide the interactions between contralateral pairs of vulval cells (Dalpe et al., 2005). Later during morphogenesis, CEH-20 is replaced by another, unknown LIN-39 co-factor (Takacs-Vellai et al., 2007). LIN-39 and this new co-factor maintain the expression of VAB-23 in cooperation with the EGFR/RAS/MAPK pathway. The late VAB-23 expression is required both for the repression of EFF-1-mediated vulval cell fusion as well as for the expression of the VulE and VulF specific genes *lin-3* and *egl-26*.

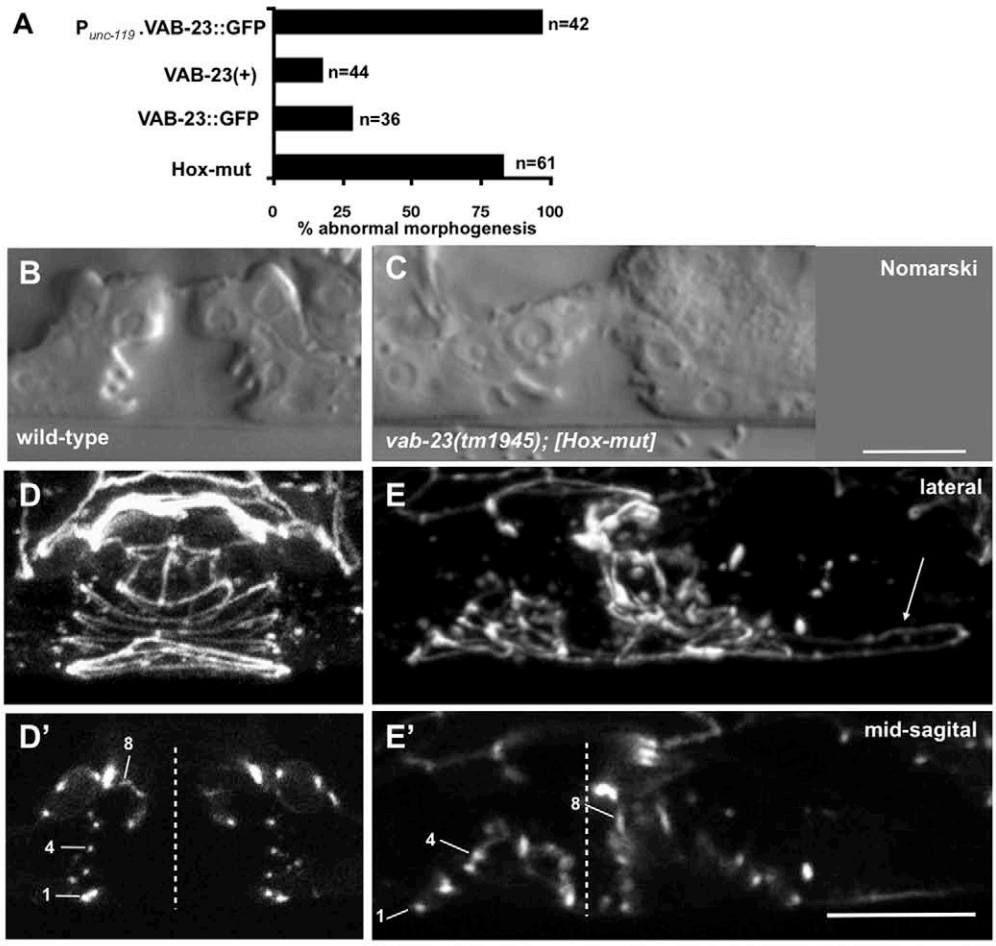

Fig. 8. The early, LIN-39-induced expression of VAB-23 is required for proper morphogenesis. (**A**) Rescue of the *vab-23(tm1945)* morphogenesis defects. VAB-23(+) represents a transgene covering the entire genomic locus (Pellegrino et al., 2009). Transgenic L4 larvae were inspected by Nomarski optics and the percentage of animals with abnormal vulval morphology was calculated. 'n' refers to the number of animals inspected for each transgene. (**B**,**C**) Nomarski images of wild-type (B) and *vab-23(tm1945); [Hox-mut]* (C) L4 larvae. (**D-E'**) Toroid structures of wild-type (D) and *vab-23(tm1945); [Hox-mut]* (E) L4 larvae visualized with the DLG-1::dsRED reporter as described in Fig. 1. D' and E' are mid-sagittal cross sections showing the junctions between toroids (numbered). The arrow in E indicates abnormal migration of VulA, and the dotted lines mark the vulval midline. Scale bars: 10 μm.

Similar functions of VAB-23 during embryo and vulval morphogenesis

Loss of VAB-23 function in the embryo causes the formation of ectopic cell contacts between ipsilateral ventral epidermal cells, resulting in defective ventral closure (Pellegrino et al., 2009). Interestingly, VAB-23 plays an analogous role during toroid formation by guiding cells towards the vulval midline, which forms an axis of symmetry for the developing organ (Fig. 1A). Similar to the embryonic phenotype, cells of the same sub-fate cannot form contacts across the vulval midline, resulting in the malformation or absence of toroids. The *vab-23* phenotype is in part due to reduced SMP-1 expression. To our knowledge, VAB-23 is the first example of a Semaphorin regulator, which links vulval morphogenesis via LIN-39 to the EGFR/RAS/MAPK pathway. However, both the vulval and embryonic morphogenesis defects of *smp-1* mutants are less penetrant and generally milder than the defects observed in *vab-23* mutants, suggesting that VAB-23 controls the expression of additional effectors of morphogenesis acting in parallel with SMP-1 (Dalpe et al., 2005). For example, the Rac GTPase MIG-2 and the guanine-nucleotide exchange factor UNC-73 are both required for vulval cell migration in parallel with the SMP-1/PLX-1 pathway (Dalpe et al., 2005; Kishore and Sundaram, 2002; Lundquist et al., 2001; Zipkin et al., 1997). Thus, VAB-23 might regulate multiple target genes performing diverse functions during vulval morphogenesis.

We have previously shown that during embryogenesis VAB-23 acts from the underlying neuroblasts in a cell non-autonomous manner to guide the ventral epidermal cells (Pellegrino et al., 2009). Although VAB-23 expression was detected predominantly in the 1° cell lineage (except for the weaker, later expression in VulC and VulD) and VAB-23 only controls the patterning of VulE and VulF cells, *vab-23* mutants display defects in the formation of all toroids. Even the distal-most VulA cells often failed to migrate towards the midline and form a toroid. It thus appears that during vulval morphogenesis, VAB-23 guides vulval cells in a cell non-autonomous manner, possibly by regulating the production of multiple secreted cues.

VAB-23 regulates various aspects of vulval and uterine morphogenesis

In addition to controlling the formation of homotypic cell contacts, VAB-23 inhibits cell fusions at a later stage of vulval morphogenesis. Ectopic expression of the fusogen EFF-1 in *vab-23* mutants is likely to be responsible for these abnormal fusions, as loss of *eff-1* function almost completely restored the normal number of cell junctions. LIN-39 acts upstream of *eff-1* to negatively regulate VPC cell fusions prior to vulval induction by inducing the GATA factors *egl-18* and *elt-6* (Koh et al., 2002; Shemer and Podbilewicz, 2002). It is possible that LIN-39 represses late vulval cell fusions indirectly by inducing *vab-23* expression. Interestingly, the cell lineage is unchanged in *vab-23* mutants, whereas the VPCs fail to proliferate in *lin-39(0)* single or *egl-18(0); elt-6(0)* double mutants. Thus, cell proliferation is controlled by LIN-39 through a VAB-23-independent branch of the cell fate execution pathway (Fig. 9).

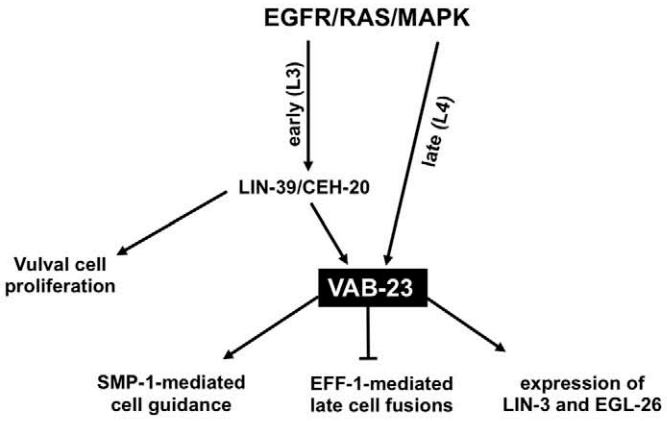

Fig. 9. Model for the regulation and function of *vab-23* during vulval morphogenesis. During early vulval development (Pn.p to Pn.pxx stage), EGFR/RAS/MAPK signaling induces *vab-23* transcription via LIN-39 together with its co-factor CEH-20. Early VAB-23 expression is required for cell guidance by regulating SMP-1 expression. Late VAB-23 expression (Pn.pxxx stage), which is maintained by EGFR/RAS/MAPK signaling acting in parallel with LIN-39 and CEH-20, is necessary to prevent cell fusions through inhibition of EFF-1. Furthermore, VAB-23 activates the expression of EGL-26 and LIN-3, which are necessary for the execution of the 1° VulE and VulF sub-fates. LIN-39 additionally promotes vulval cell proliferation independently of VAB-23.

Besides *eff-1* and *smp-1*, *vab-23* also regulates the later expression of *egl-26* and *lin-3* in VulE and VulF cells, respectively. Proper patterning of the VulE and VulF cells is necessary for vulval morphogenesis and uterine development. *egl-26* is required to maintain the shape of the VulF toroid after the AC has retracted (Estes and Hanna-Rose, 2009; Estes et al., 2007; Hanna-Rose and Han, 2002), and LIN-3 is required for the specification of the uv1 fate by activating LET-23 signaling in the ventral uterine cells. Therefore, the reduced LIN-3 expression in VulF cells probably accounts for the uterine-seam cell defects in *vab-23* mutants (Chang et al., 1999).

Based on our previous data it was not possible to distinguish whether VAB-23 acts as a transcriptional or post-transcriptional regulator of gene expression (Pellegrino et al., 2009). Here, we show that VAB-23 binds to regulatory regions in two of its target genes: to the first intron of *smp-1* and, more weakly, to the 5′ regulatory region of *egl-26*. Finally, we have detected specific binding of VAB-23 to a relatively large number of sites throughout the genome. Although we could not extract an obvious consensus sequence from the VAB-23 binding sites identified by ChIPseq, the palindromic TTCNGAA motif in the center of the conserved regulatory element in *smp-1* is around sevenfold over-represented in the VAB-23 binding sites. (The TTCNGAA motif was found 286 times versus the 40 times that would be expected in a random distribution.) These results indicate that VAB-23 acts as a transcription factor that controls the expression of multiple target genes regulating various aspects of epidermal morphogenesis.

Vulval cell fate specification and morphogenesis are linked processes

During the specification of segment-specific structures and individual organs, the hox genes are thought to regulate a large number of target genes in a context-specific manner (Hueber and Lohmann, 2008). However, only a relatively small number of hox targets that are directly involved in morphogenesis, the so-called 'realisators', have been identified. Furthermore, the conserved EGFR/RAS/MAPK, Notch and WNT signaling pathways control various aspects of epithelial morphogenesis in *Drosophila* and *C. elegans*, but their transcriptional targets during morphogenesis are poorly characterized (Galindo et al., 2005; O'Keefe et al., 2007; Rasmussen et al., 2008).

vab-23 reveals how EGFR/RAS/MAPK signaling coordinates via LIN-39 different aspects of organogenesis after the cell fate decisions have been made. *let-60* has previously been reported to regulate cell migration and fusions (Shemer et al., 2000), and *smp-1* is expressed in the pseudovulvae of *let-60(gf)* worms (Dalpe et al., 2005), suggesting that SMP-1 expression is indeed linked to EGFR/RAS/MAPK signaling. Moreover, conditional inactivation of *sos-1* indicates that continuous EGFR/RAS/MAPK signaling after induction is necessary to maintain VAB-23 expression in the 1° cell lineage. VAB-23 thus acts as a link between the cell fate specification and execution pathways. Although LIN-39 mediates most of the regulation of VAB-23 by the EGFR/RAS/MAPK pathway, LIN-39 clearly performs additional, VAB-23-independent functions. LIN-39 prevents VPC fusion before and promotes cell proliferation after vulval induction (Shemer and Podbilewicz, 2002). Owing to the lack of cell proliferation, it is difficult to determine whether any vulval sub-fates are specified and, thus, whether proper cell contacts are formed in *lin-39(0)* mutants. However, the few (usually one to four) toroids that are formed in *lin-39(0); eff-1(0)* double mutants appear disorganized (Shemer and Podbilewicz, 2002).

In summary, this study shows that vulval fate specification and morphogenesis are more tightly linked than previously thought, as there exists a considerable temporal overlap between these two phases of organogenesis. Continuous signaling by the EGFR/RAS/MAPK pathway after vulval fate specification might be necessary to induce and maintain the expression of key regulators of epidermal morphogenesis. The identification of additional late EGFR/RAS/MAPK targets might shed light on the regulatory network controlling vulval morphogenesis.

Acknowledgements
We thank the members of our group for critical discussion and J.M. Escobar and M. Walser for comments on the manuscript. We are also grateful to the *C. elegans* genetics center and S. Mitani (Japan Knockout Consortium) for providing strains, to the Functional Genomics Center Zurich for SOLiD4 sequencing, and to Andrew Fire for vectors.

Funding
This work was supported by a postgraduate scholarship from the University of Melbourne, the Dr Sue Newton Research Award, and a travel grant from the Australia Research Council and the National Health and Medical Research Council Parasitology Research Network to M.W.P.; the Australian Academy of Science; a grant from the Forschungskredit of the University of Zürich to S.F.; a grant from the Australian Research Council to R.B.G.; and a grant from the Swiss National Science Foundation to A.H.

Competing interests statement
The authors declare no competing financial interests.

Supplementary material
Supplementary material for this article is available at
http://dev.biologists.org/lookup/suppl/doi:10.1242/dev.071951/-/DC1

References
Aroian, R. V. and Sternberg, P. W. (1991). Multiple functions of let-23, a *Caenorhabditis elegans* receptor tyrosine kinase gene required for vulval induction. *Genetics* **128**, 251-267.

Beitel, G. J., Clark, S. G. and Horvitz, H. R. (1990). *Caenorhabditis elegans ras* gene *let-60* acts as a switch in the pathway of vulval induction. *Nature* **348**, 503-509.
Berset, T., Hoier, E. F., Battu, G., Canevascini, S. and Hajnal, A. (2001). Notch inhibition of RAS signaling through MAP kinase phosphatase LIP-1 during *C. elegans* vulval development. *Science* **291**, 1055-1058.
Bossinger, O., Klebes, A., Segbert, C., Theres, C. and Knust, E. (2001). Zonula adherens formation in *Caenorhabditis elegans* requires *dlg-1*, the homologue of the *Drosophila* gene discs large. *Dev. Biol.* **230**, 29-42.
Brenner, S. (1974). The genetics of *Caenorhabditis elegans*. *Genetics* **77**, 71-94.
Brunschwig, K., Wittmann, C., Schnabel, R., Burglin, T. R., Tobler, H. and Muller, F. (1999). Anterior organization of the *Caenorhabditis elegans* embryo by the labial-like Hox gene ceh-13. *Development* **126**, 1537-1546.
Burdine, R. D., Branda, C. S. and Stern, M. J. (1998). EGL-17(FGF) expression coordinates the attraction of the migrating sex myoblasts with vulval induction in *C. elegans*. *Development* **125**, 1083-1093.
Celniker, S. E., Dillon, L. A., Gerstein, M. B., Gunsalus, K. C., Henikoff, S., Karpen, G. H., Kellis, M., Lai, E. C., Lieb, J. D., MacAlpine, D. M. et al. (2009). Unlocking the secrets of the genome. *Nature* **459**, 927-930.
Chang, C., Newman, A. P. and Sternberg, P. W. (1999). Reciprocal EGF signaling back to the uterus from the induced *C. elegans* vulva coordinates morphogenesis of epithelia. *Curr. Biol.* **9**, 237-246.
Chang, C., Hopper, N. A. and Sternberg, P. W. (2000). *Caenorhabditis elegans* SOS-1 is necessary for multiple RAS-mediated developmental signals. *EMBO J.* **19**, 3283-3294.
Chisholm, A. (1991). Control of cell fate in the tail region of *C. elegans* by the gene *egl-5*. *Development* **111**, 921-932.
Clark, S. G., Chisholm, A. D. and Horvitz, H. R. (1993). Control of cell fates in the central body region of *C. elegans* by the homeobox gene *lin-39*. *Cell* **74**, 43-55.
Cui, M. and Han, M. (2003). Cis regulatory requirements for vulval cell-specific expression of the *Caenorhabditis elegans* fibroblast growth factor gene *egl-17*. *Dev. Biol.* **257**, 104-116.
Dalpe, G., Brown, L. and Culotti, J. G. (2005). Vulva morphogenesis involves attraction of plexin 1-expressing primordial vulva cells to semaphorin 1a sequentially expressed at the vulva midline. *Development* **132**, 1387-1400.
Eisenmann, D. M., Maloof, J. N., Simske, J. S., Kenyon, C. and Kim, S. K. (1998). The beta-catenin homolog BAR-1 and LET-60 Ras coordinately regulate the Hox gene *lin-39* during *Caenorhabditis elegans* vulval development. *Development* **125**, 3667-3680.
Estes, K. A. and Hanna-Rose, W. (2009). The anchor cell initiates dorsal lumen formation during *C. elegans* vulval tubulogenesis. *Dev. Biol.* **328**, 297-304.
Estes, K. A., Kalamegham, R. and Hanna-Rose, W. (2007). Membrane localization of the NlpC/P60 family protein EGL-26 correlates with regulation of vulval cell morphogenesis in *Caenorhabditis elegans*. *Dev. Biol.* **308**, 196-205.
Fernandes, J. S. and Sternberg, P. W. (2007). The tailless ortholog *nhr-67* regulates patterning of gene expression and morphogenesis in the *C. elegans* vulva. *PLoS Genet.* **3**, e69.
Galindo, M. I., Bishop, S. A. and Couso, J. P. (2005). Dynamic EGFR-Ras signalling in *Drosophila* leg development. *Dev. Dyn.* **233**, 1496-1508.
Greenwald, I. (2005). LIN-12/Notch signaling in *C. elegans* (August 4, 2005). In *WormBook* (ed. The *C. elegans* Research Community, Wormbook), pp. 1-16. http://www.wormbook.org
Guerry, F., Marti, C. O., Zhang, Y., Moroni, P. S., Jaquiery, E. and Muller, F. (2007). The Mi-2 nucleosome-remodeling protein LET-418 is targeted via LIN-1/ETS to the promoter of *lin-39/hox* during vulval development in *C. elegans*. *Dev. Biol.* **306**, 469-479.
Hanna-Rose, W. and Han, M. (2002). The *Caenorhabditis elegans* EGL-26 protein mediates vulval cell morphogenesis. *Dev. Biol.* **241**, 247-258.
Hill, R. J. and Sternberg, P. W. (1992). The gene *lin-3* encodes an inductive signal for vulval development in *C. elegans*. *Nature* **358**, 470-476.
Hobert, O. (2002). PCR fusion-based approach to create reporter gene constructs for expression analysis in transgenic *C. elegans*. *Biotechniques* **32**, 728-730.
Hombria, J. C. and Lovegrove, B. (2003). Beyond homeosis – HOX function in morphogenesis and organogenesis. *Differentiation* **71**, 461-476.
Hueber, S. D. and Lohmann, I. (2008). Shaping segments: Hox gene function in the genomic age. *BioEssays* **30**, 965-979.
Inoue, T., Sherwood, D. R., Aspock, G., Butler, J. A., Gupta, B. P., Kirouac, M., Wang, M., Lee, P. Y., Kramer, J. M., Hope, I. et al. (2002). Gene expression markers for *Caenorhabditis elegans* vulval cells. *Mech. Dev.* **119 Suppl. 1**, S203-S209.
Kamath, R. S., Martinez-Campos, M., Zipperlen, P., Fraser, A. G. and Ahringer, J. (2001). Effectiveness of specific RNA-mediated interference through ingested double-stranded RNA in *Caenorhabditis elegans*. *Genome Biol.* **2**, RESEARCH0002.
Kenyon, C. (1986). A gene involved in the development of the posterior body region of *C. elegans*. *Cell* **46**, 477-487.
Kishore, R. S. and Sundaram, M. V. (2002). *ced-10* Rac and *mig-2* function redundantly and act with *unc-73* trio to control the orientation of vulval cell divisions and migrations in *Caenorhabditis elegans*. *Dev. Biol.* **241**, 339-348.
Koh, K., Peyrot, S. M., Wood, C. G., Wagmaister, J. A., Maduro, M. F., Eisenmann, D. M. and Rothman, J. H. (2002). Cell fates and fusion in the *C. elegans* vulval primordium are regulated by the EGL-18 and ELT-6 GATA factors - apparent direct targets of the LIN-39 Hox protein. *Development* **129**, 5171-5180.
Lackner, M. R. and Kim, S. K. (1998). Genetic analysis of the *Caenorhabditis elegans* MAP kinase gene *mpk-1*. *Genetics* **150**, 103-117.
Lundquist, E. A., Reddien, P. W., Hartwieg, E., Horvitz, H. R. and Bargmann, C. I. (2001). Three *C. elegans* Rac proteins and several alternative Rac regulators control axon guidance, cell migration and apoptotic cell phagocytosis. *Development* **128**, 4475-4488.
Maloof, J. N. and Kenyon, C. (1998). The Hox gene *lin-39* is required during *C. elegans* vulval induction to select the outcome of Ras signaling. *Development* **125**, 181-190.
McGinnis, W. and Krumlauf, R. (1992). Homeobox genes and axial patterning. *Cell* **68**, 283-302.
Mohler, W. A., Simske, J. S., Williams-Masson, E. M., Hardin, J. D. and White, J. G. (1998). Dynamics and ultrastructure of developmental cell fusions in the *Caenorhabditis elegans* hypodermis. *Curr. Biol.* **8**, 1087-1090.
Mohler, W. A., Shemer, G., del Campo, J. J., Valansi, C., Opoku-Serebuoh, E., Scranton, V., Assaf, N., White, J. G. and Podbilewicz, B. (2002). The type I membrane protein EFF-1 is essential for developmental cell fusion. *Dev. Cell* **2**, 355-362.
Mukhopadhyay, A., Deplancke, B., Walhout, A. J. and Tissenbaum, H. A. (2008). Chromatin immunoprecipitation (ChIP) coupled to detection by quantitative real-time PCR to study transcription factor binding to DNA in *Caenorhabditis elegans*. *Nat. Protoc.* **3**, 698-709.
O'Keefe, D. D., Prober, D. A., Moyle, P. S., Rickoll, W. L. and Edgar, B. A. (2007). Egfr/Ras signaling regulates DE-cadherin/Shotgun localization to control vein morphogenesis in the *Drosophila* wing. *Dev. Biol.* **311**, 25-39.
Pellegrino, M. W., Gasser, R. B., Sprenger, F., Stetak, A. and Hajnal, A. (2009). The conserved zinc finger protein VAB-23 is an essential regulator of epidermal morphogenesis in *Caenorhabditis elegans*. *Dev. Biol.* **336**, 84-93.
Rasmussen, J. P., English, K., Tenlen, J. R. and Priess, J. R. (2008). Notch signaling and morphogenesis of single-cell tubes in the *C. elegans* digestive tract. *Dev. Cell* **14**, 559-569.
Shemer, G. and Podbilewicz, B. (2002). LIN-39/Hox triggers cell division and represses EFF-1/fusogen-dependent vulval cell fusion. *Genes Dev.* **16**, 3136-3141.
Shemer, G., Kishore, R. and Podbilewicz, B. (2000). Ring formation drives invagination of the vulva in *Caenorhabditis elegans*: Ras, cell fusion, and cell migration determine structural fates. *Dev Biol.* **221**, 233-248.
Simske, J. S., Kaech, S. M., Harp, S. A. and Kim, S. K. (1996). LET-23 receptor localization by the cell junction protein LIN-7 during *C. elegans* vulval induction. *Cell* **85**, 195-204.
Sternberg, P. W. (2005). Vulval development. In *WormBook* (ed. The *C. elegans* Research Community, Wormbook), pp. 1-28. http://www.wormbook.org
Szabo, E., Hargitai, B., Regos, A., Tihanyi, B., Barna, J., Borsos, E., Takacs-Vellai, K. and Vellai, T. (2009). TRA-1/GLI controls the expression of the Hox gene *lin-39* during *C. elegans* vulval development. *Dev. Biol.* **330**, 339-348.
Takacs-Vellai, K., Vellai, T., Chen, E. B., Zhang, Y., Guerry, F., Stern, M. J. and Muller, F. (2007). Transcriptional control of Notch signaling by a HOX and a PBX/EXD protein during vulval development in *C. elegans*. *Dev. Biol.* **302**, 661-669.
Tan, P. B., Lackner, M. R. and Kim, S. K. (1998). MAP kinase signaling specificity mediated by the LIN-1 Ets/LIN-31 WH transcription factor complex during *C. elegans* vulval induction. *Cell* **93**, 569-580.
Van Auken, K., Weaver, D. C., Edgar, L. G. and Wood, W. B. (2000). *Caenorhabditis elegans* embryonic axial patterning requires two recently discovered posterior-group Hox genes. *Proc. Natl. Acad. Sci. USA* **97**, 4499-4503.
Wagmaister, J. A., Miley, G. R., Morris, C. A., Gleason, J. E., Miller, L. M., Kornfeld, K. and Eisenmann, D. M. (2006). Identification of cis-regulatory elements from the *C. elegans* Hox gene *lin-39* required for embryonic expression and for regulation by the transcription factors LIN-1, LIN-31 and LIN-39. *Dev. Biol.* **297**, 550-565.
Wang, Y., Han, K. J., Pang, X. W., Vaughan, H. A., Qu, W., Dong, X. Y., Peng, J. R., Zhao, H. T., Rui, J. A., Leng, X. S. et al. (2002). Large scale identification of human hepatocellular carcinoma-associated antigens by autoantibodies. *J. Immunol.* **169**, 1102-1109.
Yang, L., Sym, M. and Kenyon, C. (2005). The roles of two *C. elegans* HOX co-factor orthologs in cell migration and vulva development. *Development* **132**, 1413-1428.
Zipkin, I. D., Kindt, R. M. and Kenyon, C. J. (1997). Role of a new Rho family member in cell migration and axon guidance in *C. elegans*. *Cell* **90**, 883-894.

6 Concluding remarks

6.1 The *C. elegans* vulva as a model for studying regulation of morphogenesis

6.1.1. Notch and Ras signaling regulate cell fate decison

Notch signaling is important for various binary cell fate decisions. It is dysregulated in many cancers, and faulty notch signaling is implicated in many diseases including T-ALL (T-cell acute lymphoblastic leukemia), CADASIL (Cerebral Autosomal Dominant Arteriopathy with Sub-cortical Infarcts and Leukoencephalopathy), MS (Multiple Sclerosis), Tetralogy of Fallot, Alagille syndrome, and many other disease states (Lai, 2004). Inhibition of notch signaling has been shown to have anti-proliferative effects on T-ALL in cultured cells and in mouse model (Lai, 2004). In most of the above disorders, the phenotypic output of Notch signaling pathway are cell fate decisions. Similarly Ras proteins function as binary molecular switches that control intracellular signaling networks. Ras-regulated signaling pathways control such processes as actin cytoskeletal integrity, proliferation, differentiation, cell adhesion, apoptosis and cell migration. Ras and ras-related proteins are often deregulated in cancers, leading to increased invasion and metastasis, and decreased apoptosis (Campbell et al., 1998). These signaling pathways affect several processes. These interactions among different pathways form important part of cell as a system and hence further investigation of these combinatorial interactions becomes more important.

Defects in morphogenesis lead to disorders in the living system (Shah et al., 2004). The core components of both Notch and Ras signaling are highly conserved among different species (Campbell et al., 1998; Lai, 2004) and hence their role in regulating the execution or morphogenesis becomes more and more important.

6.1.2. Notch and Ras signaling regulate vulval morphogenesis

Using the *C.elegans* vulva as a model for morphogenesis, I have uncovered the molecular nature of the regulation of the force generating machinery during its morphogenesis. I have been able to show that the universal Notch and Ras signaling pathways converge on the LIN-1 ETS transcription factor to attain a fine balance of the forces generated for shaping the vulval tissue. This study opens up another important question about the targets of the LIN-1 ETS transcription factor, which, regulate morphogenesis. Mostly, Notch activates signaling via the CSL family of transcription factors (Christensen S, 1996).

However, the Notch-Rho-kinase signaling connection is a new example of an indirect CSL-independent regulation via ETS.

Also, in collaboration with Dr. Mark Watson Pellegrino, we have shown that Ras activates the novel DNA binding protein VAB-23 via the LIN-39 Hox protein, which further regulates important genes such as *eff-1* and *smp-1* to regulate morphogenesis. Thus, LIN-1 and VAB-23 could be the master regulators of morphogenesis in 2° and 1° vulval cells respectively. Further experiments showing the interaction between these two genes would give us good insight about cooperation/antagonism between 1° and 2° cells during morphogenesis.

6.2 The vulva as a model for epithelial tube formation

6.2.1. The vulva is a fluid filled epithelial tube

From this study, the *C. elegans* vulva has emerged as a good model for tube formation since the final organ forms a tube for allowing laying of eggs. Twenty-two cells rearrange themselves to make a functional tube. The laser puncturing experiment indicates a role of the luminal fluid in maintaining the shape of "christmas tree" stage. It has been reported that *sqv1-8* mutants, whose genes encode proteoglycan-modifying proteins, show a vulval lumen defect wherein, there is an apparent partial collapse of the invagination and an elongation of the central vulval cells. Out of several predictions for the cause of *sqv* phenotype, one of the possibilities is in agreement with our understanding i.e. the expansion of the invagination space takes place by the accumulation of fluid with hygroscopic proteoglycans and it is an active process that could require *sqv* gene function (Herman et al., 1999). Using *sqv* mutants, the interesting questions to follow up would be to find out the nature of the fluid, how it is secreted? Is it responsible for cross signaling among cells in the lumen? and which cells/ genes are important for maintaing the fluid in it.

6.2.2. Leaders and followers co-operate: lesson from vulval morphogenesis

Morphogenesis is a process by which a group of cells made up of different cell types change their shape, migrate to form new cellular interactions and adopt a new spatial arragement to make an organ. In doing so, they generate forces, which govern the change of position, and collectively they form tissues and organs. Any descrepancy in these processes of morphogenesis leads to severe organ malformation. So, it becomes important to unfold the contribution of each individual cell type in forming a complete organ. Owing to simplistic

organization of the vulval cell types in *C.elegans* vulva (1°, 2° and AC), we investigated the individual force contributions of the different cell types. During vulval morphogenesis, If we consider the dorsal movement of the vulval cells, the AC is leading in front while the 2° cells are lagging behind. The common belief would lead to the hypothesis that the AC and 1° cells should behave as leaders, which generate all the forces, and the rest as the followers, which just passively follow the group. On the contrary, we found that AC does provide a pulling force but the 1° cells are passive and do not provide any pulling force to the 2° cells lagging behind them. Not only that, the 2° cells provide a pushing force to the 1° cells. This study takes us a step further in defining individual role of a particular cell type in force contribution during organogenesis. Our results lead to several new questions for example; do the cells of the same cell type behave differently in terms of force contribution? Owing to the ease of manipulating worms, this could be done by laser ablating the individual cells of the 2° group and see if some of them are providing more force than others. This experiment would further differentiate the behaviour of individual cells in the same cell type. Also, another important question is to determine the molecular nature of the newly described pulling force by AC.

6.2.3. A new paradigm for actomyosin contraction: Vulval morphogenesis

Actin and myosin are the core components of the force generating machinery during morphogenesis. By analyzing the expression of polymerized actin and distribution of myosin in the vulva, we obtained new insights into the presence of acto-myosin mediated contraction. Usually, the notion is that wherever the myosin heavy chain is present, the rest of the components of myosin II should be present. On the contrary, we observed that the regulatory myosin light chain is selectively expressed in specific toroids only. This showed that the distribution of polymerized actin and regulatory myosin light chain could be a regulating step during acto-myosin mediated contraction. It would be very interesting to identify molecular regulators for the differential distribution of actin and myosin light chain.

6.2.4. Real time imaging gives new insights in vulval morphogenesis

For the first time, real time imaging of vulval morphogenesis led to the identification of transient processes like the requirement of AC for maintaining proper 1° lumen size. The same 4D microscopy approach could be used to describe the transient behaviour of the cytoskeleton as well as the signaling molecules for e.g. EGF, EGFR, Actin, myosin motors etc. This would give us a very good idea about the transient changes in cytoskeletal components with respect to the signaling molecules.

From this study, vulval development has become a very simple but informative model for morphogenesis. Several new questions are there to be addressed. The only drawback of this model organ at the same time its advantage and its simple organization. But owing to the possibility to manipulate the individual cells by laser dissection, *C. elegans* serves as one of the best model organisms for studying epithelial morphogenesis.

References:

Campbell, S. L., Khosravi-Far, R., Rossman, K. L., Clark, G. J. and Der, C. J. (1998). Increasing complexity of Ras signaling. *Oncogene* **17**, 1395-413.
Christensen S, K. V., Bosenberg M, Friedman L, Kimble J. (1996). lag-1, a gene required for lin-12 and glp-1 signaling in Caenorhabditis elegans, is homologous to human CBF1 and Drosophila Su(H). *Development* **122**, 1373-83.
Herman, T., Hartwieg, E. and Horvitz, H. R. (1999). sqv mutants of Caenorhabditis elegans are defective in vulval epithelial invagination. *Proc Natl Acad Sci U S A* **96**, 968-73.
Lai, E. C. (2004). Notch signaling: control of cell communication and cell fate. *Development* **131**, 965-73.
Shah, M. M., Sampogna, R. V., Sakurai, H., Bush, K. T. and Nigam, S. K. (2004). Branching morphogenesis and kidney disease. *Development* **131**, 1449-62.

Acknowledgements

Firstly, I heartily thank my mentor and supervisor, Prof. Alex Hajnal for not only providing me this opportunity to work on this project but also for his constant guidance throughout my PhD. Specially, encouraging me during bad times in the begining of PhD by saying that ”during discussions, you listen more in the begining, you argue more in the middle and you win the arguement often at the end of your PhD” which was the case in my PhD. Secondly, I would like to thank dearly, Dr. Mark W. Pellegrino, for showing me the door of ’ morphogenesis’ and shaping my knowledge base through fruitful discussion and excellent arguements in and out of the lab. I cannot forget Prof. H. S. Dhaliwal, my mentor during my M.Sc. thesis, for introducing me to the path of research.

Special thanks to my thesis committee members for guiding me through and shaping my project in a very systematic and organised way. Specially, helping me in deciding what to focus on and what to leave aside. It was great learning experience to chose the feasible among experiments.

I got immense pleasure while working with Ivo Rimann, Sara Vassali, Peter Gutierrez, Claudia Walser, Christina Herrmann, Stefanie Nusser, Itay Nakdimon, Michael Walser, Juan Escobar, Tobias Schmidt, Matthias Morf, Magdalene Adamcyk, Daniel Roiz, and Erika Frohli, who made me feel like being at home away from home in the lab. Special thanks to Stefanie Nusser for helping me out with Zussamensung part of my PhD thesis

I would like to thank members of the Joint Worm Meeting (JWM) which is held every thursday for brain storming discussions and critical inputs for my project. Special thanks to Lukas Neukomm, Kimon Doukoumetzidis and Erica Bogan for helping out with inputs and reagents. Also, I would like to thank, Dominique Forster, and other lab members of Prof. Christian Lehner’s/Dr.Stefan Luschnig’s group for assistance with confocal microscopy.

For personal funding of this project, I would like to acknowledge the University of Zurich for the Forschungskredits Grant, Julius Klaus Stifftung and Molecular Life Science PhD programme for sponsoring my travel to different conferences and the Swiss National Science Foundation (to Alex Hajnal).

All along, I cannot forget Asim Siddique, Nicola Pasquale, Paolo Salvioni, Laida Alberdi, Chetak Shetty, Lena Matveeva, Isabel Gruber, Shabir Hasan, Farooque Razvi, Shoib Siddiqui, Himanish Ghosh, Krishna Vadodaria, Marrielle Oggier, Viola Gunther and several others who made my life easier and happier outside the lab.

Final and foremost, to Papa, Ammi, Naheed Bajee, Tanveer, Taukeer, Yousuf and Sherin, words cannot describe how grateful I am to all of you for your support and encouragement throughout this project, as well as for all of other endeavors in my life. All of my successes are devoted to you.

7 Curriculum Vitae

Personal information

Name: **Farooqui**
First, middle name: **Sarfaraz Hussain**
Degrees: B.Sc., M.Sc., PhD (final year)
Nationality: Indian
Date of birth: November 10, 1981
Current position: Doctoral Fellow
E-mail: sarfarazhussain.farooqui@imls.uzh.ch, farooqui.raz@gmail.com

Contact address

University of Zurich
Institute of Molecular Life Science
Winterthurerstrasse 190
Zurich, Switzerland 8057
Phone no. 00-41-786642078

Educational and research experience

Doctor of Philosophy (PhD), University of Zurich (Switzerland), 2006 onwards.
Research topic: Characterization of NOTCH/LIN-12 signaling pathway and ETS/LIN-1as an architect of vulval morphogenesis via ROCK/*LET-502* in *C.elegans*.

Master of Science in Biotechnology, Indian Institute of Technology, Roorkee (IIT, India), 2003-2005.
Subjects: Biochemical engineering, Vaccine production and technology, Mathematics, Computers science, Water quality and environment, Instrumental method of analysis, Cell Biology and other fundamental biology subjects.
Research topic: QTL mapping of plant height in wheat genome using QTL cartographer

Bachelor of Science (Distinction), St. Xaviers College (India), 2000-2003.
Subjects: Biochemistry, Chemistry, Physics, Immunology etc
Research topic: Inducing thermo-tolerance in *Lactuca sativa*

Research Publications

Farooqui S., Pellegrino M.W.,Rimann I., Morph M., Froehli E., and Hajnal A. 2011. Lin-12 Notch and LIN-1 ETS co-ordinately control *C. Eelegans* vulval morphogenesis via LET-502 RHO KINASE (*manuscript submitted to dev cell*).

Pellegrino M.W., **Farooqui S**., Froehli E., Gasser R.B., and Hajnal A. 2011. *C.elegans vab-23* is transcriptionally activated by Ras/MAPK and LIN-39/Hox to execute vulval morphogenesis (*Development*).

Conference proceedings

-Presented **poster** at "European worm meeting" held in Crete, Greece 2006.
-Presented **poster** at 3rd, 4rth and 5th MLS PhD retreat.
-Presented **poster** at "International *C.elegans* meeting" in Los Angles, USA 2007.
-Presented **poster** at "*C.elegans* Development and Evolution meeting" in Wisconsin, Madison, USA 2008.
-Presented **poster** at "Mechanisms and models of cancer" meeting at CSHL, NY, USA in 2008.
-Presented **talk** at "International *C.elegans* meeting" in Los Angles, USA 2009.
-Presented **poster** at " Morphogenesis and Dynamics of multicellular systems" in Heidelberg, Germany 2009.
-Presented **poster** at " *C.elegans*: Development and Gene expression" in Heidelberg,

Germany 2010.
-Presented **poster** at " Seeing is believing" in EMBL Heidelberg, Germany 2011.
-Attended Regional worm meetings at FMI Basel Switzerland in 2006, 2007, 2008,2009

Scholarships/ Awards/Grants

Awarded **SHARAD A. ZHALA MEMORIAL GOLD MEDAL** by Gujarat University for getting First rank in the university biology Programme in 2001.

Awarded **JOSEPH GRACIOUS RESEARCH FELLOWSHIP** for the year 2002-2003 by St.Xavier's College Ahmedabad.

Awarded **DBT fellowship** of 800 Rs/month for pursuing M.Sc. in Biotechnology at IIT Roorkee in India.

Qualified **GATE** (Graduate Aptitude test for Engineering), with 95.75 Percentile (out of 100 percentile) in 2005, conducted by IIT (INDIA) for award of Fellowship for doing PhD in India. (Turned down in favor of doing PhD in Prof. Dr. Alex Hajnals lab at University of Zurich)

Awarded **CSIR JRF,** December 2004, conducted by Council of Scientific and Industrial Research (CSIR, Government of INDIA) for award of junior research fellowships for doing PhD in CSIR or other labs in India. (Turned
down in favor of doing PhD in Prof. Dr. Alex Hajnals lab at University of Zurich)

Awarded **DBT JRF** June, 2005, conducted by Department of Biotechnology, (DBT, Government of INDIA for award of junior research fellowships for doing PhD in CSIR or other labs in India. (Turned down in favor of doing PhD in Prof. Dr. Alex Hajnals lab at University of Zurich)

Awarded **Forschungskredit Grant** covering the monthly salary for two years (2008-2009) from Forschungskredit at University of Zurich for the project "A reporter-based screen for the Notch target genes during vulval development".

Awarded **Grant** from JULIUS KLAUS-STIFTUNG (August 2008) covering the expenses for attending the conference "**Mechanisms and models of cancer"** held at Cold Spring Harbor Labs, NY, USA.

Awarded **Grant** from Molecular life Science PhD programme (October 2009) covering the expenses for attending the conference **"Morphogenesis and Dynamics of Multicellular systems"** held at Heidelberg, Germany.

Selected one of the 50 participants of **ITP** (International Talent Programme for Life Sciences & Health held in The Netherlands from May 17th – May 21st 2010 sponsored by Govt of Netherland and Hyphen Projects of BCFjobs) to get to know the people, the research climate and the employers in the Dutch Life Sciences & Health sector.

Supervision of research students

Supervised Undergraduate, Diploma, Masters and summer students during their research projects

Languages Known

Hindi (fluent in oral and written (mother tongue))
English, Gujarati, Urdu (fluent in oral and written)
Sanskrit, German (Elementary)